2013

Characterization of the retina in the alpha 7 nicotinic acetylcholine receptor knockout mouse

Marci Lynn Smith
University of Alabama at Birmingham

CHARACTERIZATION OF THE RETINA IN THE α7 NICOTINIC ACETYLCHOLINE RECEPTOR KNOCKOUT MOUSE

by

MARCI L. SMITH

KENT T. KEYSER, CHAIR
FRANKLIN R. AMTHOR
DAVID C. KNIGHT
LORI L. MCMAHON
CHRISTIANNE E. STRANG

A DISSERTATION

Submitted to the graduate faculty of the University of Alabama at Birmingham,
in partial fulfillment of the requirements for the degree of
Doctor of Philosophy

BIRMINGHAM, ALABAMA

2013

CHARACTERIZATION OF THE RETINA IN THE α7 NICOTINIC ACETYLCHOLINE RECEPTOR KNOCKOUT MOUSE

MARCI L. SMITH

BEHAVIORAL NEUROSCIENCE, PSYCHOLOGY

ABSTRACT

Acetylcholine receptors (AChRs) are involved in visual processing and are expressed by inner retinal neurons in all species studied to date (Keyser et al., 2000; Dmitrieva et al., 2007; Liu et al., 2009), but their distribution in the mouse retina remains unknown. Reductions in α7 nicotinic AChRs (nAChRs) are thought to contribute to memory and visual deficits observed in Alzheimer's and schizophrenia (Coyle et al., 1983; Nordberg et al., 1999; Leonard et al., 2006). However, the α7 nAChR knockout (KO) mouse has a mild phenotype (Paylor et al., 1998; Fernandes et al., 2006; Young et al., 2007; Origlia et al., 2012). The purpose of this study was to determine the expression of AChRs in wildtype (WT) mouse retina and to assess whether up-regulation of other AChRs in the α7 nAChR KO retina may explain the minimal deficits described in the KO mouse.

Reverse-transcriptase PCR (RT-PCR) showed that mRNA transcripts for α2-7, α9, α10, β2-4 nAChR subunits and m1-m5 muscarinic AChR (mAChR) subtypes were present in WT murine retina. Western blot analysis confirmed the presence of α3-5, α9, and m1-m5 AChR proteins and immunohistochemical analysis demonstrated nAChR and mAChR proteins expressed by subsets of bipolar, amacrine and ganglion cells. This is the first reported expression of α9 and α10 nAChR transcripts and α9 nAChR proteins in the retina of any species.

Quantitative RT-PCR (qPCR) showed changes in AChR transcript expression in the α7 nAChR KO mouse retina relative to WT. Within whole retina α2, α9, α10, β4, m1 and m4

AChR transcripts were up-regulated, while α5 nAChR transcripts were down-regulated. However, cell populations showed subtle differences; m4 mAChR transcripts were up-regulated in the ganglion cell layer and outer portion of the inner nuclear layer (oINL), while β4 nAChR transcript up-regulation was limited to the oINL. Surprisingly, α2, α9, β4, m2 and m4 transcripts were down-regulated in the inner portion of the INL. These results indicate that compensation is mediated by differential regulation of more than one receptor type and changes in mRNA expression vary between cell populations.

ACKOWLEDGEMENTS

I would like to thank all of the members of my dissertation committee for volunteering your precious time to support my education. First and foremost, I would like to thank my doctoral mentor, Dr Kent Keyser. I appreciate you giving me the chance and taking me on as a student. Through your mentorship I have learned so much. I have learned to be a better writer, a better speaker, a better critical thinker, and a better scientist. I will forever be indebted to you for sharing your extensive knowledge with me. You are also one of the kindest men I have ever known and have been supportive of me through sickness, deaths in the family, and frustrating technical difficulties. I would like to thank Dr Christianne Strang. You have been a great committee member, friend, sounding board, and sometimes substitute mentor. You have helped me get through the day to day grind of graduate school and are always willing to answer my multitudes of questions or just talk about doggies with me. I have said it before, but I really do not know what I would have done without your constant support and encouragement. I would like to thank Dr Frank Amthor who served on both my qualifying and dissertation committee, who helped to give me a start in science by hiring me as a lab technician while I was getting my bachelor's degree, attended countless lab meetings, and has been a constant force in my graduate career. I would like to thank Dr David Knight for agreeing to serve on my committee even though it is so far out of your area of interest. Your comments and suggestions have been very helpful, and I think your unique viewpoint has strengthened my work and made me take a step back and fill in some of the blanks in my reasoning. I would like to thank Dr Lori McMahon for your spot-on input and

advice and for your friendly and cheerful interactions which always buoy my mood. Finally, I would like to thank both Dr Lori McMahon and Dr Christianne Strang for being such great role-models of women in science.

I also want to thank the Psychology department and the Behavioral Neuroscience program for admitting me to the program and providing such great support. There are too many people in the department who have supported me to list them all, but I will name a few. First, I would like to thank Dr Alan Randich, who has served as my program director throughout much of my graduate career. You have always been supportive, encouraging, and available no matter how busy you were and I have learned a lot from you, particularly through the behavioral neuroscience seminar course. I would also like to thank Terri Roberson for helping me through all the paperwork and difficulties of finally graduating. Finally, I would like to thank Dr Rozalyn Weller and Dr James Cox who have been great instructors through much of my graduate coursework and both served on my qualifying committee. I would also like to thank Dr Rozalyn Weller for our many conversations on teaching, which really helped me improve my teaching strategies.

I also want to thank the many people in the Vision Science department who have supported me. Specifically, Dr Ramona Hart, David Parkinson, and Clifford Kennon who have always treated me like I was a member of the department, included me in department functions, and helped me far more than was required. I think Ramona is the heart of the program and her tireless defense of and support for the students is definitely one of the greatest assets of the vision science department. I would like to thank Dr Virginia Wotring, who took a girl who had never held a pipette before and taught her molecular biology. I learned so much from you and I am a better scientist for it. I would like to thank the many

people in the department who provided scientific support and in some way helped me learn new techniques, troubleshoot technical difficulties, or just provided materials or space, in particular Dr Steven Pittler, Dr Shu-Zhen Wang, and Hank Fortinberry.

I would like to thank Dr Barbara Morley at Boystown Research Hospital, who provided the α7 nAChR knockout mouse retinal tissue. Additionally, I would like to thank the Eye Foundation of Alabama, the National Institutes of Health, and the National Eye Institute for providing funding for my experiments.

I would like to thank all my fellow students and the entire Keyser lab, past and present. You have been great friends, frequent lunch companions, and great listeners. In particular, I would like to express appreciation to Dr Jordan Renna and Dr Ryan Splittgerber who helped me through my first couple years, always looking out for the new girl, always being there to talk to or commiserate with, and later answering questions about how to get a job and what to expect after graduation. I also need to thank Dr Konstantin Gavrikov, for being so friendly and dependable. I always know when I come into lab; you will be there with a greeting and a smile. You are always willing to talk, always willing to explain the strange and mystical science that is electrophysiology, and always willing to do the "manly" thing and reach, open, or lift things for me. I would like to thank Fred Souza and Kady Bruce for giving me the chance to try my hand at supervising a student and for helping me to collect data and troubleshoot techniques during their rotations in the lab. I would also like to thank Fred for your joyful personality, you always brighten my day; no matter what is going on in your life you always try to be happy and positive.

I would like to thank Dr Heather Williamson and Dr Sandrine Niyongere, some of my closest friends in the world who were my roommates and study companions for many years. I

cannot believe we are all finally doctors! I love you both and miss you dearly. You both have bolstered my spirits and been great peer role-models. I was truly blessed to meet both of you and to have you in my life.

I would like to thank my family for their support and encouragement. I am excited to be reaching the end of my graduate career and to finally get my doctorate but it is also bittersweet as I mourn those who saw me receive my bachelor's degree, but are no longer here to see me get my doctorate. I miss you so much and wish you were here, I know how proud you would be. My siblings have been such an important part of my life and have all supported me in their own ways. I love you all for your support through the good and hard times, through the difficulties our family has faced in the last few years. While we often disagree and argue, I always know that if I need any of you, you will be there for me and I truly appreciate it!

Lastly, I would like to thank my parents, Bobby and Linda Smith. You have been steadfast supporters throughout my education, whether it was reading with me as a child, testing me with flashcards, reading my papers, paying for advanced placement courses, providing a quiet home where I could study, providing an allowance so I could focus on school and not work, or just providing emotional support through difficult coursework. I am certain that your influence has been one of the largest forces allowing me to reach the goal of obtaining a doctorate. I love you both so much, and what your love and support have given me truly cannot be measured. Thank you.

TABLE OF CONTENTS

Page

LIST OF TABLES

Table *Page*

LIST OF FIGURES

Figure *Page*

INTRODUCTION

DISTRIBUTION OF ACETYLCHOLINE RECEPTORS IN THE MOUSE RETINA

ACETYLCHOLINE RECEPTORS IN THE RETINAS OF THE α7 NICOTINIC ACETYLCHOLINE RECEPTOR KNOCKOUT MOUSE

ABBREVIATIONS

α-BGT	α-bungarotoxin
AC	adenylate cyclase
ACh	acetylcholine
AChR	acetylcholine receptor
AD	Alzheimer's disease
AMPA	α-amino-3-hydroxy-5-methyl-4-isoxazoleproprionic acid
Aβ	amyloid-β peptides
BTNRH	Boys Town National Research Hospital
cAMP	cyclic adenosine monophosphate
cDNA	complementary deoxyribonucleic acid
ChAT	choline acetyltransferase
Ct	cycle threshold
DKNS	donkey normal serum
DNA	deoxyribonucleic acid
DNAse	deoxyribonuclease
DS	directionally selective
FΔ	fold change
FD	fold difference
GABA	γ-aminobutyric acid
GCL	ganglion cell layer

GluRs	ionotropic glutamate receptors
IgG	immunoglobulin G
IHC	immunohistochemistry
iINL	inner portion of the inner nuclear layer
INL	inner nuclear layer
IPL	inner plexiform layer
Kcnj4	inwardly rectifying potassium subfamily J, member 4 channel
KO	knockout
LCM	laser capture microdissection
mAChR	muscarinic acetylcholine receptor
mGluR	metabotropic glutamate receptor
mRNA	messenger ribonucleic acid
nAChR	nicotinic acetylcholine receptor
NFL	nerve fiber layer
NMDA	n-methyl-d-aspartic acid
oINL	outer portion of the inner nuclear layer
ONL	outer nuclear layer
OPL	outer plexiform layer
OS	outer segments
PBS	phosphate buffered saline
PCR	polymerase chain reaction
PFA	paraformaldehyde
qPCR	quantitative real-time reverse transcriptase polymerase chain reaction

RNA	ribonucleic acid
RNAse	ribonuclease
RyR3	ryanodine receptor 3
RT	reverse transcriptase
RT-PCR	reverse transcriptase polymerase chain reaction
SD	standard deviation
SEM	standard error of the mean
UAB	University of Alabama at Birmingham
WT	wildtype

GLOBAL INTRODUCTION

The Mammalian Retina and Visual Processing

Transduction and coding of light information by the retina is the first stage in visual processing. The retina is the light sensitive tissue that lines a portion of the inner surface of the eye. It is a highly laminar structure with five basic neuronal types, including the photoreceptors, bipolar cells, ganglion cells, horizontal cells, and amacrine cells, each of which has several subtypes (Figure 1). In the absence of light, photoreceptors are depolarized while light increments result in photoreceptor hyperpolarization. The rod photoreceptors are responsible for phototransduction under scotopic (dim light) conditions while the cone photoreceptors are responsible for phototransduction under photopic (bright light) conditions (Kolb & Famiglietti, 1974; Wassle & Boycott, 1991). In the mammalian retina, there are parallel information processing pathways for detecting light increments, the ON pathway, and decrements in light, the OFF pathway. These pathways arise at the level of the photoreceptor synapses and, for photopic vision, are preserved throughout the retina, including bipolar and ganglion cells which respond preferentially to light decrements or increments (Kolb & Marshak, 2003).

The first step in visual processing is phototransduction by the photoreceptors; these photoreceptors synapse onto the dendrites of bipolar cells and horizontal cells in the outer plexiform layer (OPL). Horizontal cells provide lateral feedback to photoreceptors while the bipolar cells transmit information to the ganglion cells. Retinal bipolar cell

types have been extensively characterized in many species and it has been determined that, similar to other mammalian species, the mouse retina has four types of OFF bipolar cells, five types of ON bipolar cells, and one type of ON rod bipolar cell (Wassle & Boycott, 1991; Ghosh et al., 2004). Bipolar cells synapse with ganglion cell and amacrine cell dendrites in the inner plexiform layer (IPL). Amacrine cells provide lateral feedback at the bipolar and ganglion cell, while the ganglion cells integrate inputs from bipolar and amacrine cells. The ganglion cell axons form the optic nerve and transmit the information from the retina to subcortical visual areas and non-visual areas, such as the suprachiasmatic nucleus, in the form of action potential trains (Fukuda & Stone, 1974; Leventhal et al., 1981; Perry & Cowey, 1984; Perry et al., 1984; Leventhal et al., 1985).

In the mammalian retina there are more than 20 classes of ganglion cells that comprise two broad categories; concentric and complex ganglion cells (Barlow et al., 1964; Levick, 1967; Kolb et al., 1981; Amthor et al., 1984; Amthor et al., 1989a; Amthor et al., 1989b; Badea & Nathans, 2004; Kong et al., 2005; Volgyi et al., 2009). The concentric ganglion cells have center-surround receptive field organization consisting of either an ON center and OFF surround (ON center) or an OFF center and an ON surround (OFF center). The firing rate of ON center cells increases when light falls on the center of the receptive field and the firing rate decreases when light falls in the surround of the receptive field. In contrast, the firing rate of OFF center cells decreases when light falls on the center of the receptive field and the firing rate increases when light falls in the surround of the receptive field. Concentric ganglion cells can be further divided into brisk transient, brisk sustained, sluggish transient and sluggish sustained cells based upon the timing and length of their responses to light (Barlow et al., 1964; Levick, 1967; Amthor

et al., 1989b). The receptive field surrounds can be either suppressive or antagonistic. Light stimuli that impinge on a suppressive surround decrease the center response while light stimuli that impinge on an antagonistic surround give rise to an excitatory response opposite to that of the center. There are also several types of complex ganglion cells including orientation-selective, directionally selective (DS), local edge detectors, and uniformity detectors which respond preferentially to more complex features of visual stimuli such as movement in a specific direction or light increment or decrement only in the center of the receptive field (Amthor et al., 1989a; Amthor et al., 1989b; Amthor & Grzywacz, 1993; Bloomfield, 1994; Merwine et al., 1995).

The electrical signals of photoreceptors, bipolar cells, and ganglion cells are modulated by two types of interneurons; horizontal cells and amacrine cells. In the outer retina, the horizontal cells release the inhibitory neurotransmitter, λ-aminobutyric acid (GABA) in the OPL. Horizontal cell dendrites are a component of the photoreceptor bipolar cell triad ribbon synapse, which consists of three or more postsynaptic components including bipolar cell dendrites and at least two horizontal cell dendrites (Leicester & Stone, 1967; Wassle & Boycott, 1991). Amacrine cells also receive input from bipolar cells and release neurotransmitters such as GABA, glycine, and acetylcholine (ACh) in the IPL (Leicester & Stone, 1967; Nelson & Kolb, 1985; Wassle & Boycott, 1991). Thus, the synaptic connections in the IPL provide substrates for complex modulation of visual information.

As previously mentioned, the mammalian retina has ON and OFF pathways which allow for perception of contrast (Kolb & Marshak, 2003). The ON pathway begins with cones that synapse with the ON cone bipolar cells. The OFF pathway begins with

cones that synapse with OFF cone bipolar cells in the OPL. The IPL is divided into several sublaminas; sublamina 1 at the border of the inner nuclear layer (INL) and the IPL to sublamina 5 at the border of the ganglion cell layer (GCL) and the IPL. OFF bipolar, ganglion, and amacrine cell processes stratify in sublamina 1, 2, and 3. ON bipolar, ganglion, and amacrine cell processes stratify in sublamina 3, 4, and 5 (Famiglietti & Kolb, 1976; Nelson et al., 1978; Kolb, 1979; Famiglietti, 1983).

Information about visual stimuli is transmitted through the retina as electrical signals produced by neurotransmitter activity (Figure 2, Table 1). The major excitatory neurotransmitter in the retina is glutamate, which exerts its actions through two classes of receptors: ionotropic and metabotropic. The α-amino-3-hydroxy-5-methyl-4-isoxazolepropionic acid (AMPA), kainate, and N-Methyl-D-aspartic acid (NMDA) receptors are ionotropic glutamate receptors (Slaughter & Miller, 1981; Slaughter & Miller, 1983; Dingledine et al., 1999). AMPA/kainate receptors are expressed by OFF bipolar cells, horizontal cells, and retinal ganglion cells; these receptors depolarize the cell in response to glutamate release (Slaughter & Miller, 1981; Slaughter & Miller, 1983; Aizenman et al., 1988; Kleckner & Dingledine, 1988; Massey & Miller, 1988; Massey & Miller, 1990; Cohen & Miller, 1994; Euler et al., 1996; Sasaki & Kaneko, 1996; Pin & Duvoisin, 1995; Dingledine et al., 1999). Thus, bipolar cells that express ionotropic glutamate receptors (GlurRs) are OFF bipolar cells since they depolarize to light decrements. The OFF bipolar cells stratify in the outer sublaminas of the IPL and make flat contacts at the cone triad synapse. NMDA receptors are expressed by retinal ganglion cells; these receptors also depolarize the cell in response to glutamate release from bipolar cells with the additional requirements for glycine or serine binding and an

initial membrane depolarization prior to activation (Aizenman et al., 1988; Kleckner & Dingledine, 1988; Massey & Miller, 1988; Massey & Miller, 1990; Cohen & Miller, 1994; Pin & Duvoisin, 1995; Dingledine et al., 1999; Stevens et al., 2003). Eight types of metabotropic glutamate receptors (mGluRs) have been described, mGluR1-mGluR8. mGluRs are classified as Type I, Type II, or Type III (Swanson et al., 2005). Type I mGluRs include mGluR1 and mGluR5, which activate the Gq-α G-protein and activate the phospholipase signaling pathway. This raises intracellular Ca^{2+} levels and activates protein kinase C, eventually resulting in potentiation of NMDA receptor currents (Chu & Hablitz, 2000; Skeberdis et al., 2001; Lea et al., 2002; Endoh, 2004; Swanson et al., 2005). Type II mGluRs include mGluR2 and mGluR3, which activate the Gi-α G-protein and inhibit adenylate cyclase. This decreases intracellular Ca^{2+} levels and inhibits cyclic adenosine monophosphate production, eventually resulting in an attenuation of NMDA receptor currents (Ambrosini et al., 1995; Swanson et al., 2005). Type III mGluRs include mGluR4, mGluR6, mGluR7, and mGluR8, which also activate the Gi-α G-protein and inhibit adenylate cyclase (Ambrosini et al., 1995; Swanson et al., 2005). mGluR6 receptors are expressed by ON bipolar cells and activation of these receptors hyperpolarizes the cell in response to glutamate release (Slaughter & Miller, 1981; Slaughter & Miller, 1983; Euler et al., 1996). ON bipolar cells make invaginating contacts at the cone triad synapse. ON bipolar cells that express mGluR6 stratify in the inner sublaminas of the IPL and respond to increments of light via activation of the Gi-α G-protein.

In summary, light increments hyperpolarize the photoreceptors, resulting in decreased glutamate release. Reduced glutamate binding to AMPA/kainate receptors on

the OFF bipolar cells then results in hyperpolarization of the OFF bipolar cell and reduces the amount of glutamate it releases, which in turn releases less glutamate onto the OFF ganglion cells, which signal light decrements to other parts of the brain via a decreased firing rate (Slaughter & Miller, 1981; Slaughter & Miller, 1983; Aizenman et al., 1988; Massey & Miller, 1988; Massey & Miller, 1990; Cohen & Miller, 1994; Euler et al., 1996). Light decrements cause photoreceptor depolarization and increased glutamate release which results in depolarization of OFF bipolar cells and increased firing rates of OFF ganglion cells as well as hyperpolarization of ON bipolar cells and decreased firing rates of ON ganglion cells (Slaughter & Miller, 1981; Slaughter & Miller, 1983; Aizenman et al., 1988; Massey & Miller, 1988; Massey & Miller, 1990; Cohen & Miller, 1994; Euler et al., 1996). The cells of the parallel ON pathway depolarize in response to the reduced glutamate release due to light increments via a sign-inversion at the photoreceptor bipolar cell synapse. Reduced glutamate binding to the mGluRs on the ON bipolar cells results in depolarization, via a second messenger cascade, and increases the amount of glutamate the bipolar cell releases, which in turn increases the firing rate of the corresponding ON ganglion cell (Figure 2 & Table 1; Cohen & Miller, 1994; Dingledine et al., 1999). Both pathways are modulated by lateral interactions with horizontal cells and amacrine cells.

Acetylcholine in the Retina

In addition to glutamate, another excitatory neurotransmitter expressed in the retina is ACh. Activation of ACh receptors (AChRs) by ACh effects the response of ganglion cells (Masland & Ames; 1976; Ikeda & Sheardown, 1982; Masland et al., 1984;

Schmidt et al., 1987; Baldridge, 1996; Reed et al., 2002; Reed et al., 2004; Strang et al., 2007; Taylor & Smith, 2012). ACh is synthesized from choline and Acetyl Co-A by the enzyme choline acetyltransferase (ChAT). There are two sources of ACh in the retina: the populations of starburst amacrine cells and displaced starburst amacrine cells. Starburst amacrine cells have cell bodies in the INL, project to the OFF sublamina of the IPL, and release ACh in response to light decrements (Famiglietti, 1983; Masland et al., 1984). Displaced starburst amacrine cells have cell bodies in the GCL, project to the ON sublamina of the IPL, and release ACh in response to light increments (Famiglietti, 1983; Masland et al., 1984). Both populations receive inputs from cone bipolar cells, via kainate receptors, and release GABA as well as ACh (Masland et al., 1984). Additionally, there is light-independent tonic release of ACh in the retina (Masland et al., 1984). ACh binds to nicotinic ACh receptors (nAChRs) or muscarinic ACh receptors (mAChRs), which are expressed by subpopulations of horizontal, bipolar, amacrine, and ganglion cells (Zucker & Yazulla, 1982; Keyser et al., 1988; Britto et al., 1992; Keyser et al., 2000; Yamada et al., 2003; Dmitrieva et al., 2007; Liu et al., 2009; Strang et al., 2010).

AChR Subtypes and Expression Patterns in the Retina

The nAChRs are ligand-gated cation channels, composed of five subunits arranged around a central pore, activated by ACh (Figure 3). They are members of the ligand-gated ion channel superfamily that includes glycine receptors, $GABA_A$ and $GABA_C$, and 5HT3 receptors (Karlin, 2002; Alexander et al., 2007). α2-α6 subunits can combine with β2-β4 subunits to create αβ heteromeric nAChR subtypes. α7 and α9 subunits usually combine into homomeric nAChRs containing only α subunits

(McGehee, 1999; Lindstrom, 2000; Clementi et al., 2000; Khiroug et al., 2002). However, there is one report suggesting that α7 subunits may combine with β2 subunits to form heteromers (Khiroug et al., 2002) and the α9 subunit combines with the α10 subunits to form an α-only heteromeric nAChR (Weisstaub et al., 2002; Plazas et al., 2005). Subunit composition determines the pharmacological and physiological properties of the channel; including the rate of desensitization, channel opening time, ligand affinity, and conductance (Lindstrom et al., 1996; Arias, 2000). All of the nAChRs are permeable to Ca^{2+}, but those composed of only α7 subunits have the highest Ca^{2+} permeability (Fucile, 2004). nAChRs have two, or in the case of α-only homomers, five agonist binding sites, and different receptors have varying permeability to calcium (Lindstrom, 2000; Dani, 2001). Receptors with α9 subunits or both α9 subunits and α10 subunits also have high Ca^{2+} permeability (Katz et al., 2000; Weisstaub et al., 2002; Fucile, 2004). Finally, when the α5 subunit is added to either the α3β2 or the α3β4 receptors to form α3β2α5 and α3β4α5 nAChRs, respectively, these receptors have Ca^{2+} permeabilities similar to that of the α7 nAChR (Gerzanich et al., 1998; Fucile, 2004). Increased intracellular Ca^{2+} can have many effects, including, depolarization of the cell membrane, increased presynaptic vesicle release, and activation of postsynaptic G-protein signaling cascades (Berridge et al., 2000).

Immunocytochemical studies have shown nAChR subunit expression by bipolar, amacrine, displaced amacrine, and ganglion cells in the rabbit and rhesus monkey retina (Zucker & Yazulla, 1982; Keyser et al., 1988; Britto et al., 1992; Keyser et al., 2000; Dmitrieva et al., 2007; Liu et al., 2009). Specifically, α7 nAChRs are expressed by bipolar, amacrine, displaced amacrine, and ganglion cells, while the non-α7, β-containing

nAChRs are expressed by amacrine, displaced amacrine, and ganglion cells. Further, the activation of nAChRs affects the responses of ganglion cells; including increasing baseline firing rate and light responses (Masland & Ames, 1976; Ikeda & Sheardown, 1982; Masland et al., 1984; Baldridge, 1996; Reed et al., 2002; Reed et al., 2004; Strang et al., 2007). ACh, via activation of nAChRs, also affects the responses of DS ganglion cells, cells which respond preferentially to movement in one direction. GABA release inhibits the null direction, opposite of preferred direction, while ACh enhances the preferred direction response to moving bars (Masland et al., 1984). The preferred direction response to moving gratings requires ACh and could potentially be mediated through α7 nAChRs (Grzywacz et al., 1998; Reed et al., 2002; Reed et al., 2004). However, these DS responses are likely mediated by more than one nAChR subtype (Strang et al., 2007). The majority of DS ganglion cells that respond preferentially to movement in the temporal direction express only α7 nAChRs, whereas the majority of DS ganglion cells that respond preferentially to movement in the nasal direction express non-α7, β-containing nAChRs (Strang et al., 2007). DS ganglion cells expressing both α7 nAChRs and non-α7 nAChRs respond preferentially to movement away from or toward the visual streak (superior and inferior direction) as well as movement in the nasal direction (Strang et al., 2007).

mAChRs are metabotropic G-protein coupled receptors that are activated by ACh. mAChR subtypes include m1-m5 subtypes (Figure 4), each of which is encoded by a specific gene (Caulfield & Birdsall, 1998). The mAChR subtypes can be distinguished by their affinities to ligands, susceptibility to toxins and antagonists, and their responses to agonists (Caulfield & Birdsall, 1998). The subtypes also activate different intracellular

signaling pathways (Caulfield & Birdsall, 1998). The m1, m3, and m5 subtypes couple with the Gq-α G-protein subunit and activate the phosphatidyl inositol or phospholipase signaling pathways. When activated, they produce excitation through increased intracellular Ca^{2+} release or decreased K^{+} conductance (Brown et al., 1997). The m2 and m4 subtypes couple with the Gi-α G-protein subunit and inhibit adenylate cyclase and cyclic adenosine monophosphate production. When activated, they produce inhibition through decreased intracellular Ca^{2+} release and increased K^{+} conductance (Wess, et al., 1997). Thus, the effects of activation of the m1, m3, and m5 mAChR subtypes are generally excitatory, while the effects of activation of the m2 and m4 mAChR subtypes are generally inhibitory.

Immunohistochemical studies have shown mAChR expression by subpopulations of bipolar, horizontal, amacrine, displaced amacrine, and ganglion cells in the retina (Cheon et al., 2001; Yamada et al., 2003; Strang, et al., 2010). m1 and m4 mAChRs have been reported to be expressed by subpopulations of amacrine and ganglion cells (Cheon et al., 2001; Strang et al., 2010). m2 and m5 mAChRs are expressed by subpopulations of bipolar, amacrine, and ganglion cells (Cheon et al., 2001; Yamada et al., 2003; Strang et al., 2010). Finally, m3 mAChRs are expressed by subpopulations of horizontal, bipolar, amacrine, and ganglion cells (Yamada et al., 2003; Strang et al., 2010). Activation of mAChRs has been shown to increase and decrease ganglion cell maintained firing rates and directional selectivity (Kittila & Massey, 1997). In addition, mAChRs may play a role in development of the retina and amacrine cell mosaic tiling, and in the generation and propagation of retinal waves (Zhou & Zhao, 2000; Syed et al., 2004; Stanke et al., 2008).

Physiology and Expression of the α7 nAChRs in the Mammalian Retina

Homomeric α7 nAChRs are expressed throughout the mammalian nervous system. They bind and are blocked by α-bungarotoxin (α-BGT), a protein from banded krait snake venom (Nelson & Lindstrom, 1999). These receptors have lower sensitivity to ACh than other nAChRs, and desensitize rapidly to high agonist concentrations (Bertrand et al., 1990; Couturier et al., 1990; Papke et al., 1996; Chen & Patrick, 1997; Nelson & Lindstrom, 1999; Papke et al., 2000). In the brain, α7 nAChRs have been reported to have many functional roles which include mediating postsynaptic excitatory currents (Alkondon et al., 1998; Orr-Urtreger et al., 1997; Frazier et al., 1998), synchronizing and maintaining the synchronization of firing of groups of neurons (Chang & Berg, 1999), producing cytoprotective effects (Kihara et al., 2001; Jonnala & Buccafusco, 2001; Jonnala et al., 2003), and regulating the release of other neurotransmitters such as GABA (Albuquerque et al., 2000; Alkondon & Albuquerque, 2001; Marchi et al., 2002; Zhang & Berg, 2007).

In the rabbit retina, α7 nAChRs are expressed by a number of retinal cell types including subpopulations of ON cone bipolar cells, subpopulations of glycinergic and GABAergic amacrine cells, subpopulations of ON and OFF ganglion cells, and subpopulations of directionally selective ganglion cells in the rabbit retina (Dmitrieva et al., 2003; Strang et al., 2005; Dmitrieva et al., 2007; Renna et al., 2007; Strang et al., 2007). The distribution of AChRs in the mouse retina, including α7 nAChRs, have not yet been described, even though in other mammals they have been shown to be expressed throughout the retina and to play a role in visual processing.

Several of the populations of cells in the retina that are involved in the ON/OFF pathway express α7 nAChRs, including three subtypes of ON cone bipolar cells, subpopulations of amacrine cells, and ON and OFF ganglion cells (Dmitrieva et al., 2007). Activation of α7 nAChRs expressed by ganglion cells may affect the response properties of ganglion cells directly. Additionally, α7 nAChRs expressed by glycinergic amacrine cells and some GABAergic amacrine cells could affect the response properties of ganglion cells indirectly by activating receptors expressed by amacrine cells that release inhibitory neurotransmitters and cause inhibition or disinhibition, as has been seen in hippocampus (Alkondon & Albuquerque, 2001). There is also evidence that α7 nAChRs are involved in the development of the retina. First, retinal waves, spontaneous bursts of action potentials thought to be involved in developing circuitry within the developing retina and between ganglion cells and cells of the lateral geniculate nucleus, are cholinergic, thus cholinergic activation may contribute to early retinal patterning (Zhou & Zhao, 2000; Feller, 2002; Syed et al., 2004). There is also evidence that during the development of the visual system, α7-containing receptors (either heteromeric or homomeric) may be expressed in retinal ganglion cell axon terminals and modulate glutamatergic signaling at retinogeniculate and retinocollicular synapses (Zhou & Zhao, 2000; Feller, 2002; Debski & Cline, 2002). The widespread expression of α7 nAChRs in the nervous system, including the retina, as well as their functional role in visual processing suggests that changes in the expression of α7 nAChRs may lead to changes in visual processing.

Visual Dysfunctions and α7 nAChRs in Alzheimer's disease

Interestingly, changes in nAChR expression and cholinergic function have been reported in disease states such as Alzheimer's disease (AD). AD is a degenerative dementia characterized by the development of amyloid plaques formed by amyloid-β peptides (Aβ) as well as neurofibrillary tangles formed by aggregates of hyperphosphorylated tau proteins in the cortex (Palmer, 2002; Ni et al., 2013). Mouse models of AD and a few human studies have provided evidence that Aβ plaques form in the retina prior to formation in the cortex (Hinton et al., 1986; Katz & Rimmer, 1989; Trojanowski et al., 1993; Loffler et al., 1995; Blanks et al., 1996a; Blanks et al., 1996b; Parisi et al., 2001; Hardey & Selkoe, 2002; Parisi, 2003; Greeve et al., 2004; Ning et al., 2008; Dutescu et al., 2009; Liu et al., 2009; Perez et al., 2009; Koronyo et al., 2011; Koronyo et al., 2012). AD results in progressive cognitive dysfunction, especially in learning and memory tasks (Palmer, 2002) and AD patients also exhibit a number of visual deficits. For example, visual acuity is decreased in AD and studies have shown a higher number of AD patients with myopia and hyperopia, as compared to age matched controls (Uhlmann et al., 1991; Viertio et al., 2007). AD patients have a higher rate of anomalous trichromacy, a color discrimination dysfunction in which the observer's spectral sensitivities are different from those of the standard observer (Wolin, 1994; Cronin-Golomb et al., 1995; Cronin-Golomb, 1995). AD patients exhibit poor spatial and temporal visual resolution, meaning they are less adept than controls at discriminating between two closely spaced objects and two stimuli closely spaced in time (Cronin-Golomb et al., 1995). AD patients exhibit higher contrast thresholds than controls; the lowest contrast detected by AD patients is significantly higher than the lowest contrast

detected by controls (Hutton et al., 1993; Cronin-Golomb et al., 1995; Cronin-Golomb, 1995). AD patients also have deficits in visuospatial functions, which results in a decrease in the ability to produce or recognize figures as well as a decrease in the capacity to recognize relationships among spatial locations (Kaskie & Storandt, 1995). Finally, AD patients exhibit deficits in backwards masking, which is the ability to identify an object which is revealed and then partly blocked from view by other objects (Cronin-Golomb et al., 1995; Cronin-Golomb, 1995). Further, AD patients exhibit a reduced density of ganglion cells and their axons in the optic nerve, including a 43% reduction of ganglion cells in the central retina and 25% reduction in the peripheral retina (Hinton et al., 1986; Sadun & Bassi, 1990; Blanks et al., 1996). Retinal ganglion cell loss could lead to impairments in visual acuity, color vision, contrast discrimination, and spatial resolution (Kandel et al., 2000). So, while some of the deficits observed in AD may arise at the cortical level, other deficits may be mediated by changes in visual processing as a result of retinal ganglion cell loss.

α7 nAChR subtypes in particular have been reported to be associated with some of the deficits observed in AD (Lindstrom, 1997). Nicotine, a cholinergic agonist which binds with high affinity to α7 nAChRs, has been shown to protect against cell death in cells expressing amyloid precursor protein (Wang et al., 2000; Oddo & LaFerla, 2006; Brown et al., 2013). Also, the progression of symptoms in AD is mirrored by a decline in cortical ACh and a decrease in α7 nAChR expression, as measured in postmortem brain tissue, particularly in the cortex and hippocampus (Coyle et al., 1983; Levin, 1992; Nordberg, 1999; Perry et al., 2000). Additionally, α7 nAChRs are found in plaques, and α7 nAChRs are positively correlated in postmortem AD brain tissue with neurons that

amass hyperphosphorylated tau and extracellular Aβ (Wevers et al., 1999; Wang et al., 2000). Visual deficits observed in AD are partially attributable to deficits in AChR activation in the non-retina areas of the brain, but may also arise at the level of the retina, increasing the importance of determining the expression patterns of AChRs in the retina.

Visual Dysfunctions and α7 nAChRs in Schizophrenia

Changes in nAChR expression and cholinergic function have also been reported in patients with schizophrenia, a disorder characterized by abnormalities in the perception of reality (Mueser & McGurk, 2004; van Os & Kapur, 2009). Positive symptoms include hallucinations and delusions, whereas negative symptoms include blunted emotions and social withdrawal (Mueser & McGurk, 2004). Neurocognitive deficits such as reduced or impaired memory, attention, problem-solving, executive function, and social cognition are common in schizophrenics (Mueser & McGurk, 2004; van Os & Kapur, 2009). Schizophrenic patients also exhibit visual dysfunctions similar to those observed in AD patients, including impairments in acuity, spatial and temporal resolution, contrast sensitivity, and backwards masking (Uhlmann et al., 1991; Hutton et al., 1993; Wolin, 1994; Kaskie & Storandt, 1995; Cronin-Golomb et al., 1995). In addition, people suffering from schizophrenia also exhibit deficits in stereoacuity, which is the ability to distinguish differences in distance using three-dimensional cues (Viertio et al., 2007; Lindstrom, 1997). In order to measure stereoacuity, the smallest difference that can be accurately detected between images presented to the two eyes is determined, and schizophrenic patients are unable to detect small differences in the distance of the images (Viertio et al., 2007; Lindstrom, 1997). These visual deficits have been linked to

abnormalities in the cortex, but visual deficits linked to changes in the non-retina part of the brain of schizophrenics could correlate to changes in the retina. However, there are no reports of the retina of schizophrenic patients being examined, so whether there are actually retinal abnormalities in schizophrenia is unknown.

While schizophrenia is most commonly associated with abnormalities in dopaminergic transmission, cholinergic abnormalities also contribute to schizophrenia (Seeman et al., 1975; Creese et al., 1976). Schizophrenics have a much higher prevalence of smoking than the general population, with as many as 80-90% of schizophrenics smoking (Hughes et al., 1996). This high incidence of smoking in schizophrenics, often thought to be a form of self-medication, may be evidence for involvement of nAChRs in schizophrenia. The α7 nAChR subtype in particular has been strongly implicated in the development of schizophrenia since abnormalities in α7 nAChR expression have been observed in schizophrenics. The chromosomal site of the α7 nAChR gene, 15q13-14, has a specific dinucleotide polymorphism that is reported in schizophrenics and their first-degree relatives (Freedman et al., 1997; Xu et al., 2001; Leonard & Freedman, 2006). Schizophrenics, and their first degree relatives, are more likely to have abnormalities in auditory evoked responses to repeated stimuli, which may make it difficult for them to properly filter auditory stimuli (McGhie & Chapman, 1961; Freedman et al., 1987; Adler et al., 1992; Griffith et al., 1998). In cochlear hair cells ACh has been shown to increase the Ca^{2+}-dependent potassium current via activation of α9 nAChRs, resulting in hyperpolarization (Fuchs & Murrow, 1992). In normal auditory processing, presentation of an auditory stimulus results in nAChR mediated inhibition of auditory responses to a second auditory stimulus because the hair cells are hyperpolarized after the initial

stimulus (Fuchs & Murrow, 1992). Schizophrenics show a reduction in this inhibition; in other words, they exhibit a smaller decrease in response to the second auditory stimulus compared to healthy controls (Freedman et al., 1987; Freedman et al., 1994; Fernandes et al., 2006). This abnormality can be normalized with nicotine administration via smoking or nicotine gum, indicating that the deficit is mediated by decreased cholinergic transmission (Waldo et al., 1991; Adler et al., 1992; Freedman et al., 1994; Fernandes et al., 2006). In rats, the normal auditory filtering response is reduced, as it is in schizophrenic patients, following administration of α-bungarotoxin in the hippocampus (Luntz-Leybman et al., 1992).

Further, postmortem studies have shown morphological differences in the brains of schizophrenics compared to controls, which include reduced α-BGT binding in the hippocampus. The reduction in α-BGT binding may be due to a reduction in hippocampal α7 nAChR expression (Freedman et al., 2000). Another piece of evidence linking α7 nAChRs to schizophrenia is that one of the genes linked to susceptibility for schizophrenia, neuregulin 1, regulates α7 nAChR messenger ribonucleic acid (mRNA) expression (Mathew et al., 2007). One study suggested that in the disease state, neuregulin 1 may cause down-regulation of α7 nAChR mRNA expression (Mathew et al., 2007). Taken together, these data support the idea that decreases in cholinergic transmission contribute to symptoms of schizophrenia.

Mouse Models and the α7 nAChR KO Mouse

Understanding the changes that occur in an α7 nAChR knockout (KO) mouse may provide a better understanding of the mechanisms by which the cholinergic deficits

in AD and schizophrenia exert their effects, leading to the potential for better treatment and symptom management. Because some visual symptoms may arise at the level of the retina in diseases in which α7 nAChR expression is reduced, we used an α7 nAChR KO mouse to investigate potential changes in the retina. The α7 nAChR KO mouse was designed using 129/SvEv embryonic stem cells at Baylor College of Medicine (Orr-Urtreger et al., 1997). Jackson Laboratories backcrossed this mutation into the C57Bl/6J strain for eight generations. The C57Bl/6J mouse was used because it was one of the first strains to have its genome sequenced and is one of the most widely used strains. The gene for the α7 nAChR is located on the fifteenth chromosome, on the q arm in the thirteen to fourteen region. The α7 nAChR KO mouse has a deletion of the exons 8-10, which codes for the second, third and fourth transmembrane domains (M2, M3, and M4), the cytoplasmic loop, and the extracellular C-terminus (Figure 5). To confirm KO, deoxyribonucleic acid (DNA) from the tail was genotyped via the Jackson Laboratory protocol (Morley et al., 2004).

The α7 nAChR KO mice have been behaviorally characterized and show no difference from wildtype (WT) mice in spatial learning, conditioned fear response, prepulse inhibition, habituation to startle, exploration, and motor coordination (Paylor et al., 1998). The α7 nAChR KO mice have a mildly altered phenotype including slight impairments in sustained attention (Young et al., 2007) and working memory (Fernandes et al., 2006). Consistent with what would be expected with the loss of functional α7 nAChR, they also lack the neuroprotective effects of nicotine against glutamate neurotoxicity in the hippocampus (Egea et al., 2007) and display reduced nicotine dependence (Grabus et al., 2005) and reduced fertility (Morley & Rodriguez-Sierra,

2004). Overall, the α7 nAChR KO mouse does not display any motor dysfunctions or physiological abnormalities of the type associated with AD and schizophrenia, despite the link between α7 nAChRs and these disease states. While the visual responses of the α7 nAChR mouse have not been well-characterized, there has been one report of reduced visual acuity in the α7 nAChR KO mouse, but this study concluded that the low visual acuity was not due to a deficit present in the retina, thus, the mild phenotype extends to the retina (Origlia, et al., 2012). The question then is why are the phenotypical affects in the α7 nAChR KO mouse so modest, given the evidence that changes in α7 nAChR expression are involved in the deficits seen in AD and schizophrenia (Coyle et al., 1983; Uhlmann et al., 1991; Adler et al., 1992; Freedman et al., 1994; Cronin-Golomb, 1995; Cronin-Golomb et al., 1995; Kaskie & Storandt, 1995; Blanks et al., 1996; Freedman et al., 1997; Griffith et al., 1998; Nordberg & Svensson, 1998; Nordberg, 1999; Wevers et al., 1999; Freedman et al., 2000; Perry et al., 2000; Wang et al., 2000; Kihara et al., 2001; Xu et al., 2001; Ikonomovic et al., 2005; Leonard & Freedman, 2006; Oddo & LaFerla, 2006; Dziewczapolski et al., 2009; Brown et al., 2013; Ni et al., 2013). Identification of genes that are up-regulated in the retina of the α7 KO mouse could increase our understanding of the role of α7 nAChRs in the healthy and diseased retina and inform further studies in other parts of the brain.

Hypotheses and Specific Aims

Specific Aim I

Characterization of the distribution patterns of AChRs in the mouse retina will allow physiological predictions regarding visual processing mediated by AChR activation

and guide future physiological studies of retinal information processing in healthy and diseased retinas. Since α7 nAChRs may play an important role in normal retinal physiology and changes in expression in non-retina parts of the brain have been reported in association with disease states such as AD and schizophrenia, the current study aimed to begin to characterize the retinas of α7 nAChR KO mice. To understand changes in distribution resulting from the α7 nAChR KO, we must first understand the expression pattern in WT mice retinas. Identification of differences in AChR expression in the mouse compared to other well characterized mammals will also be useful in furthering our understanding in how visual processing in the mouse retina differs from, or is similar to, that of other mammalian visual systems. There is a particular need for increased understanding of visual processing and the retina in mice because of the widespread use of genetically engineered disease models being employed in mice. In order to accomplish this, Specific Aim I was proposed: to examine the expression patterns of nAChR and mAChRs in the retina of the WT C57BL/6J mouse. mRNA expression of nAChR subunits and mAChR subtypes was examined via reverse transcriptase polymerase chain reaction (RT-PCR), while the protein distribution pattern was examined via immunohistochemistry. This allowed us to determine exactly which nAChR subunits and mAChR subtypes are expressed and by what cell types. We predicted that in the mouse retina the distribution pattern of cholinergic amacrine cells and the AChRs would be similar to that already reported in the non-murine mammalian retina.

Specific Aim II

We hypothesized that the mild phenotype of the α7 nAChR KO mouse is due to the up-regulation of other genes that can partially compensate for the loss of α7 nAChRs. Consistent with our hypothesis, Yu et al. reported a slight, but statistically significant up-regulation of α3 and α4 in the brain of young α7 nAChR KO mice, but changes in the retina were not investigated. A limitation of KO studies in general is that the subunit of interest is lacking in the animal throughout development. Therefore, changes in expression of other genes may occur that compensate for the lack of the receptor of interest. Consequently, we proposed Specific Aim II, to determine if there is up- or down-regulation of nAChR subunits, mAChR subtypes or other receptors or channels that may have similar effects as α7 nAChRs, in the retinas of α7 nAChR KO mice. We hypothesized that in the retinas of α7 nAChR KO mice, there is up-regulation of other AChR subunits, particularly those with moderate to high calcium permeability since α7 nAChRs have high calcium permeability. Specifically, we predict that those nAChRs with high calcium permeability, such as α9, α9α10, α3β2α5 and α3β4α5 nAChRs, as well as excitatory mAChRs will be up-regulated (Gerzanich et al., 1998; Katz et al., 2000; Weisstaub et al., 2002; Fucile, 2004).

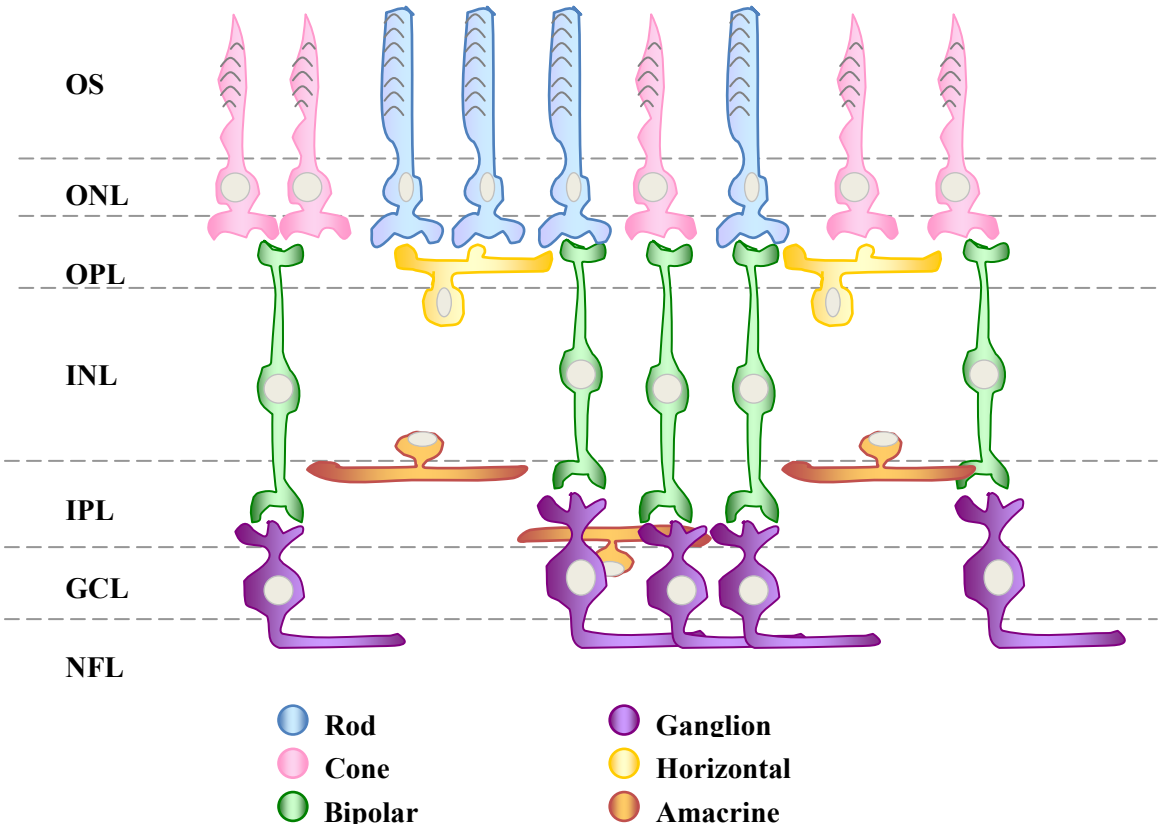

Figure 1. Cartoon depicting a simplified cross-sectional view of the retina and identifying the different cell classes and layers of the retina. Outer segments (OS), outer nuclear layer (ONL), outer plexiform layer (OPL), inner nuclear layer (INL), inner plexiform layer (IPL), ganglion cell layer (GCL), nerve fiber layer (NFL).

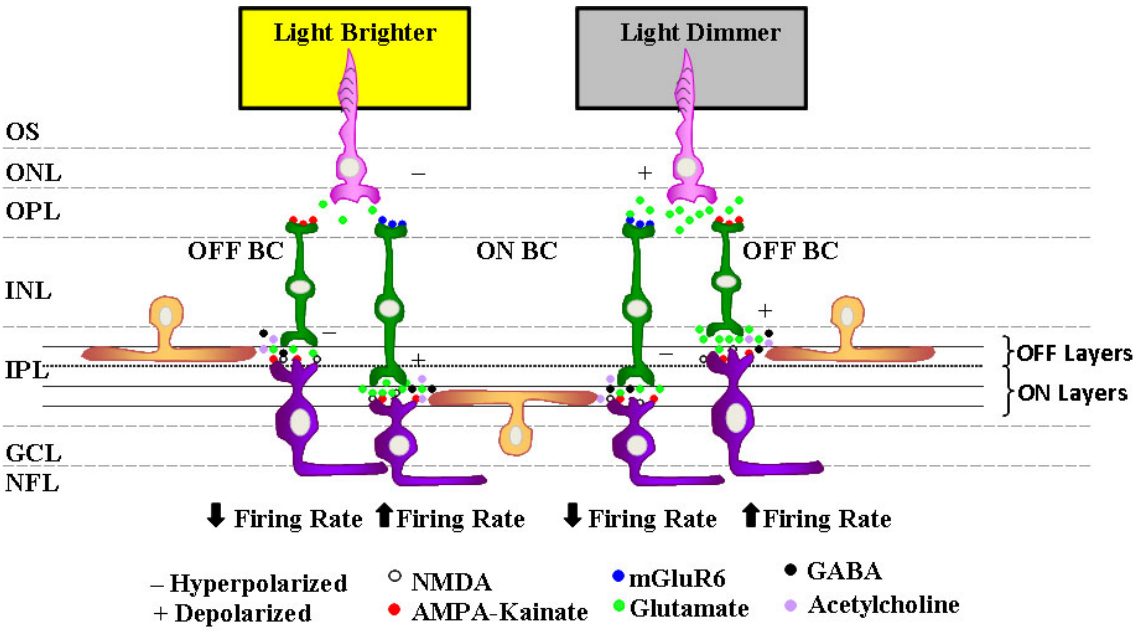

Figure 2. Cartoon depicting the electrochemical signaling of the vertical visual pathway, for both ON and OFF bipolar cells, under light or dark conditions.

Table 1. Glutamate Receptors on Retinal Neurons

Retinal Cell Type	AMPA/Kainate Receptors	NMDA Receptors	mGluR6 Receptors	References
OFF-bipolar cells	++			Slaughter & Miller, 1981; Slaughter & Miller, 1983; Euler et al., 1996; Sasaki & Kaneko, 1996.
ON-bipolar cells			++	Slaughter & Miller, 1981; Slaughter & Miller, 1983; Euler et al., 1996.
Ganglion cells	++	++		Aizenman et al., 1988; Massey & Miller, 1988; Massey & Miller, 1990; Cohen & Miller, 1994

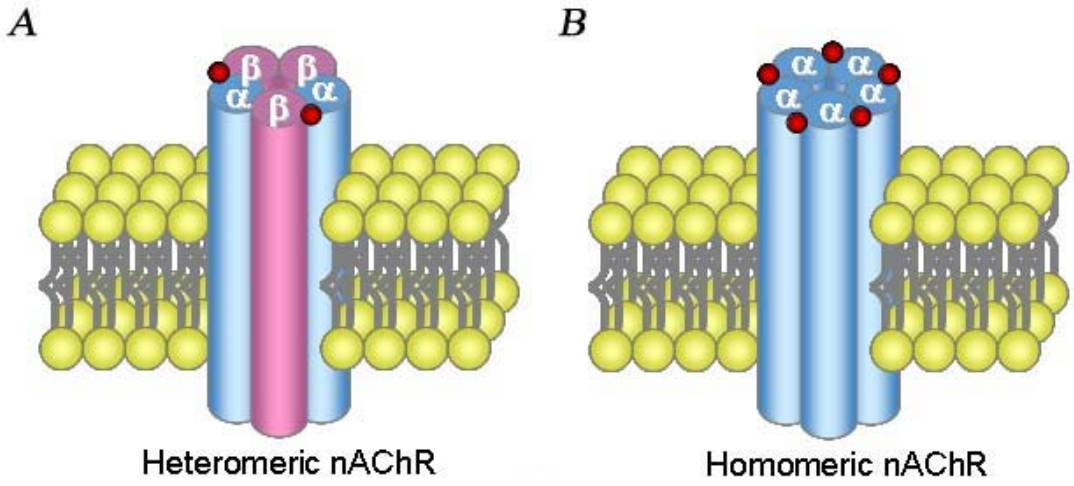

Figure 3. Cartoon representing the structure of nicotinic receptors. (A) Heteromeric nicotinic ACh receptors (nAChRs) and (B) homomeric nAChRs (McGehee, 1999; Lindstrom et al., 2000; Clementi, 2000; Dani, 2001; Khiroug et al., 2002).
● = ACh binding sites

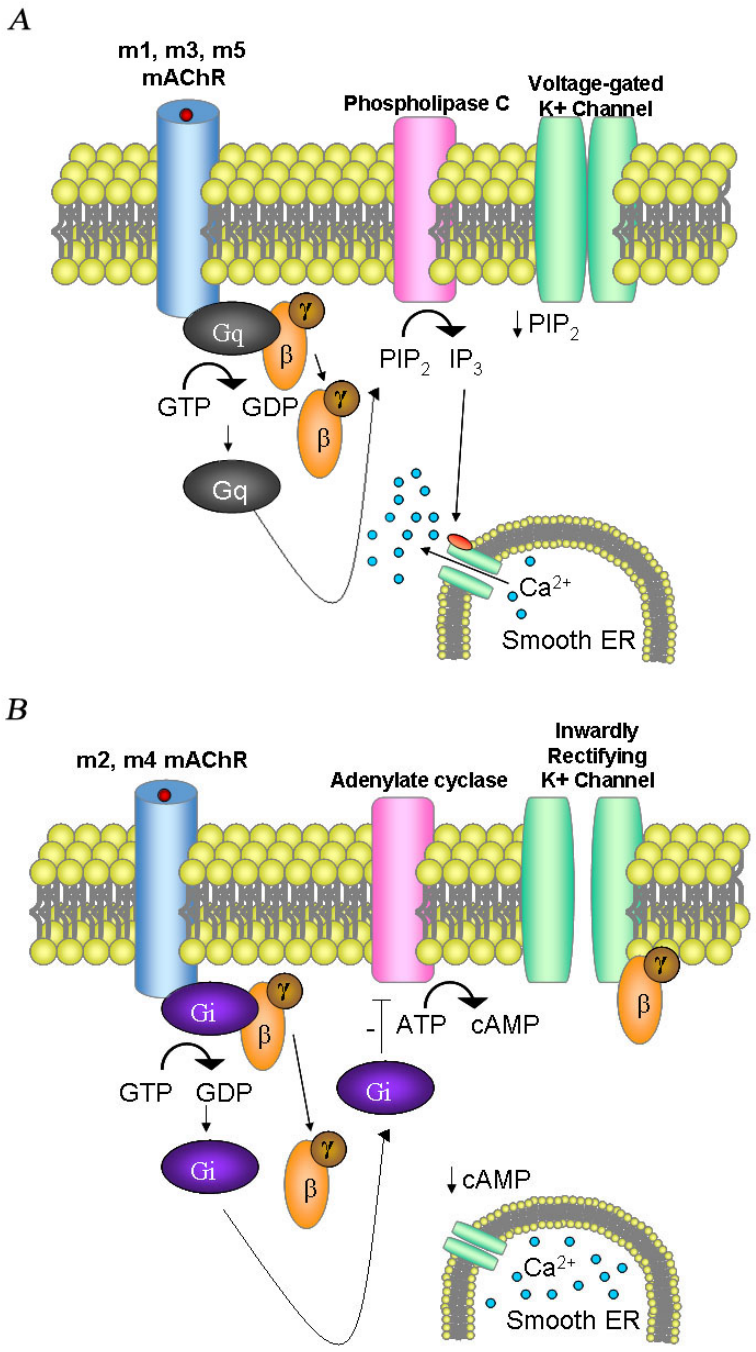

Figure 4. Cartoon representing the structure and signaling pathways of the muscarinic ACh receptors. (A) m1, m3, and m5 mAChRs and the (B) m2 and m4 mAChRs (Brown et al., 1997; Wess et al., 1997; Caulfield & Birdsall, 1998). ● = ACh binding site

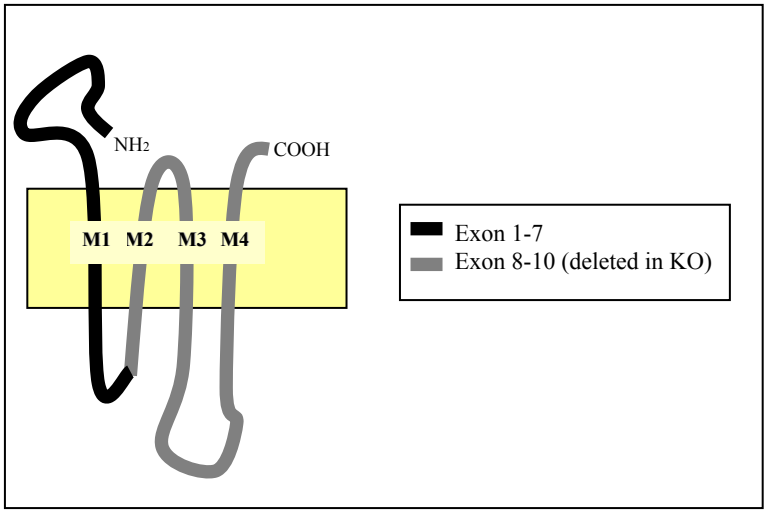

Figure 5. Cartoon of the structure of α7 nAChR subunits, depicting the areas deleted in the α7 nAChR KO mouse. Depicts the deletion of the exons 8-10 in the KO mouse, which codes for the second, third and fourth transmembrane domains (M2, M3, and M4), the cytoplasmic loop, and the extracellular C-terminus (Dajas-Bailador & Wonnacott, 2004; Jones & Wonnacott, 2005)

DISTRIBUTION OF ACETYLCHOLINE RECEPTORS IN THE MOUSE RETINA

by

M.L. SMITH, K.S. BRUCE, C.E. STRANG, B.J. MORLEY, K.T. KEYSER

In preparation for Visual Neuroscience

Format adapted for dissertation

Abstract

Acetylcholine (ACh) receptors (AChRs) are expressed throughout the mammalian nervous system including: retina, cochlea, thalamus, autonomic ganglia, hippocampus, striatum, and nucleus accumbens (Mihovilovic and Roses, 1991; Chini et al., 1992; Willoughby et al., 1993; Elliott et al., 1996). Neuronal nicotinic AChRs (nAChRs) are pentameric ligand-gated cation channels activated by ACh. Muscarinic AChRs (mAChRs) are G-protein coupled receptors which are also activated by ACh and are expressed throughout the nervous system (Caulfield & Birdsall, 1998). Immunohistochemical studies have shown AChR expression by ganglion, bipolar, amacrine, displaced amacrine, and horizontal cells in the rabbit retina (Keyser et al., 1988; Strang et al., 2010; Keyser et al., 2000; Strang et al., 2005; Dmitrieva et al., 2007). Despite their widespread expression in the nervous system, analysis of the expression patterns of nAChRs and mAChRs in the mouse retina has not been described.

The purpose of this study was to determine the presence of AChR ribonucleic acid (RNA) transcripts and protein expression in the mouse retina. Qualitative reverse-transcriptase polymerase chain reaction (RT-PCR) experiments confirmed the presence of α2-7, α9, α10, β2- β4 nAChR subunit and m1-m5 mAChR subtype mRNA transcripts.

Western blot experiments confirmed protein expression and the specificity of antibodies against α3-α5, and α9 nAChR subunits and m1-m5 mAChR subtypes in mouse retina. Immunohistochemical experiments using specific antibodies against nAChR subunits or mAChR subtypes indicated that AChR expression in the mouse retina is generally consistent with rabbit and monkey retina expression patterns in that AChRs are expressed by subsets of bipolar, amacrine, and ganglion cells (Dmitrieva et al., 2007; Liu

et al., 2009; Strang et al., 2010). In mouse retinas, a subset of bipolar cells appears to express a non-α7 nAChR subtype, whereas in the rabbit retinas a subset of cone bipolar cells express α7 nAChRs. (Dmitrieva et al., 2007). In addition, m1 mAChRs were not expressed by amacrine cells in the inner nuclear layer (INL), while m4 mAChRs were expressed by bipolar cells. These differences in expression patterns of AChRs suggest that physiological responses in the mouse retina differ from the responses observed in other mammals.

Introduction

The neurotransmitter ACh activates two classes of receptors: nicotinic and muscarinic. Neuronal nicotinic ACh receptors (nAChRs) are pentameric ligand-gated cation channels which have two or, in the case of α7 nAChRs, five agonist binding sites, and different receptors have differing permeabilities to calcium (Gerzanich et al., 1998; Berridge et al., 2000; Katz et al., 2000; Weisstaub et al., 2002; Fucile, 2004). They are members of the ligand-gated ion channel superfamily that includes glycine receptors, λ-aminobutyric acid A and C ($GABA_A$/$GABA_C$), and serotonin receptors (Karlin, 2002; Alexander et al., 2007). The nAChRs are comprised of the α2-α6, α10, and β2-β4 subunits, which can combine heteromerically, and the α7, α8 and α9 subunits, which can combine either into heteromers or homomers consisting of only α subunits (McGehee, 1999; Lindstrom, 2000; Clementi et al., 2000; Khiroug et al., 2002). Subunit composition determines the pharmacological and physiological properties of the channel, including the rate of desensitization, channel opening time, agonist and antagonist affinity, and conductance (Lindstrom et al., 1996; Arias, 2000).

Muscarinic AChRs (mAChRs) are metabotropic G-protein coupled receptors which are activated by ACh. The mAChRs include m1-m5 subtypes, each encoded by a specific gene which can be identified by affinity to agonists or antagonists as well as susceptibility to toxins. The mAChRs can be divided into two functional groupings based upon the G-protein that binds to the receptor and their associated intracellular signaling pathways (Caulfield & Birdsall, 1998). First, the m1, m3, and m5 subtypes typically couple with the Gq-α G-protein, which, upon ligand binding, activates the phosphatidyl inositol or phospholipase signaling pathways. Effects on downstream targets of these

pathways produce excitation through activation of cation channels, increased intracellular Ca^{2+} levels and inhibition of K^+ channels (Brown, et al., 1997). In contrast, the m2 and m4 subtypes typically couple with the Gi-α G-protein subunit which, upon ligand binding, inhibits adenylate cyclase (AC) and reduces cyclic adenosine monophosphate (cAMP) production. This reduction of cAMP affects downstream targets in the signaling cascade, resulting in inhibition through activation of K^+ channels (Wess, et al., 1997). Thus, mAChR activation can produce either excitatory effects (m1, m3, and m5) or inhibitory effects (m2 and m4).

Immunocytochemical studies have described nAChR subunit expression by bipolar, amacrine, displaced amacrine, and ganglion cells in the rabbit and rhesus monkey retina (Keyser et al., 1988; Britto et al., 1992; Keyser et al., 2000; Yamada et al., 2003; Dmitrieva et al., 2007; Liu et al., 2009). Neuronal nAChR expression correlates with functional responses in that activation of nAChRs has been shown to modulate the responses of ON, OFF, and directionally selective (DS) ganglion cells; including baseline firing rate, light responses, and preferred direction for ganglion cells with complex response properties (Masland & Ames, 1976; Ikeda & Sheardown, 1982; Masland et al., 1984; Baldridge, 1996; Reed et al., 2002; Reed et al., 2004; Strang et al., 2007).

In the rabbit retina, mAChRs are expressed by bipolar, amacrine, displaced amacrine, ganglion, and horizontal cells (Strang, et al., 2010). The mAChRs effect ganglion cell maintained firing rates and responses of DS ganglion cells (Kittila & Massey, 1997). There is also evidence that mAChRs play a role in the development of the retina and amacrine cell mosaic tiling (Zhou & Zhao, 2000; Syed et al., 2004; Stanke et al., 2008).

The increased use of mouse models in the study of the retina makes the analysis of the mouse retina essential. Much has been determined about the distribution and functions of GABA, glycine, and the distribution of their receptors in the mouse retina (Jeon et al., 1998; Haverkamp & Wassle, 2000; Heinze et al., 2007; Haverkamp et al., 2008; Wässle et al., 2009). Conversely, the distribution patterns of AChRs have not been described in the mouse retina. There are many AChR transgenic mouse models directed at studying the function and distribution of AChRs as well as studying diseases in which AChRs have been implicated, such as schizophrenia and Alzheimer's disease (AD; Kedmi et al., 2004; Morley et al., 1999; Egea et al., 2007; Yu et al., 2007). Schizophrenia and AD both include visual deficits at the level of the cortex and while the schizophrenic retina has not been described, a reduction in the number and density of ganglion cells has been described in AD retinas (Hinton et al., 1986; Sadun & Bassi, 1990; Freedman et al., 1994; Cronin-Golomb et al., 1995). Characterization of the pattern of AChR expression in the mouse retina would increase our understanding of the role of ACh in the mouse retina and help to guide functional studies of AChRs in normal and diseased retinas. This is the first study to describe the expression patterns of nAChRs and mAChRs in the mouse retina.

Methods

Animals

C57BL/6J mouse retinas and brains were provided by Dr. Barbara Morley at Boys Town National Research Hospital (BTNRH) and Dr Steve Pittler at the University of Alabama at Birmingham (UAB) from animals being used for unrelated studies. Albino

rabbit retinas were provided by Dr Kent Keyser at UAB, also from animals being used for unrelated studies. Animal care and surgical procedures were approved by the BTNRH and UAB Institutional Animal Care and Use Committee (IACUC).

Reverse Transcriptase Polymerase Chain Reaction (RT-PCR)

To determine presence of AChR ribonucleic acid (RNA) transcripts, reverse transcriptase polymerase chain reaction (RT-PCR) was performed using primers specific for each AChR subunit/subtype. After enucleation, retinas to be used for RT-PCR were dissected from the eyecup and flash frozen. Prior to RNA extraction, retinas were stored at -80°C. RNA was extracted from frozen retinas using the RNAqueous -4PCR Kit (Ambion; Austin, TX). The procedure included the following steps: homogenization of tissue in a lysis solution, application to a filter which selectively bound mRNA, washing to remove residual impurities, proteins, and other contaminants, and then elution with nuclease free water. The RNA then underwent a deoxyribonuclease (DNAse I) treatment, to remove any deoxyribonucleic acid (DNA) contamination, which involved incubation of DNAse I Buffer and DNAse I with the RNA followed by incubation with a DNAse inactivation reagent and centrifugation to pellet. RNA precipitation was performed on the supernatant resulting from the DNAse I treatment while the pellet was discarded. RNA precipitation involved the addition of 5M ammonium acetate, glycogen, and 100% ethanol to the RNA. Centrifugation (Eppendorf 5810R; Westbury, NY) was performed at maximum speed, cold rotor, for 10 minutes to pellet the RNA. The supernatant was removed and a 75% ethanol wash was performed, followed by another centrifugation. The RNA pellet was dried at 37°C and resuspended in nuclease-free water. The quality

and quantity of the RNA was assessed using the Nanodrop ND-1000 spectrophotometer (Thermo Scientific; Wilmington, DE).

AChR primers were designed using Beacon Designer (Table 1). Primers were optimized using RNA extracted from mouse whole brain tissue using the RNAqueous - 4PCR Kit. The best annealing temperature and primer concentration ratio, as determined by optimization, was used. RNA was converted to complementary DNA (cDNA) using an iScript cDNA synthesis kit (BioRad; Hercules, CA). RNA was added to a cDNA synthesis mix containing 5x iScript buffer, iScript reverse transcriptase (included an RNase inhibitor), and RNAse-free water. The cDNA synthesis mix was placed in the MyCycler Personal Thermocycler (BioRad; Hercules, CA) and incubated at 25°C for 5 minutes, at 45°C for 30 minutes, and 85°C for 5 minutes. For amplification, resulting cDNA was added to a PCR mix containing iQ SYBR green supermix (containing DNA polymerase and deoxyribonucleotide triphosphates), nuclease-free water, and primers. The cDNA/PCR mix was placed in the thermocycler (BioRad iQ5) and underwent an initial hot start at 95°C for 3 minutes followed by 40 cycles of 95°C for 10 seconds (denaturation), optimum annealing temperature for 30 seconds (annealing), and 72°C for 30 seconds (elongation). The resulting DNA transcripts were validated by electrophoresis on a 2.5% agarose gel. PCR products were purified using the Qiaquick PCR Purification kit (Qiagen; Valencia, CA) and then sequenced to confirm product identity (Heflin Center for Genomic Sciences; UAB; Birmingham, Al).

Western Blotting

Western blotting was performed to confirm the specificity of the AChR antibodies and to confirm that proteins corresponding to the RNA transcripts were expressed. Retinas to be used for western blotting were dissected from the eyecup, flash frozen, and stored at-80°C. In order to isolate the protein, retinas were homogenized in five volumes of lysis buffer that contained 1% NP-40, 0.5% sodium deoxycholate, 0.1% sodium dodecyl sulfate, and protease inhibitor cocktail. This mixture was incubated for 30 min at 4°C and then centrifuged (Eppendorf 5810R; Westbury, NY) at 15,000g for 20 minutes. The supernatant was extracted and then mixed with an equal volume of sample buffer that contained 1.0M tris-HCL, 25% glycerol, 10% SDS, 10% bromophenol blue, and 5% β-mercaptoethanol. The mixture was incubated at 95°C for 5 minutes. Protein concentrations were determined using the Nanodrop ND-1000 spectrophotometer (Thermo Scientific; Wilmington, DE) and then protein samples were stored at -80°C until use. Gel electrophoresis was used to separate protein into bands onto a 10% polyacrylamide gel. Electrophoresis was carried out for 1 hour at 200V with 10-20μg of protein. The proteins were then transferred to a nitrocellulose membrane. Membranes were either blocked overnight at 4°C followed by incubation with primary antibody (Table 2) for 1 hour at room temperature or membranes were blocked for 2 hours at room temperature and incubated in primary antibody overnight at 4°C. The blocking solution used in both protocols was 3% non-fat dry milk (Bio-Rad; Hercules, CA) containing 1% bovine serum albumin (BSA; FisherScientific; Pittsburgh, PA) in phosphate buffered saline (PBS) containing Tween. Then the membrane was incubated in secondary antibodies, conjugated to horseradish peroxidase, for 2 hours. Immunoreactive bands

were detected using colorimetric detection (Opti-4CN; Bio-Rad; Hercules, CA). In some cases the signal was amplified prior to detection using the Western Blot Amplification Module (Bio-Rad; Hercules, CA). All controls were performed in parallel with experimental conditions. To ensure primary antibody specificity, matched concentrations of protein immunoglobulin G (IgG), from the animal the primary antibody was made in, were used. To control for secondary antibody specificity, the primary antibody was omitted and membranes were incubated in blocking medium instead of primary antibody.

Immunohistochemistry

The same antibodies used for western blot were also used for immunohistochemistry (IHC), with two exceptions. First, the mAb210 antibody was used for IHC in place of its commercially available form, the Ab24719 antibody, which was used for western blot. Second, the mAb35 antibody was used for IHC in place of its commercially available form, the Ab24668 antibody. Neither mAb35 nor Ab24668 were used in western blot, as mAb35 was only used to confirm immunoreactivity patterns obtained with mAb210. Mouse and rabbit eyecups to be used for IHC were obtained by enucleation followed by hemisection. Eyecups were fixed by immersion in 1% paraformaldehyde (PFA) with 0.34% L-lysine and 0.05% sodium-m-periodate in 0.1M phosphate buffer or 4% PFA for 2 hours at room temperature. Eyecups were then cryoprotected by sequential immersion in 0.1M phosphate buffer with graded concentrations of sucrose (10%, 20%, and 30%) for 30 minutes each and then stored at 4°C. For cryosectioning, eyecups were embedded in a block of 50% optimum cutting temperature medium (Sakura Finetek, Torrance, CA) and 50% aquamount (VWR

Scientific; West Chester, PA), frozen, sectioned into 10-12µm vertical cryosections (Leica CM 3050), then mounted onto superfrost slides (VWR Scientific; West Chester, PA), and stored at -20°C.

Immediately prior to use, the sections were warmed for 45 minutes, washed in 3 changes of 0.1M PBS, and in some cases incubated in 0.8% β-mercaptoethanol in PBS/0.3% Triton for 1 hour at room temperature to improve tissue antigenicity, followed by three more washes. All sections were then incubated in 10% donkey normal serum (Jackson ImmunoResearch) for 1 hour at room temperature followed by incubation for 24 hours in primary antibody at 4°C (Table 2), washed again in three changes of 0.1M PBS, incubated with the secondary antibody, conjugated to a fluorescent dye, for 1 hour, washed again, cover slipped and stored at 4°C until imaging. Appropriate controls, including matched IgG protein concentrations and omission of primary antibody, were performed. All primary antibodies were obtained from Abcam (Cambridge, MA), Chemicon (Billerica, MA), Santa Cruz (Santa Cruz, CA) or generously provided by Dr. Jon Lindstrom. Secondary antibodies were raised in donkey and obtained from Jackson Immunoresearch Laboratories (West Grove, PA).

All IHC images were collected with a Leica TCS SP confocal laser scanning microscope. Brightness and contrast were adjusted using Adobe Photoshop (Adobe Systems; San Jose, CA). Brightness and contrast adjustments were applied identically for all images within a figure.

Results

RNA and Protein Expression

The goal of this study was to characterize the distribution of ACh receptors in the mouse retina. To determine which nAChR subunit and mAChR subtype mRNA transcripts were expressed in mouse retina, RNA extracted from whole retina was screened for the presence of AChR mRNA transcripts. Qualitative RT-PCR using primers specific for nAChR subunits and mAChR subtypes showed the presence of α2-α7, α9, α10, β2- β4, and m1-m5 AChR mRNA in mouse retina (Figure 1). Amplified AChR products, separated by elecrophoresis on 2.5% agarose gels, are shown. Products obtained were at the size expected for each target. RT-PCR products were sequenced and compared to Genbank entries for their respective mouse AChR entries; homology of sequences ranged from 81-99% (Table 1). No products were amplified in the no-template controls (data not shown).

In order to determine whether or not the presence of mRNA transcripts indicated expression of the corresponding proteins, and to ensure specificity of the antibodies used in immunohistochemistry experiments, Western blot analyses were performed. Protein used in Western blotting was extracted from whole mouse retina. The results of Western blot analyses with antibodies to mAChR subtypes and nAChR subunits resulted in single bands of the predicted size (Figure 2A, Table 2). Predicted sizes were obtained from the Universal Protein Resource (UniProt) protein sequence database. This indicated the presence of mAChR and nAChR protein and the single bands showed that each antibody was specific for the expected protein. Specifically, AB5590, an antibody specific to amino acids 568-588 of the rat nAChR α4 protein, displayed a band at the expected 70kD

size. AB24719, an antibody specific to the main immunogenic region on the extracellular surface of human muscle α1 nAChR as well as the α3 and α5 neuronal nAChR subunit proteins, displayed a band at the expected 51kD size. AB49065, an antibody specific for the N-terminal region of the human α9 nAChR protein, displayed a band at the expected 53kD size, but no bands with protein from an α9 nAChR KO mouse retina. AB5164, an antibody specific to amino acids 227-353 of the human m1 mAChR protein, displayed a band at the expected 60kD size. mAB367, an antibody specific to amino acids 225-359 of the human m2 mAChR protein, displayed a band at the expected 52kD size. AS-3741S, an antibody specific to the amino acids 580-589 of the human m3 mAChR protein, displayed a band at the expected 75kD size. mAB1578, an antibody specific to the i3 intracellular loop of the human m4 mAChR protein, displayed a band at the expected 53kD size. Finally, AB9454, an antibody specific to the 3rd cytoplasmic domain of the human m5 mAChR protein, displayed a band at the expected 70kD size. m5 mAChR western blot experiments used protein extracted only from the brain as the antibody was discontinued prior to probing with retinal extracts. These results indicated the presence of α3-α5 and α9 nAChR as well as m1-m5 mAChR proteins in mouse retina. AB24719, the commercially available form of the mAb210 antibody (Keefe et al., 2009), was used in western blotting experiments, while mAb210 was used in immunohistochemistry experiments. mAb35 was used in immunohistochemistry simply to confirm the results of mAb210 immunohistochemistry experiments and was not included in the Western blotting experiments. Primary antibody omission and IgG controls yielded no bands (Figure 2B). Only antibodies that yielded a single band on western blot, with no bands on control membranes, were used in immunohistochemistry studies.

AChR Expression Patterns

In order to assess the distribution of AChRs, indirect immunohistochemistry was performed. Antibodies against specific nAChR subunits yielded labeling in ganglion cells, amacrine cells, bipolar cells, and in dendrites throughout the inner plexiform layer (IPL). In the mouse retina incubation with mAb210, an antibody that is specific for α3 and α5 nAChRs in retina (Lindstrom, 1996; Keyser et al., 2000), resulted in labeling of neurons throughout the inner nuclear layer (INL) and the ganglion cell layer (GCL); including presumptive amacrine cells, bipolar cells, and ganglion cells (Figure 3). Immunoreactivity to mAb210 was also observed in two broad bands of dendrites spanning much of the IPL. At the level of the outer plexiform layer (OPL), there was mAb210 immunoreactivity (Figure 4, Figure 5A). In contrast, the rabbit retina, amacrine and ganglion cells displayed mAb210 immunoreactivity consistent with previous publications (Keyser et al., 2000). Additionally, in the rabbit retina there was immunoreactivity across the IPL with two brighter bands. Finally, the OPL of rabbit retina had no mAb210 immunoreactivity. Regardless of species, mAb210 immunoreactivity outlined the cell bodies, indicating the presence of α3 and α5 nAChRs synthesized in the endoplasmic reticulum and not yet transported to the synapse. In order to confirm these differences in mAb210 labeling in mouse as compared to rabbit, another antibody specific for α3 and α5 nAChRs, mAb35, was used. Incubation with mAb35 showed patterns of immunoreactivity in the mouse retina similar to that observed with mAb210. Specifically, presumptive bipolar, amacrine, and ganglion cells as well as in two diffuse bands in the IPL displayed labeling (Figure 4). Dendrites immunoreactive for mAb210 and mAb35 were evident throughout much of the IPL, suggesting that α3 and

α5 nAChRs are expressed by both ON and OFF ganglion, bipolar, and amacrine cells. Both mAb210 and mAb35 also recognize the main immunogenic region on the extracellular surface of the muscle α1 nAChR, but α1 subunit is not thought to be present in neuronal tissue (Lindstrom, 1996).

Incubation with AB5590, an antibody specific for α4 nAChRs, also displayed patterns of immunoreactivity similar to that seen with mAb210 and mAb35 with immunoreactivity observed in presumptive bipolar, amacrine and ganglion cells as well as in two broad diffuse bands in the IPL (Figure 5A). Additionally, there was AB5590 immunoreactivity in the OPL. As with mAb 210 and mAb35, dendrites in the IPL displayed immunoreactivity throughout much of the IPL, suggesting that α4 nAChRs are expressed by both ON and OFF bipolar, amacrine, and ganglion cells. Incubation with AB49065, an antibody specific for α9 nAChRs, showed immunoreactivity by a broad variety of cell types including, amacrine, bipolar, and ganglion cells as well as throughout the IPL (Figure 5B). However, α9 nAChR immunoreactivity within the IPL differed from other nAChR subunit immunoreactivity. Instead of two broad, diffuse bands in the IPL with evenly distributed immunoreactive processes, α9 nAChRs immunoreactivity in the IPL was densest in a single, broad band in the center at approximately the same level as the dim area in the center of mAb 210 immunoreactivity.

Antibodies specific for just α2, α3, α6 or α10 nAChRs were also tested (not shown), but yielded uninterpretable or irreproducible immunoreactivity patterns and/pr had multiple bands on westerns indicating lack of specificity and so were excluded from this study. Furthermore, consistent with previous reports (Herber et al., 2004) we have observed (data not shown) that commercially available antibodies against α7 nAChRs

yielded labeling patterns in α7 nAChR knockout (KO) retinas similar to those seen in wildtype (WT) retinas or yielded no labeling at all; therefore, α7 nAChR antibodies were not used in this study.

Experiments using antibodies against mAChR subtypes showed immunoreactivity in ganglion cells, amacrine cells, bipolar cells, and throughout the IPL (Figure 6). Antibodies against m1 mAChRs labeled neurons throughout the GCL and two narrow bands of immunoreactive processes, at sublamina 2 and sublamina 4, as well as diffuse background labeling throughout the IPL. Antibodies against m2 mAChRs revealed immunoreactivity in large cell bodies in the GCL, presumably ganglion cells, as well as presumptive amacrine and bipolar cells in the INL. As was seen with m1 mAChR antibodies, antibodies against m2 mAChRs showed two narrow bands of immunoreactive processes in the IPL at sublamina 2 and sublamina 4. In addition, diffuse background labeling throughout the IPL was observed. However, the two bands in the IPL were more intense following incubation with antibodies against m2 mAChRs than with m1 mAChR antibodies. Finally, antibodies against m3, m4, and m5 mAChRs all produced similar patterns of immunoreactivity; presumptive ganglion cells, amacrine cells, and bipolar cells as well as labeling throughout the IPL. However, immunoreactivity for m4 and m5 mAChRs was more intense in the inner IPL, suggesting a higher amount of m4 and m5 mAChRs localized on ON bipolar, amacrine, and ganglion cell processes. Finally, m2 and m3 mAChR immunoreactivity had more defined bipolar cell processes. This is the first report of mAChR expression patterns in the mouse retina. For all antibodies, concentration matched IgG controls displayed weak, non-specific labeling that did not

resemble the experimental immunoreactivity patterns (data not shown). Omission of primary antibody resulted in no labeling.

Discussion

In this study we examined AChR expression in mouse retina in order to understand the specific expression patterns and compare these patterns to those already reported in the retina of other species. AChRs are widely expressed and play many functional roles in the retina of other mammals, particularly in modulating the responses of ganglion cells (Masland & Ames, 1976; Masland et al., 1984; Baldridge, 1996; Alkondon et al., 1998; Reed et al., 2002; Reed et al., 2004; Strang et al., 2007). The widespread expression of AChRs, their functional importance in visual processing, and the widespread use of genetic models makes it important to examine the expression of AChRs in mouse retina in order to further understand the role of AChRs in visual processing in the mouse.

To begin with, it was necessary to determine which AChR subtypes were expressed in the mouse retina. RT-PCR data indicated that mRNA transcripts for all and mAChR subtypes and all nAChR subunits were present in the mouse retina, with the exception of α1 and α8 nAChR subunits. α1 nAChR subunits are not expressed in neuronal tissues while α8 nAChR subunits have not been observed in mammalian systems. Western blot analyses confirmed the protein expression as well as specifity of the AChR antibodies used in this study. This is the first study demonstrating α9 nAChR protein expression in mammalian retina.

Immunohistochemical analysis using antibodies against AChRs resulted in immunoreactivity by amacrine cells, bipolar cells, ganglion cells and in processes throughout the IPL in C57BL/6J WT mice. Immunoreactivity to mAb210 antibody (α3 and α5 nAChR) was observed in amacrine cells, bipolar cells, ganglion cells, and in processes throughout the IPL. However, consistent with previous reports in mammalian retina, mAb210 immunoreactivity was only observed by presumptive amacrine and ganglion cell types in the rabbit retina. Unlike mouse, in which mAb210 immunoreactivity was detected in bipolar cells, in rabbit retina bipolar cells have not been reported to be mAb210 immunoreactive (Keyser et al., 2000). Further, mAb210 immunoreactivity in the rabbit was detectable in two bright, narrow bands in addition to diffuse labeling throughout much of the IPL while in the mouse two broad bands were present. In order to confirm the presence of non-α7 nAChRs on bipolar cells in the mouse retina, another antibody, mAb35, specific for α1, α3, and α5 nAChRs was used. The mAb 35 neuronal immunoreactivity was similar to that of mAb210 with the addition of bipolar cells. Additionally, AB5590, which recognizes α4 nAChR subunits, displayed similar patterns of labeling in the mouse retina and, like mAb210 and mAb35, revealed α4 nAChR subunit expression by bipolar cells. In brain, α4 containing nAChRs are the most abundant nAChR subunit. While the distribution pattern of the α4 nAChR subunit has not been determined in rabbit retina, previous reports in pig and rhesus monkey showed α4 nAChR labeling predominately in ganglion cells (Court et al., 1994; Aubert et al., 1996; Thompson et al., 2006; Liu et al., 2009). To summarize, α3, α4, and α5 immunoreactivity was observed in bipolar cells in the mouse retina, while α7 nAChRs are present on bipolar cells in the rabbit retina. The α7 nAChR response to high concentrations of

agonist is transient with fast desensitization, while the response of non-α7 nAChRs results in less rapid desensitization (Papke et al., 1996; Papke et al., 2000). This suggests that ganglion cell light responses that are mediated by cholinoceptive bipolar cells may be more sustained, due to enhanced glutamate release, in the mouse than the rabbit. Future studies will include examination of physiological light responses in the mouse retina, particularly that of the bipolar cells.

This study is the first to show α9 or α10 nAChR mRNA expression in the mammalian retina. Additionally, AB49065, an antibody specific for α9 nAChRs, resulted in immunoreactivity within the retina, indicating that α9 nAChR protein is present within the retina. Specificity of AB49065 was confirmed with western blot and, when protein extracted from a α9 nAChR KO mouse was used, incubation with AB49065 did not result in a band (Figure 2). α9 nAChRs have a distinct pharmacological profile which differs from that of the other AChRs. The narrow brighter bands in the center of the IPL may be at the level of the dimmer region of mAb 210 immunoreactivity, indicating that cells that stratify in the middle of the IPL express α9 nAChRs more densely than α3 and α5 nAChRs

In general, nAChRs are activated by nicotine but blocked by curare, while mAChRs are activated by muscarine but blocked by atropine (Taylor, 1990). AChRs also have varying permeabilities to Ca^{2+}, with the α7 nAChRs having the highest permeability (Fucile, 2004). Additionally, α7 nAChRs are blocked by low micromolar concentrations of strychnine as well as by α-bungarotoxin (Renna et al., 2007). However, α9 nAChRs have a different pharmacological profile; instead, α9 nAChRs are activated by ACh and choline, but not nicotine, blocked by α-bungarotoxin (α-BGT) and strychnine and have

high Ca^{2+} permeability (Housley & Ashmore, 1991; Fuchs & Murrow, 1992; Elgoyhen et al., 1994; Erostegui et al., 1994; Johnson et al., 1995; Dulon & Lenoir, 1996; Evans, 1996; Rothlin et al., 1999; Katz et al., 2000). The expression of α9 nAChRs in the retina may have a significant effect on the response properties of the retina due to the mixed nicotinic-muscarinic pharmacological profile of the α9 nAChRs. Thus, experiments using nicotine to probe for AChR expression would miss α9 nAChRs. So to determine whether α9 nAChRs are expressed in other mammalian retina, choline in concert with MLA and nicotine would need to be used. The presence of α9 nAChRs could also effect conclusions of previous studies using α-BGT to block α7 nAChRs in the retina, as this would have also been blocking α9 nAChRs.

AB5164 antibody (m1 mAChR) immunoreactivity was observed in ganglion cells and in two bands in the IPL, with no immunoreactivity in somata in the INL. Yet, in the rabbit retina both horizontal and amacrine cells showed immunoreactivity following incubation with the AB5164 antibody. This indicates a possible reduction in excitatory mAChR inputs in the IPL of the mouse retina as compared to the rabbit retina. However, the AS3741S antibody (m3 mAChRs) and the AB9454 antibody (m5 mAChRs) immunoreactivity were observed in ganglion cells, amacrine cells, bipolar cells and throughout the IPL. Thus, excitatory mAChR subtypes are present in the mouse INL; there just appear to be fewer m1 mAChR containing cells in the INL of the mouse. An additional difference in the distribution of excitatory mAChR subtypes in the mouse retina is the lack of m1 and m3 mAChR expression by horizontal cells. Finally, in the rabbit retina m3 mAChR immunoreactivity was seen in two narrow bands in the IPL, while in the mouse retina there is immunoreactivity throughout the IPL. This indicates

different specialization, within the ON and OFF pathways, of mAChR in the mouse retina than is seen in rabbit retina (Strang et al., 2010).

Differences between mouse and other mammals were also seen in the distribution of m2 and m4 mAChRs, which typically have inhibitory actions. In the mouse the mAB367 antibody (m2 mAChR) immunoreactivity was observed in ganglion cells, bipolar cells, and amacrine cells as well as in two narrow, intense bands in the IPL. However, in the rabbit retina IPL immunoreactivity was intense in the central IPL and weaker in sublamina 1 and 5 (Strang et al., 2010). This could indicate a difference in the subtypes of cells expressing m2 mAChRs. Immunoreactivity for mAb1578 (m4 mAChRs) was observed in ganglion, bipolar, and amacrine cells and throughout the IPL in the mouse retina. Yet, in the rabbit retina, m4 mAChRs were not detected in bipolar cells (Strang et al., 2010). This may indicate an increase in m4 mAChR- mediated inhibition in the mouse retina, as compared to the rabbit retina. These data suggest that there may be a decrease in mAChR-mediated excitation and an increase in mAChR-mediated inhibition.

We observed many differences in the types of AChRs expressed by bipolar cells in the mouse. Thus, determination of the types of bipolar cells expressing AChRs could be beneficial in furthering our understanding of visual processing in the mouse. This understanding is crucial in establishing a baseline by which to measure differences in mouse models of disease states, particularly those with visual dysfunction.

References

Arias, H.R. (2000). Localization of agonist and competitive antagonist binding sites on nicotinic acetylcholine receptors. Neurochemistry International, 36, 595-645.

Alexander, S.P., Mathie, A. & Peters, J.A. (2007). Guide to Receptors and Channels, 2nd edition (2007 Revision). British Journal of Pharmacology, 150, 1-168.

Alkondon, M., Pereira, E.F. & Albuquerque, E.X. (1998). α-bungarotoxin- and methyllycaconitine-sensitive nicotinic receptors mediate fast synaptic transmission in interneurons of rat hippocampal slices. Brain Research, 810, 257-263.

Aubert, I., Cecyre, D., Gauthier, S. & Quirion, R. (1996). Comparative otogenetic profile of cholinergic markers including nicotinic and muscarinic receptors in the rat brain. Journal of Comparative Neurology, 369, 34-55.

Baldridge, W.H. (1996). Optical recordings of the effects of cholinergic ligands on neurons in the ganglion cells layer of mammalian retina. Journal of Neuroscience, 16, 5060-5072.

Berridge, M.J., Lipp, P. & Bootman, M.D. (2000). The versatility and universality of calcium signaling. Nature Reviews Molecular Cell Biology, 1, 11-21.

Britto, L.R., Hamassaki-Britto, D.E., Ferro, E.S., Keyser, K.T., Karten, H.J. & Lindstrom, J.M. (1992). Neurons of the chick brain and retina expressing both α-bungarotoxin-sensitive and α-bungarotoxin-insensitive nicotinic acetylcholine receptors: an immunohistochemical analysis. Brain Research, 590, 193-200.

Brown, D.A., Abogadie, F.C., Allen, T.G., Buckley, N.J., Caulfield, M.P., Delmas, P., Haley, J.E., Lamas, J.A. & Selvanko, A.A. (1997). Muscarinic mechanisms in nerve cells. Life Sciences, 60, 1137-1144.

Caulfield, M.P. & Birdsall, N.J. (1998). International Union of Pharmacology. XVII. Classification of muscarinic acetylcholine receptors. Pharmacological Review, 50, 279-290.

Chini, B., Clementi, F., Hukovic, N. & Sher, E. (1992). Neuronal-type alpha-bungarotoxin receptors and the alpha 5-nicotinic receptor subunit gene are expressed in neuronal and non-neuronal cell lines. Proceedings of the National Academy of Sciences, 89, 1572-1576.

Clementi, F., Fornasari, D. & Gotti, C. (2000). Neuronal nicotinic acetylcholine receptors: from structure to therapeutics. Trends in Pharmacological Sciences, 21, 35-37.

Court, J.A., Lloyd, S., Johnson, M., Griffifths, M., Birdsall, N.J., Piggorr, M.A., Oakley, A.E., Ince, P.G., Perry, E.K. & Perry, R.H. (1997). Nicotinic and muscarinic

cholinergic receptor binding in the human hippocampal formation during development and aging. Development Brain Research, 101, 93-105.

Cronin-Golomb, A., Corkin, S. & Growdon, J.H. (1995). Visual dysfunction predicts cognitive deficits in Alzheimer's disease. Optometry & Vision Science, 72, 168-176.

Dmitrieva, N.A., Strang, C.E. & Keyser, K.T. (2007). Expression of α7 nicotinic acetylcholine receptors by bipolar, amacrine, and ganglion cells of the rabbit retina. Journal of Histochemical Cytochemistry, 55, 461-476.

Dulon, D., Lenoir, M. (1996). Cholinergic responses in developing outer hair cells of the rat cochlea. European Journal of Neuroscience, 8, 1945-1952.

Egea, J., Rosa, A.O., Sobrado, M., Gandia, L., Lopez, M.G. & Garcia, A.G. (2007). Neuroprotection afforded by nicotine against oxygen and glucose deprivation in hippocampal slices is lost in α7 nicotinic receptor knockout mice. Neuroscience, 145, 866-872.

Elgoyhen, A.B., Johnson, D.S., Boulter, J., Veter, D.E. & Heinemann, S. (1994) A9; an acetylcholine receptor with novel pharmacological properties expressed in rat cochlear hair cells. Cell, 79, 705-715.

Elliott, K.J., Ellis, S.B., Berckhan, K.J., Urrutia, A., Chavez-Noriega, L.E., Johnson, E.C., Velicelebi, G. & Harpold, M.M. (1996). Comparative structure of human neuronal alpha 2-alpha 7 and beta 2-beta 4 nicotinic acetylcholine receptor subunits and functional expression of the alpha2, alpha3, alpha4, alpha7, beta 2, and beta 4 subunits. Journal of Molecular Neuroscience, 7, 217-228.

Erostegui, C., Norris, C.H., Bobbin, R.P. (1994). In vitro characterization of a cholinegic receptor on outer hair cells. Hearing Research, 74, 135-147.

Evans, M. (1996). Acetylcholine activates two currents in guinea-pig outer hair cells. Journal of Physiology, 491, 563-578.

Freedman, R., Adler, L.E., Bickford, P., Byerley, W., Coon, H., Cullum, C.M., Griffith, J.M., Harris, J.G., Leonard, S. & Miller, . (1994). Schizophrenia and nicotinic receptors. Harvard Review Psychiatry, 2, 179-192.

Fuchs, P.A. & Murrow, B.W. (1992). A novel cholinergic receptor mediates inhibition of chick cochlear hair cells. Proceedings: Biological Sciences, 248, 35-40.

Fucile S. (2004). Ca2+ permeability of nicotinic acetylcholine receptors. Cell Calcium, 35, 1-8.

Gerzanich, V., Wang, F., Kuryatov, A. & Lindstrom, J. (1998). α5 subunit alters desensitization, pharmacology, Ca^{++} permeability and Ca^{++} modulation of human

neuronal α3 nicotinic receptors. The Journal of Pharmacology and Experimental Therapeutics, 286, 311-320.

Haverkamp, S. & Wassle, H. (2000). Immunocytochemical analysis of the mouse retina. The Journal of Comparative Neurology, 424, 1-23.

Haverkamp, S., Specht, D., Majumdar, S., Zaidi, N.F., Brandstatter, J.H., Wasco, W., Wassle, H. & Tom Dieck S. (2008). Type 4 OFF cone bipolar cells of the mouse retina express calsenilin and contact cones as well as rods. Journal of Comparative Neurology, 507, 1087-1101.

Heinze, L., Harvey, R.J., Haverkamp, S. & Wassle, H. (2007). Diversity of glycine receptors in the mouse retina: localization of the alpha4 subunit. Journal of Comparative Neurology, 500, 693-707.

Herber, D.L., Severance, E.G., Cuevas, J., Morgan, D. & Gordon, M.N. (2004). Biochemical and histochemical evidence of nonspecific binding of alpha7 nAChR antibodies to mouse brain tissue. Journal of Histochemistry & Cytochemistry, 52, 1367-1375.

Hinton, D.R., Sadun, A.A., Blanks, J.C. & Miller, C.A. (1986). Optic-nerve degeneration in Alzheimer's disease. New England Journal of Medicine, 315, 485-487.

Housley, G.D., Ashmore, J.F. (1991). Direct measurement of the action of acetylcholine on isolated outer hair cells of the guinea pig cochlea. Proceedings of the Royal Society London B, 244, 161-167.

Ikeda, H. & Sheardown, M.J. (1982) Acetylcholine may be an excitatory transmitter mediating visual excitation of "transient" cells with the periphery effect in the cat retina: iontophoretic studies in vivo. Neuroscience, 7, 1299-1308.

Jeon, C.J., Strettoi, E. & Masland, R.H. (1998). The major cell populations of the mouse retina. Journal of Neuroscience, 18, 8936-8946.

Johnson, D., Martinez, J., Elgoyhen, A., Heinemann, S., McIntosh, J. (1995). α-Conotoxin Im1 exhibits subtype-specific nicotinic acetylcholine receptor blockade: preferential inhibition of homomeric α7 and α9 receptors. Molecular Pharmacology, 48, 194-199.

Karlin, A. (2002). Emerging structure of the nicotinic acetylcholine receptors. National Review of Neuroscience, 3, 102-114.

Katz, E., Verbitsky, M., Rothlin, C.V., Vetter, D.E., Heinemann, S.F. & Elgoyhen, A.B. (2000). High calcium permeability and calcium block of the alpha9 nicotinic acetylcholine receptor. Hearing Research, 141, 117-128.

Kedmi,M., Beaudet,A.L. & Orr-Urtreger,A. (2004). Mice lacking neuronal nicotinic acetylcholine receptor β4-subunit and mice lacking both α5- and β4-subunits are

highly resistant to nicotine-induced seizures. Physiological Genomics, 17, 221-229.

Keefe, D., Hess, D., Bosco, J., Tzartos, S., Powell, J., Lamsa, J. & Josiah, S. (2009). A rapid, fluorescence-based assay for detecting antigenic modulation of the acetylcholine receptor on human cell lines. Cytometry Part B: Clinical Cytometry, 76, 206-212.

Keyser, K.T., Hughes, T.E., Whiting, P.J., Lindstrom, J.M. & Karten, H.J. (1988). Cholinoceptive neurons in the retina of the chick: an immunohistochemical study of the nicotinic acetylcholine receptors. Visual Neuroscience, 269, 109-117.

Keyser, K.T., MacNeil, M.A., Dmitrieva, N., Wang, F., Masland, R.H. & Lindstrom, J.M. (2000). Amacrine, ganglion, and displaced amacrine cells in the rabbit retina express nicotinic acetylcholine receptors. Visual Neuroscience, 17, 743-752.

Khiroug, S.S., Harkness, P.C., Lamb, P.W., Sudweeks, S.N., Khiroug, L., Millar, N.S. & Yakel, J.L. (2002). Rat nicotinic ACh receptor α7 and β2 subunits co-assemble to form functional heteromeric nicotinic receptor channels. Journal of Physiology, 540, 425-434.

Kittila, C.A. & Massey, S.C. (1997). Pharmacology of directionally selective ganglion cells in the rabbit retina. Journal of Neurophysiology, 77, 675-689.

Lindstrom, J., Anand, R., Gerzanich, V., Peng, X., Wang, F. & Wells, G. (1996). Structure and function of neuronal nicotinic acetylcholine receptors. Progress in Brain Research, 109, 125-137.

Lindstrom, J.M. (2000). The structures of neuronal nicotinic receptors. In Handbook of Experimental Pharmacology, Vol 144, ed. Clementi, F., Fornasari, D. & Gotti, C., pp. 101-162. Berlin Heidelburg: Springer-Verlag.

Liu, J., McGlinn, A.M., Fernandes, A.I., Milam, A.H., Strang, C.E., Andison, M.E., Lindstrom, J.M., Keyser, K.T. & Stone, R.A. (2009). Nicotinic acetylcholine receptor subunits in rhesus monkey retina. Investigative Ophthalmology and Vision Sciences, 50, 1408-1415.

Masland, R.H & Ames, A. (1976). Responses to acetylcholine of ganglion cells in an isolated mammalian retina. Journal of Neurophysiology, 39, 1220-1235.

Masland, R.H., Mills, J.W. & Cassidy, C. (1984). The functions of acetylcholine in the rabbit retina. Proceedings of the Royal Society B: Biological Sciences, 223, 121-139.

McGehee, D.S. (1999). Molecular diversity of neuronal nicotinic acetylcholine receptors. Annals of the New York Academy of Sciences, 868, 565-577.

Mihovilovic, M. & Roses, A.D. (1991). Expression of mRNAs in human thymus coding for the alpha 3 subunit of neuronal acetylcholine receptor. Experimental Neurology, 111, 175-180.

Morley, B.J. & Rodriguez-Sierra, J.F. (2004). A phenotype for the α7 nicotinic acetylcholine receptor null mutant. Brain Research, 1023, 41-47.

Morley, B., Li, H., Hiel, H., Drescher, D. & Elgoyhen, A. (1998) Identification of the subunits of the nicotinic cholinergic receptors in the rat cochlea using RT-PCR and in situ hybridization. Molecular Brain Research, 53, 78-87.

Papke, R.L., Bencherif. M. & Lippiello, P. (1996). An evaluation of neuronal nicotinic acetylcholine receptor activation by quaternary nitrogen compounds indicates that choline is selective for the α7 subtype. Neuroscience Letters, 213, 201-204.

Papke, R.L., Meyer, E. & Uteshev, V.V. (2000). α7 Receptor-selective agonists and modes of α7 receptor activation. European Journal of Pharmacology, 393, 179-195.

Plazas, P.V., Katz, E., Gomez-Casati, M.E., Bouzat, C. & Elgoyhen, A.B. (2005). Stoichiometry of the alpha9alpha10 nicotinic cholinergic receptor. Journal of Neuroscience, 25, 10905-10912.

Reed, B.T., Amthor, F.R. & Keyser, K.T. (2002). Rabbit retinal ganglion cell responses mediated by alpha-bungarotoxin-sensitive nicotinic acetylcholine receptors. Visual Neuroscience, 19, 427-438.

Reed, B.T., Amthor, F.R. & Keyser, K.T. (2004). MLA-sensitive cholinergic receptors involved in the detection of complex moving stimuli in retina. Visual Neuroscience, 21, 861-872.

Renna, J.M., Strang, C.E., Amthor, F.R. & Keyser, K.T. (2007). Strychnine, but not PMBA, inhibits neuronal nicotinic acetylcholine receptors expressed by rabbit retinal ganglion cells. Visual Neuroscience, 24, 503-511.

Rothlin, C., Verbitsky, M., Katz, E., Elgoyhen, A.B. (1999). The α9 nicotinic acetylcholine receptor shares pharmacological properties with type A γ-aminobutyric acid, glycine and type 3 serotonin receptors. Molecular Pharmacology, 55, 248-254.

Sadun, A.A. & Bassi, C.J. (1990). The visual system in Alzheimer's disease. Research Publications - Association for Research in Nervous and Mental Disease, 67, 331-347.

Stanke, J.J., Lehman, B. & Fischer, A.J. (2008). Muscarinic signaling influences the patterning and phenotype of cholinergic amacrine cells in the developing chick retina. BMC Developmental Biology, 8, 13.

Strang, C.E., Andison, M.E., Amthor, F.R. & Keyser, K.T. (2005). Rabbit retinal ganglion cells express functional α7 nAChRs. American Journal of Physiology-Cell Physiology, 289, 644-C655.

Strang, C.E., Renna, J.M., Amthor, F.R. & Keyser, K.T. (2007). Nicotinic acetylcholine receptor expression by directionally selective ganglion cells. Visual Neuroscience, 24, 523-533.

Strang, C.E., Renna, J.R., Amthor, F.R. & Keyser, K.T. (2010). Muscarinic acetylcholine receptor localization and activation effects on ganglion response properties. Investigative Ophthalmology & Visual Science, 51, 2778-2789.

Syed, M.M., Lee, S., Zheng, J. & Zhou, Z.J. (2004). Stage-dependent dynamics and modulation of spontaneous waves in the developing rabbit retina. Journal of Physiology, 560, 533-549.

Taylor, P. (1990). Cholinergic agonists. The Pharmacological Basis of Therapeutics. Permagon Press, New York, 122-149.

Thompson, S.A., Smith, O., Linn, D.M. & Linn, C.L. (2006). Acetylcholine neuroprotection against glutamate-induced excitotoxicity in adult pig retinal ganglion cells is partially mediated through alpha4 nAChRs. Experimental Eye Research, 83, 1135-1145.

Wassle, H., Puller, C., Muller, F. & Haverkamp, S. (2009). Cone contacts, mosaics, and territories of bipolar cells in the mouse retina. Journal of Neuroscience, 29, 106-117.

Weisstaub, N., Vetter, D.E., Elgoyhen, A.B. & Katz, E. (2002). The alpha9alpha10 nicotinic receptor is permeable to and is modulated by divalent cations. Hearing Research, 167, 122-135.

Wess, J., Liu, J., Blin, N., Yun, J., Lerche, C. & Kostenis, E. (1997). Structural basis of receptor/G protein coupling selectivity studied with muscarinic receptors as model systems. Life Sciences, 60, 1007-1014.

Willoughby, J.J, Ninkina, N.N., Beech, M.M., Latchman, D.S. & Wood, J.N. (1993). Molecular cloning of a human neuronal nicotinic acetylcholine receptor beta 3-like subunit. Neuroscience Letters, 155, 136-139.

Yamada, E.S., Dmitrieva, N., Keyser, K.T., Lindstrom, J.M., Hersh, L.B. & Marshak, D.W. (2003). Synaptic connections of starburst amacrine cells and localization of acetylcholine receptors in primate retinas. Journal of Comparative Neurology, 16, 76-90.

Yu, W.F, Guan, Z.Z., & Nordberg, A. (2007) Postnatal upregulation of α4 and α3 nicotinic receptor subunits in the brain of α7 nicotinic receptor-deficient mice. Neuroscience, 146, 1618-1628.

Zhou, Z.J. & Zhao, D. (2000). Coordinated transitions in neurotransmitter systems for the initiation and propagation of spontaneous retinal waves. Journal of Neuroscience, 20, 6570-6577.

Table 1. Acetylcholine Receptor Primer Pairs

Subunit	Accession Number	F- Sense R- Antisense	Product (bp)	Product Homology to the Mouse Subunit Sequence
α2 nAChR	NM_144803	**F-** GTGCCCAACACTTCCGATG **R-** TGTAGTCATTCCATTCCTGCTTT	126	92%
α3 nAChR	NM_145129	**F-** CCAGTTTGAGGTGTCTATGTC **R-** TCGGCGTTGTTGTAAAGC	198	99%
α4 nAChR	NM_015730	**F-** CTCAGATGTGGTCCTTGTC **R-** GAGTTCAGATGGGATGCG	178	95%
α5 nAChR	NM_176844	**F-** CATCGTTTTGTTTGATAATGC **R-** TGCGTCCAAGTGACAGTG	90	84%
α6 nAChR	NM_021369	**F-** TGTCTCCGATCCCGTCAC **R-** TTGTTATACAGAACGATGTCAGG	213	98%
α7 nAChR	NM_007390	**F-** GGTCATTTGCCCACTCTG **R-** GACAGCCTATCGGGTGAG	130	99%
α9 nAChR	NM_001081104	**F-** ACAAGGCCACCAACTCCA **R-** ACCAACCCACTCCTCCTCTT	152	81%
α10 nAChR	NM_001081424	**F-** TCTGACCTCACAACCCACAA **R-** TCCTGTCTCAGCCTCCATGT	168	94%
β2 nAChR	NM_009602	**F-** CCGGCAAGAAGCCGGGACCT **R-** CTCGCTGACACAAGGGCTGCG	152	97%
β3 nAChR	NM_173212	**F-** AAGAAGCAGACTCCTACC **R-** AACAACCTGACTGATGAAG	123	90%
β4 nAChR	NM_148944	**F-** CTACAGGAAGCATTAGAGG **R-** CAGAATACACACAATCACG	146	84%
m1 mAChR	NM_007698	**F-** GACCCTACAGACCCCTCTCC **R-** CCCTTCCTCCAGTCACAAGA	165	93%
m2 mAChR	NM_203491	**F-** CGGCTTTCTATCTGCCTGTC **R-** GGCATGTTGTTGTTGTTTGG	169	96%
m3 mAChR	NM_033269	**F-** GTACAACCTCGCCTTTGTTTCC **R-** GACAAGGATGTTGCCGATGATG	244	99%
m4 mAChR	NM_007699	**F-** GCCTTCATCCTCACCTGGAC **R-** AGTGGCATTGCAGAGTGCAT	146	99%
m5 mAChR	NM_205783	**F-** CCATGGACTGTGGGAAGTCA **R-** CAGCGTCCCATGAGGATGTA	215	99%

**(nAChR) Nicotinic ACh Receptors, (mAChR) Muscarinic ACh Receptor, (RyR3) Ryanodine Receptor Type 3*

Table 2. Antibodies Against Acetylcholine Receptors

Antibody (antigen)	Species	Catalog No.	Supplier
α4 nAChR A synthetic peptide corresponding to amino acids 568-588 of the rat nAChR α4 protein.	guinea pig	AB5590	Chemicon, Temecula CA
α1, α3, α5 nAChR A synthetic peptide corresponding to the main immunogenic region on the extracellular surface of muscle α1 AChR subunit, as well as the α3 and α5 subunits of human neuronal AChRs. The antibody binds the α1 subunit weakly when the protein is denatured, but can only detect the α3 and α5 subunit in native forms.	rat	mAb 210 Immunohistochemistry	Gift of Dr Jon Lindstrom, University of Pennsylvania
	rat	AB24719 Western blot	Abcam, Cambridge MA
α1, α3, α5 nAChR A synthetic peptide corresponding to the main immunogenic region on the external surface of the α1, α3, and α5 subunits of human neuronal AChRs.	rat	mAb 35 Immunohistochemistry	Gift of Dr Jon Lindstrom, University of Pennsylvania
α9 nAChR A synthetic peptide corresponding to the N-terminal region of the human nAChR α9 protein**.**	rabbit	AB49065	Abcam, Cambridge MA
m1 mAChR A Glutathione S-transferase (GST) fusion protein corresponding to a part of the i3 intracellular loop of human m1 mAChR protein (227-353).	rabbit	AB5164	Chemicon, Temecula CA
m2 mAChR A GST fusion protein corresponding to a part of the i3 intracellular loop of the m2 receptor (225-359).	rat	mAB367	Chemicon, Temecula CA
m3 mAChR A peptide analogue, attached to a carrier protein, corresponding to the carboxyl terminal of the human m3 mAChR (580-589).	rabbit	AS-3741S	Research & Diagnostic Antibodies,Benicia, Ca
m4 mAChR A GST fusion protein corresponding to the i3 loop of the human m4 mAChR.	mouse	mAB1578	Chemicon, Temecula CA
m5 mAChR A synthetic peptide corresponding to the 3rd cytoplasmic domain of the human m5 mAChR.	rabbit	AB9454	Chemicon, Temecula CA

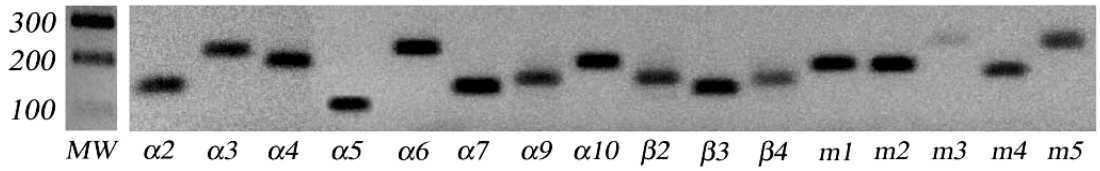

Figure 1. 2.5% agarose gel of RT-PCR transcripts. The α2, α3, α4, α5, α6, α7, α9, α10, β2, β3, and β4 nAChRs, m1, m2, m3, m4, and m5 mAChRs were amplified from WT mouse retina RNA extracts. RT-PCR products were sequenced and compared to the mouse nAChR sequences; homology of sequences ranged from 81%-99%.

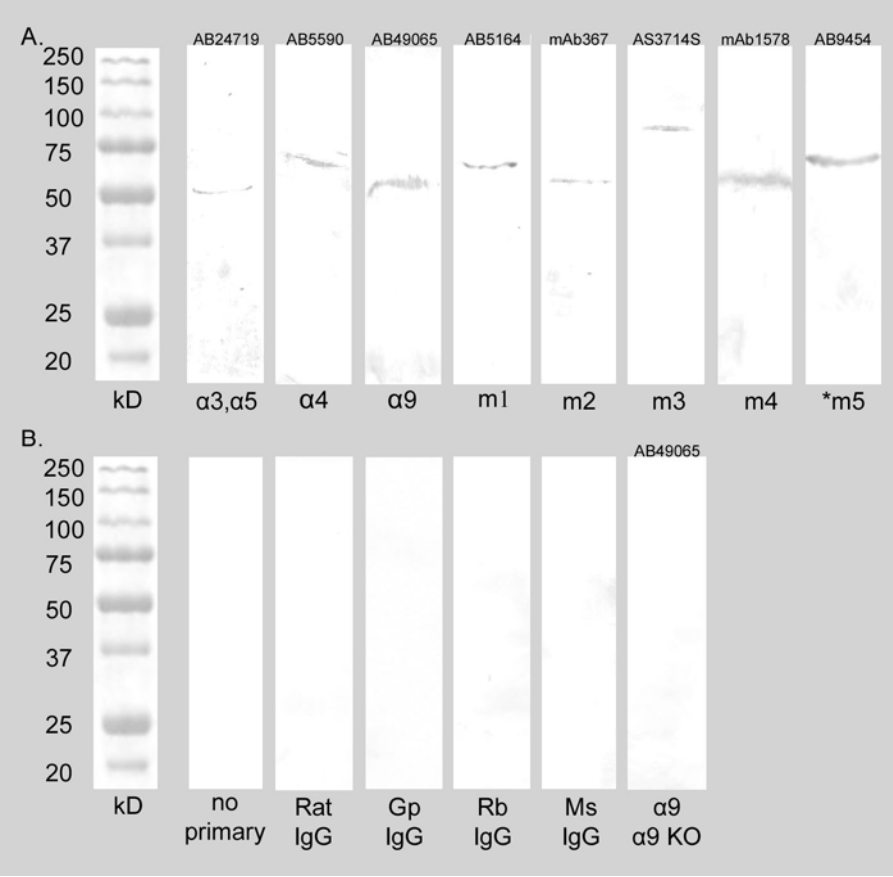

Figure 2. Western blot analyses with antibodies against acetylcholine receptors. Protein extracts from WT C57BL/6J mouse retina and, in the case of the m5 mAChR antibody, brain. (A)Western blots obtained had a single band at the predicted molecular weight. This confirmed the presence of nAChR subunit and mAChR subtype protein and antibody specificity. Blots for each antibody were obtained separately and compiled for figure. α1, α3, α5 (AB24719-Rat) 51kD; α4 nAChR (AB5590-Gp), 70kD; α9 nAChR (AB49065-Rb), 53kD; m1 mAChR (AB5164-Rb), 60kD; m2 mAChR (mAB367-Rat), 52kD; m3 mAChR (AS3714S-Rb), 75kD; m4 mAChR (mAB1578-Ms), 53kD; m5 mAChR (AB9454-Rb), 70kD. (B) Representative western blots for control conditions; clean, with no bands present. IgG: Immunoglobulin G; Gp: Guinea Pig; Rb: Rabbit; Ms: Mouse.

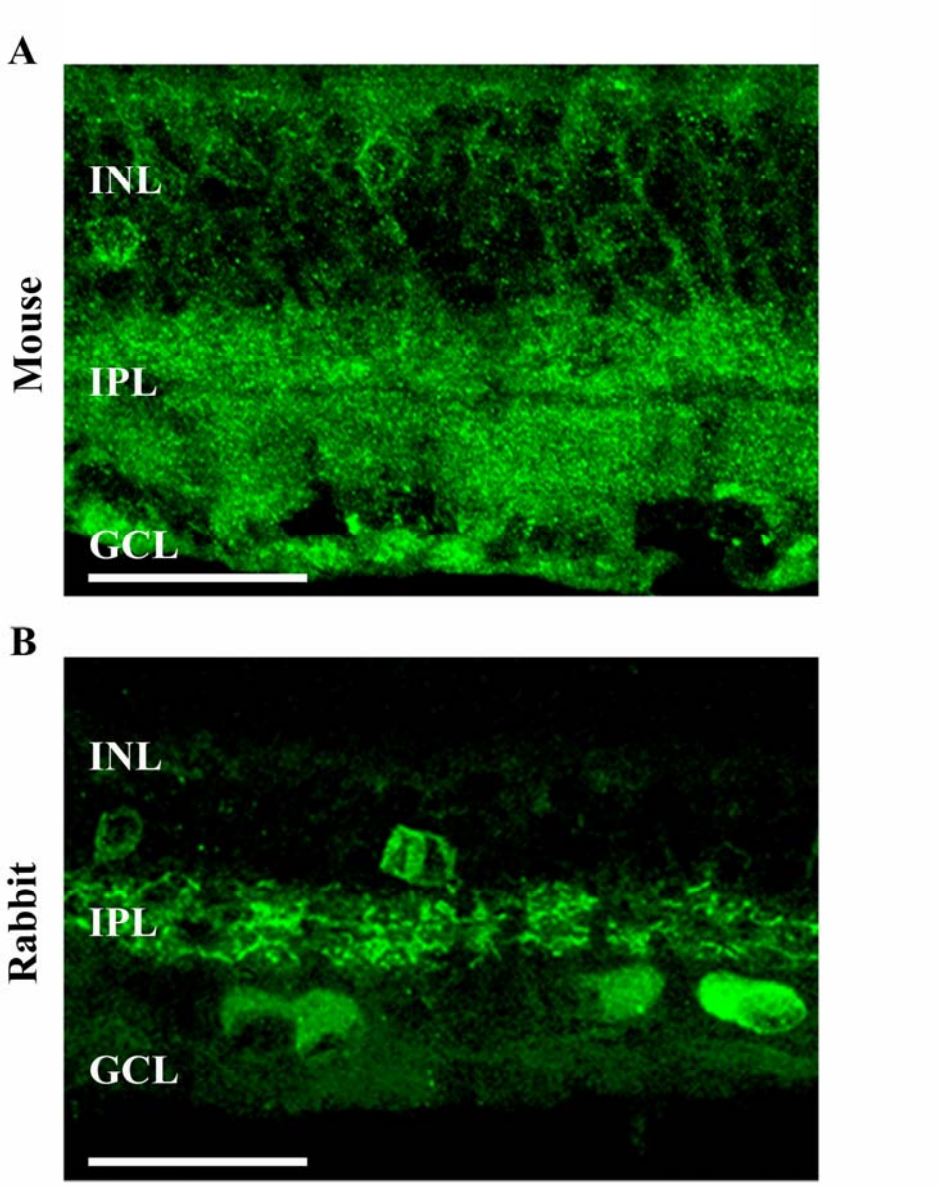

Figure 3. Labeling patterns for the mAb210 antibody, reported to recognize α1, α3, and α5 nAChR subunits, in the mouse and rabbit retina. (A) IHC revealed labeling in amacrine cells, bipolar cells, ganglion cells, and in two broad bands in the inner plexiform layer (IPL) in WT mice. (B) IHC in rabbit retina revealed patterns of mAb 210 labeling somewhat similar to that seen in mouse retina, however mAb210 does not display immunoreactivity by bipolar cells and the bands in the IPL are narrow and much more defined. Additionally, there is much less punctuate labeling. All images consist of a confocal z-stack of 5 optical sections. Scale bar, 25μm.

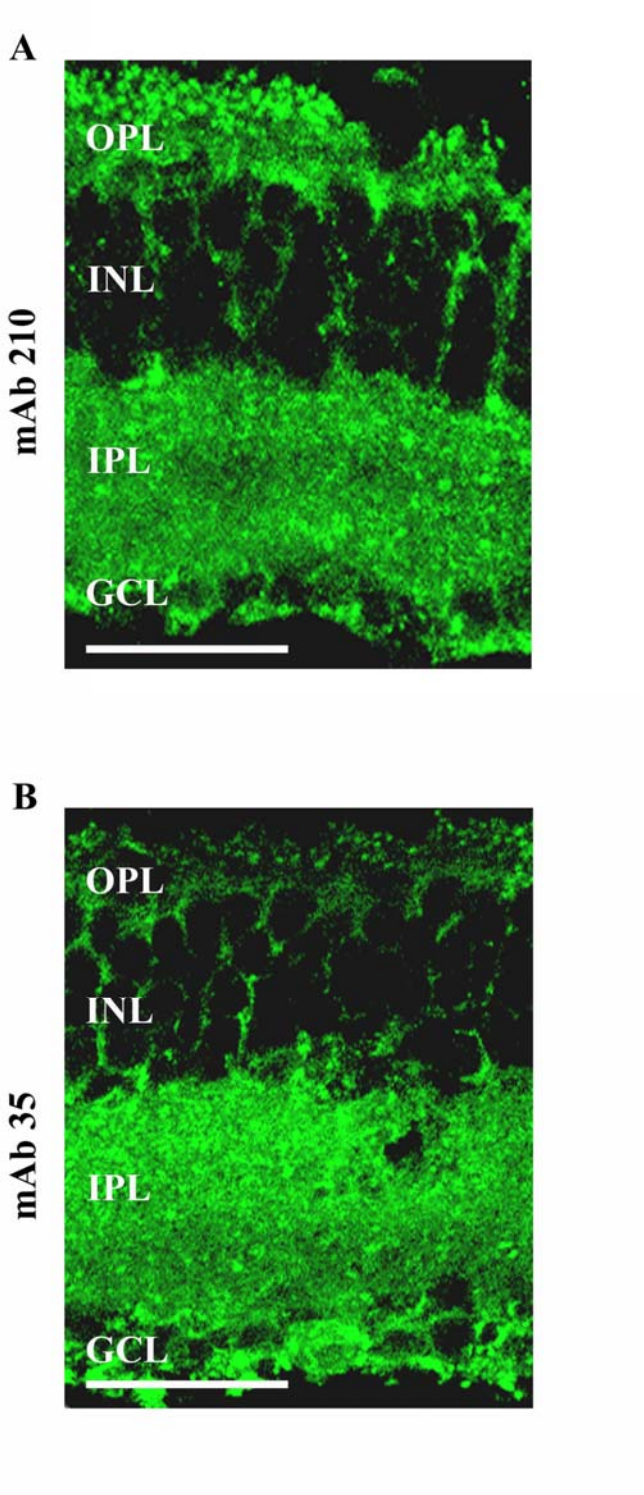

Figure 4. Comparison of labeling patterns for the mAb210 and mAb35 antibodies, reported to recognize α1, α3, and α5 nAChRs subunits, in the mouse retina. (A) mAb 210 labeling and (B) mAb 35 labeling showed similar patterns; amacrine cells, bipolar cells, ganglion cells, and in two broad bands in the IPL. All images consist of a confocal z-stack of 5 optical sections. Scale bar, 25μm.

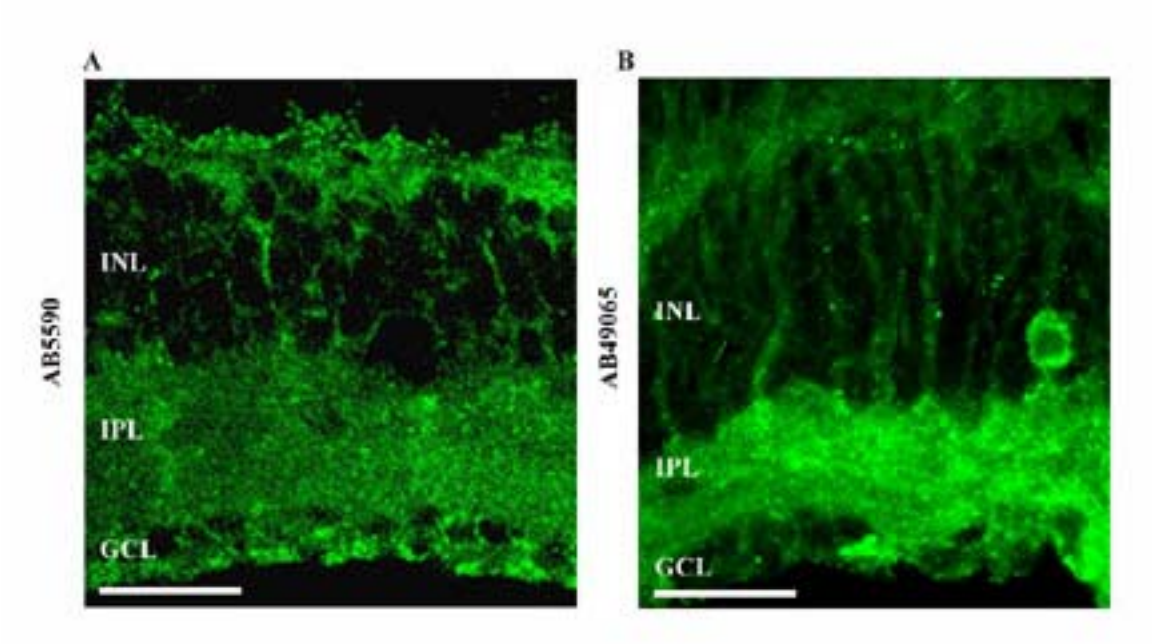

Figure 5. Labeling patterns for antibodies against α4 and α9 nAChR subunits in the mouse retina. (A) AB5590, an antibody reported to recognize α4 nAChR subunits and (B) AB49065, an antibody reported to recognize α9 nAChR subunits. Immunoreactivity was observed in amacrine cells, bipolar cells, and ganglion cells. Processes in the IPL were immunoreactive, with varying patterns of distribution across target nAChR subunit. α4 nAChRs were immunoreactive in two broad, diffuse bands within the IPL, while α9 nAChRs had more intense immunoreactivity in the center of the IPL. Scale bar = 25μm.

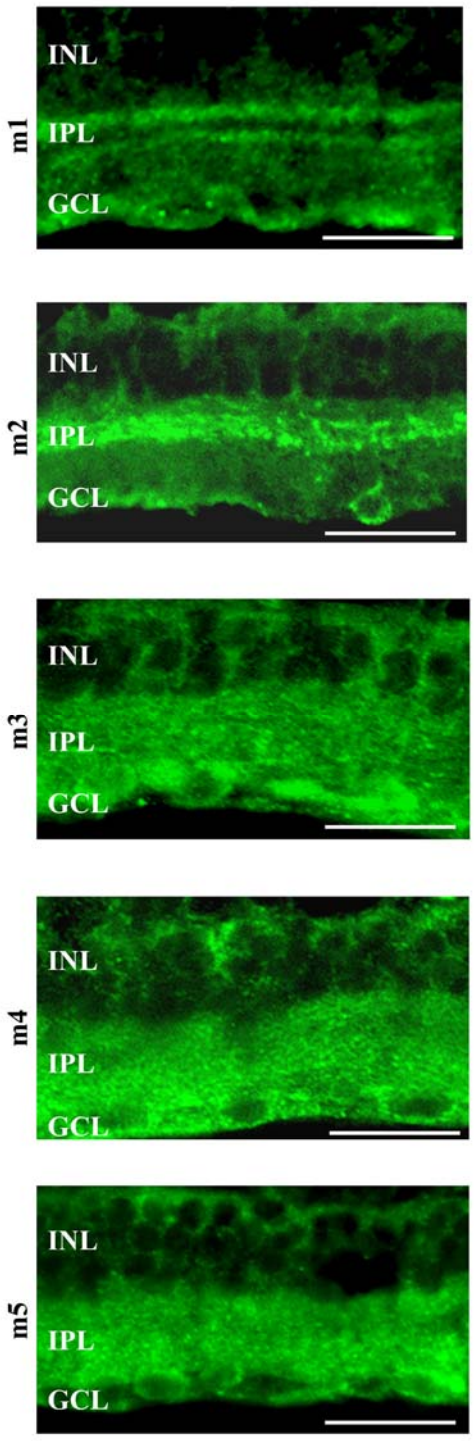

Figure 6. Labeling patterns for antibodies against muscarinic acetylcholine receptors in the mouse retina. The mAChR antibodies labeled bipolar, amacrine, and ganglion cells. Processes in the IPL were immunoreactive, with varying patterns of distribution across target mAChR subtype. All images consist of a confocal z-stack of 5 optical sections. Scale bar, 50μm.

ACETYLCHOLINE RECEPTORS IN THE RETINAS OF THE α7 NICOTINIC ACETYLCHOLINE RECEPTOR KNOCKOUT MOUSE

M.L. SMITH, F.G. SOUZA, C.E. STRANG, B.J. MORLEY, K.T. KEYSER

In preparation for Visual Neuroscience

Format adapted for dissertation

Abstract

Acetylcholine receptors (AChRs) are receptors which are activated by acetylcholine and expressed throughout the nervous system. The α7 nAChR is expressed by bipolar, amacrine, and ganglion cells in the rabbit retina, and plays a role in visual processing (McGehee, 1999; Clementi et al., 2000;). Patients suffering from Alzheimer's disease (AD) and schizophrenia display visual deficits and reductions in α7 nAChR expression. While it is not clear if the link between α7 nAChRs and disease is causal, one could predict that an α7 nAChR KO mouse would display significant phenotypic effects. However, the α7 nAChR knockout (KO) mouse has a mild phenotype, with only slight visual dysfunction (Morley & Rodriguez-Sierra, 2004; Origlia et al., 2012). This mild phenotype could be attributed to the nervous system's high plasticity early in development, compared to adulthood, and thus higher ability to compensate for loss. We predicted that up-regulation of AChR genes during development partially accounts for the α7 nAChR KO mouse's mild phenotype. We employed quantitative real-time polymerase chain reaction (qPCR) using whole retina ribonucleic acid (RNA) extracts as well as RNA extracted from selected regions of the retina, collected using laser capture microdissection (LCM), to determine any RNA expression changes. In whole retina statistically significant up-regulation of the α2, α9, α10, β4, m1, and m4 AChR subunits was observed. However, m2 and m4 mAChR subunits were significantly up-regulated and the β3 and β4 nAChR subunits were significantly down-regulated in the ganglion cell layer (GCL). α2, α9, β4, m3 and m4 AChR subunits were significantly down-regulated in the inner portion of the inner nuclear layer (iINL). β2, β4 and m4 AChR subunits were significantly up-regulated in the outer portion of the INL (oINL). Thus, rather than a

simple up-regulation of a single AChR subunit or subtype, the absence of the α7 nAChR in the KO mouse was associated with cell type specific changes in mRNA levels of a number of different AChR subunits and subtypes. These results suggest that treatment by means of simple up-regulation of cholinergic activity as with the use of acetylcholineesterase inhibitors, may not provide enough specific expression changes to treat visual symptoms, and that cholinergic agents with more specific subtype activity may be viable potential targets for drug development.

Introduction

Neuronal nicotinic ACh receptors (nAChRs) are pentameric, ligand-gated, mixed cation channels that are members of the ligand-gated ion channel superfamily (Karlin, 2002; Alexander et al., 2007). nAChRs have multiple binding sites and are one of the two classes of receptors that are activated by the neurotransmitter ACh. In general, nAChRs are activated by nicotine and blocked by curare (Taylor, 1990). Neuronal nAChRs are composed of α and β subunits, specifically, α2-α10 and β2-4. These subunits can combine into a large number of nAChRs which each have a specific pharmacological and physiological profile. The α7 subunits form homomeric or heteromeric nAChRs with β2 nAChR subunits, are sensitive to α-bungarotoxin (α-BGT), and desensitize rapidly. The α2-α6, and β2-β4 subunits combine heteromerically, are insensitive to α-BGT, and desensitize more slowly (Lindstrom et al., 1996; McGehee, 1999; Arias, 2000; Lindstrom, 2000; Clementi et al., 2000; Khiroug et al., 2002). Unlike the other nAChRs, α9 nAChRs are activated by ACh, but not nicotine. Similar to α7 nAChRs, α9 nAChRs are blocked by α-BGT and strychnine and can form homomeric or heteromeric nAChRs with α10 nAChR subunits (Housley & Ashmore, 1991; Fuchs & Murrow, 1992; Elgoyhen et al., 1994; Erostegui et al., 1994; Johnson et al., 1995; Dulon & Lenoir, 1996; Evans, 1996; Rothlin et al., 1999; Katz et al., 2000). α10 nAChR subunits cannot form homomeric receptors, they combine only with α9 nAChR subunits and the pharmacology of α9α10 nAChRs is similar to that of α9 nAChRs, but with faster desensitization (Elgoyhen et al., 2001). The α7, α9, α9α10, α3β2α5, and α3β2α5 nAChRs all have high Ca^{2+} permeability, compared to the other nAChRs (Gerzanich et al., 1998; Katz et al., 2000; Weisstaub et al., 2002).

The other class of receptors that are activated by ACh are the muscarinic ACh receptors (mAChRs). The five mAChR subtypes, m1-m5, are coupled to G-proteins. As with nAChRs, each mAChR subtype has a specific pharmacology. The mAChRs fall into two general categories (Caulfield & Birdsall, 1998). The m1, m3, and m5 subtypes all activate the phosphatidyl inositol or phospholipase signaling pathways via activation of the Gq-α G-protein. Activation of these subtypes causes the release of intracellular Ca^{2+}, inhibition of Ca^{2+}-activated K^+ channels, and activation of non-specific cation channels, which leads to excitation through cell depolarization (Brown, et al., 1997). The m2 and m4 subtypes inhibit adenylate cyclase and cyclic adenosine monophosphate production via activation of the Gi-α G-protein. Activation of these subtypes causes inhibition of Ca^{2+} channels and activation of K^+ channels, which leads to inhibition through cell hyperpolarization.

AChRs are expressed by neuronal cells throughout the mammalian retina including: bipolar, amacrine, displaced amacrine, horizontal, and ganglion cells (Keyser et al., 2000; Dmitrieva et al., 2007; Strang et al., 2010). AChR activation has been shown to modulate ganglion cell responses and AChRs have been shown to play a role in the development of the retina (Baldridge, 1996; Kittila & Massey, 1997; Zhou & Zhao, 2000). The α7 nAChR subtype is widely expressed throughout the inner retina and has been shown to affect ganglion cell responses in both a direct and indirect fashion (Alkondon & Albuquerque, 2001; Dmitrieva et al., 2007; Strang et al., 2007). First, a subset of directionally selective ganglion cells express α7 nAChRs, directly modulating the responses of these ganglion cells (Strang et al., 2007). Secondly, subsets of amacrine cells containing glycine and γ-aminobutyric acid (GABA) express α7 nAChRs

(Alkondon & Albuquerque, 2001; Dmitrieva et al., 2007). Additionally, populations of ON cone bipolar cells express α7 nAChRs (Dmitrieva et al., 2007). Activation of the α7 nAChRs presumambly depolarizes amacrine cells, leading to increased release of inhibitory neurotransmitters, providing indirect cholinergic modulation of ganglion cell responses.

Changes in α7 nAChR expression and distribution have been observed in Alzheimer's disease (AD) and schizophrenia, both of which have visual dysfunctions which have been attributed to changes at the level of the retina and in visual cortex (Coyle et al., 1983; Nordberg et al., 1999; Xu et al., 2001; Leonard et al., 2006). However, the phenotype of the α7 nAChR knockout (KO) mouse is mild, with a few impairments in working memory and reduced visual acuity, linked to changes in the cortex, but not at the level of the retina. Thus, we predict that up-regulation of other AChRs, particularly those with high Ca^{2+} permeability or that increase intracellular Ca^{2+} concentration, may partially compensate for the loss of α7 nAChRs. The first goal of this study was to determine if the loss of the α7 nAChR subunit was correlated with an overall increase in ACh. The second goal was to determine if there were changes in messenger ribonucleic acid (mRNA) expression of nAChR subunit transcripts and mAChR subtype transcripts in whole retina, to determine whether there were cell-type specific layer-specific changes, and to assess whole retina for changes in expression of other genes whose protein products may compensate in the α7 nAChR KO mouse retina.

Methods

Animals

Retinas, eyecups, and brains from the C57BL/6J wildtype (WT) and α7 nAChR KO mouse were provided by Dr. Barbara Morley at Boys Town National Research Hospital (BTNRH) from animals being used for unrelated studies. Animal care and surgical procedures were approved by the BTNRH Institutional Animal Care and Use Committee. Retinas to be used in quantitative real-time reverse transcriptase polymerase chain reaction (qPCR) experiments were obtained by enucleation and hemisection, followed by dissection from sclera and choroid. Once retinas were obtained they were flash frozen, shipped on dry ice and stored at -80°C prior to RNA extraction. A total of 11 α7 nAChR KO, 2 α9 nAChR KO, 2 α10 nAChR KO, and an equal number of WT littermates were used in whole retina qPCR experiments. Retinas from the same animal were pooled prior to RNA extraction. Eyecups to be used for laser capture microdissection (LCM) were embedded in a block of optimal cutting temperature medium immediately following enucleation (Sakura Finetek, Torrance, CA), frozen, sectioned into 8μm vertical cryosections (Leica CM 3050), mounted onto polyethylene napthalate membrane glass slides (Applied Biosystems, Foster City, California), and stored at -80°C. A total of 11 α7 nAChR KO and 11 WT mice retinas were used for LCM. Samples collected from the same retinal layer in the same animal, both right and left eyes, were pooled. Eyecups to be used for immunohistochemistry (IHC) were obtained by enucleation followed by hemisection. Eyecups were then fixed in 1% paraformaldehyde with 0.34% L-lysine and0.05% sodium-m-periodate in 0.1M phosphate buffer for 2 hours at room temperature. They were then cryprotected by immersion in graded concentrations of sucrose (10%, 20%, and then 30%) in 0.1M

phosphate buffer and then stored at 4°C. A total of 5 α7 nAChR KO and 5 WT mouse retinas were used for IHC. Brains were collected from C57BL/6J WT mice and were flash frozen immediately following removal, shipped on dry ice, and stored at -20C until RNA extraction. RNA extracted from mouse brain was used in custom primer optimization experiments.

Immunohistochemistry

Retinas to be used in choline acetyltransferase (ChAT; Millipore, Billerica, MD) wholemount IHC were processed free floating following isolation from choroid and sclera. Retinas were washed in four changes of 0.1M phosphate buffered saline (PBS) and incubated in 10% DKNS (Jackson Immunoresearch; Westgrove, PA), diluted in PBS/0.03% Triton-X, for 24 hours at 4°C. Retinas were then incubated in ChAT with 10% DKNS, and 0.3% sodium azide in PBS/0.03% Triton-X for 11 days at 4°C, washed in four changes of 0.1M PBS, incubated in Fluorescein-conjugated-donkey-anti-goat (Jackson Immunoresearch; Westgrove, PA) in 0.3% sodium azide/PBS/0.03% Triton-X for 72 hours at 4°C, mounted, and stored at 4°C until imaging. Images were collected with a Leica TCS SP confocal laser scanning microscope. Brightness contrast adjustments and figure preparation was completed in Adobe Photoshop (Adobe Systems; San Jose, CA). For each retina, cell counts were obtained from z-stack confocal images, collapsed into 5 optical sections for the INL and GCL, from three non-overlapping regions that were approximately 500um away from the optic nerve under 40X magnification (adapted from Gu et al., 2003). Each region of interest was 500um by 500um and cells were counted using a colony counter pen (Research Products International; Mount Prospect, IL). Total retinal cell counts were sum of the INL and

GCL counts. Student t-tests were performed to determine if there were differences in cell counts between the inner nuclear layer (INL) and ganglion cell layer (GCL) in both WT and α7 nAChR KO. Student t-tests were also performed to determine if there was a difference in cell counts between WT and α7 nAChR KO mice in INL, GCL, or total retina.

RNA extraction protocol

For qPCR studies, total RNA was extracted from flash frozen retinas using the RNAqueous -4PCR Kit (Ambion; Austin, TX). The protocol included the following steps: homogenization of tissue in a lysis/binding solution, application to a filter which selectively binds mRNA, washing with a salt buffer to remove residual deoxyribonucleic acid (DNA), proteins, and other contaminants, followed by elution in nuclease free water. The RNA then underwent a deoxyribonuclease (DNAse I) treatment, to remove any DNA contamination, which involved incubation of DNAse I Buffer and DNAse I with the RNA followed by incubation with a DNAse inactivation reagent and centrifugation to pellet any DNA contaminates. RNA was precipitated from the resulting supernatant by the addition of 5M ammonium acetate, 1ul glycogen, and 100% ethanol after which centrifugation (Eppendorf 5810R; Westbury, NY) was performed at 10 RPM, 4°C, for 10 minutes. The supernatant was removed and discarded, and then a 75% ethanol wash was performed on the RNA pellet, followed by another centrifugation and removal of supernatant. The RNA pellet was dried at 37°C and resuspended in nuclease-free water. The majority of extractions yielded an RNA concentration of 60-100ng/ul for each retina. The quality of the RNA was assessed using the 260/280 and 260/230 ratios as measured by the Nanodrop ND-1000 spectrophotometer (Thermo Scientific; Wilmington, DE).

The PicoPure RNA Isolation Kit (Arcturus; Sunnyvale, CA) was used to extract RNA from specific retinal layers, isolated via LCM (as described below). This protocol followed equivalent steps as the RNAqueous kit, but was optimized for samples as small as one cell.

qPCR screening

SuperArrays, (SABiosciences; Frederick, MD) custom 96 well PCR arrays containing pre-optimized and pre-validated primers, were used to determine if the α7 nAChR KO resulted in a changes in mRNA expression of 96 receptors, channels, or transporters, including AChRs. The arrays used in this study contained primers to a wide variety of neuronal receptors, channels, and transporters including GABA receptors, glycine receptors, and potassium channels (Table 1). The arrays also contained a positive PCR control, a no reverse transcriptase control, a mouse DNA positive control, and several reference genes including β-actin and glyceraldehyde-3-phosphate. Superarray primer sets were proprietary, and thus sequencing of products could not be completed as we could not obtain a primer sequences, which are needed for sequencing. However, Superarray plates enabled screening of many targets.

RNA was extracted from 8 KO and 8 WT animals and quality assessed following the same protocol previously described. The RNA was converted to complementary DNA (cDNA) using the RT^2 First Strand Kit (SABiosciences; Frederick, MD). One microgram of RNA was added to an annealing mixture containing P2 (primer and external control mix) and ribonuclease (RNAse) free water. This annealing mixture was incubated at 70°C for 3 minutes and then a reverse transcriptase (RT) mix, containing buffer, RT

enzyme mix (containing the polymerase and deoxynucleotide triphosphates), RNase inhibitor, and RNAse-free water, was added. The reverse transcriptase mixture plus annealing mixture was incubated at 37°C for 60 minutes, followed by incubation at 95°C for 5 minutes to inactive the RT. One hundred microliters of cDNA was then added to another PCR mix containing 2X SuperArray PCR Master Mix and nuclease-free water. Twenty-five microliters of the resulting PCR mix was added to each of the wells in the custom SuperArray plate containing the pre-optimized and validated primers. The loaded SuperArray plate was placed in the thermocyler (BioRad iQ5) and underwent a hot start of 95°C for 10 minutes, 40 cycles of 95°C for 15 seconds (denaturation), and 60°C for 1 minute (amplification).

Quantification

qPCR uses the level of fluorescence emitted by SYBR green, which fluoresces when bound to double stranded DNA, at each amplification step to quantify amplification of DNA within the PCR reaction. As amplification occurs, and the number of double stranded DNA strands increase, the level of fluorescence increases. Increased fluorescence as a result of DNA amplification produces an amplification curve that has a sigmoid trajectory with a linear ground phase, an early exponential phase, a log-linear phase, and a plateau phase (Tichopad et al., 2003). Threshold level is set so that the level crosses the early exponential phase of the sigmoid trajectory for the majority of the samples. The cycle at which a sample's amplification curve crosses the threshold line is the Ct. Smaller Ct values indicates faster amplification and higher copy number.

Fold change (up- or down-regulation) was determined using the ΔΔ Ct method. The ΔCt for each gene of interest was calculated by subtracting the average Ct of the reference genes from the Ct of the gene of interest:

$$\Delta Ct = Ct_{goi} - Ct_{ref}$$

Then the ΔΔ Ct was determined for each gene of interest by raising 2 to the power of the negative ΔCt:

$$\Delta\Delta Ct = 2^{-\Delta Ct}$$

Fold difference (FD) was then calculated by dividing the ΔΔCt of the KO animals by the ΔΔCt of the WT animals:

$$FD = KO\ \Delta\Delta Ct / WT\ \Delta\Delta Ct$$

If the resulting number was greater than one, this indicated a positive fold change (FΔ), or up-regulation, and the FD was also the FΔ.

$$F\Delta_{pos} = FD$$

If the resulting number was less than one, this indicated a negative FΔ, or down-regulation, and a further calculation was necessary. For down-regulation the FΔ was determined by dividing -1 by the FD:

$$F\Delta_{neg} = -1 / FD$$

A standard independent samples, two-tailed t-test was performed to determine if there was a significant difference in the KO and WT samples for each target gene. Total standard deviation for FΔ values was calculated by first determining the standard deviation (SD) of both the wildtype and knockout sample. SD for each sample was calculated by taking the square root of the average of the squared differences from the mean:

$$SD_{sample} = \sqrt{(\sum (\mathbf{X} - \bar{x})^2/(n-1))}$$

Then the sample SDs were used to calculate the total SD for fold change by taking the square root of the squared SD for the wildtype plus the squared SD for the knockout:

$$SD_{total} = \sqrt{(SD^2_{WT} + SD^2_{KO})}$$

Standard error of the mean (SEM) was calculated by dividing the SD_{total} by the square root of the sample size:

$$SEM = SD_{total}/\sqrt{(n)}$$

FΔ was reported in the following format:

$$F\Delta\ (\pm\ SEM)$$

AChR qPCR primer design and optimization

In order to confirm any changes in expression, relative to those identified in the SuperArray qPCR screening, and to perform a more fine-grained analysis of changes in nAChR subunit and mAChR subtype expression in the α7 nAChR KO mouse retina, primers were designed for nAChR subunits and mAChR subtypes using Beacon Designer (Table 2). The Ryanodine receptor 3 (RyR3) was chosen as the reference gene because the results of our qPCR screening experiments showed that its expression did not differ between WT and α7 nAChR KO mouse samples. All primer sets were purchased from Sigma-Genosis (St. Louis, MO). Primers were previously used to determine the presence of AChRs in the mouse retina (RT-PCR), but further optimization steps were performed to ensure primers were appropriate for qPCR (Nolan et al., 2006).

Optimization for quantitative PCR included determining the annealing temperature and primer ratio that resulted in the highest copy number and a single

product for each primer set. RNA for optimization experiments was extracted from WT mouse whole brain tissue using the RNAqueous -4PCR Kit, as previously described. RNA was converted to cDNA using an iScript cDNA synthesis kit (BioRad; Hercules, CA). One microgram of RNA was added to a cDNA synthesis mix containing 5x iScript buffer, iScript reverse transcriptase (includes an RNase inhibitor), and RNAse-free water. The cDNA synthesis mix was placed in the MyCycler Personal Thermocycler (BioRad; Hercules, CA) and incubated at 25°C for 5 minutes, at 45°C for 30 minutes, and 85°C for 5 minutes. For amplification, two hundred nanograms of cDNA were added to a PCR mix containing iQ SYBR green supermix (containing DNA polymerase and dNTPs; BioRad, Hercules, CA), nuclease-free water, and forward and reverse primers. The cDNA/PCR mix was placed in the thermocycler (BioRad iQ5) and underwent an initial hot start at 95°C for 3 minutes followed by 40 cycles of 95°C for 10 seconds (denaturation), optimum annealing temperature for 30 seconds (annealing temperature), and 72°C for 30 seconds (elongation). A melt curve to determine the melting point of the DNA product was performed immediately after the final elongation cycle. Negative controls, omission of cDNA, were performed in parallel.

Optimum temperature and primer ratios were determined by selecting the conditions with the smallest Ct value, which also had a melt curve containing a sharp single peak (indicating the presence of only one product). The melt peak chart was determined by plotting the negative first derivative (-dF/dt) of the relative fluorescence units versus temperature (the negative first derivative of the melt curve) using the BioRad iQ5 software. A clean melt peak chart had a single sharp peak (indicating the presence of only one product), with minimal primer dimers (the extension of self annealed primers).

A melt curve with two or more peaks indicated the presence of two or more DNA products at different melting temperatures.

The efficiency of the reactions was determined by serial dilution of the cDNA to produce a standard curve showing the relationship between Ct and log cDNA starting quantity. Each dilution was performed in triplicate and standard curves determined such that each showed a regression line with $r^2 > 0.95$, a slope between -3.2 and -3.5, reaction efficiency between 95% and 105%, and an average technical error (Ct difference between replicates) less than 1 Ct. Efficiency was calculated as $10^{(-1/slope)} - 1$. If the efficiency of the reaction did not fall within this range, the optimization steps were repeated until the target efficiency was obtained.

AChRs whole retina qPCR experiments

Total RNA was extracted from frozen retinas of 11 WT and 11 α7 nAChR KO mice and quality assessed following the same protocol as previously described (see RNA Extraction Protocol). RNA was extracted from both retinas in each mouse and pooled into one sample per animal. RNA was reverse transcribed and resulting cDNA amplified under the validated conditions determined using RNA extracted from mouse brain. Primers for α2-α7, α9, α10, β2-β4 nAChR and M1-M5 mAChR subunits were used; the reference gene was the ryanodine receptor (RyR3). Fold change was determined as previously described. Statistical significance was determined using independent samples t-tests. The DNA products resulting from the qPCR experiments were validated by electrophoresis on a 2.5% agarose gel. PCR products were purified using the Qiaquick PCR Purification kit (Qiagen; Valencia, CA) and then sequenced to confirm their identity

(Heflin Center for Genomic Sciences; University of Alabama at Birmingham; Birmingham, Al).

Laser capture microdissection (LCM) qPCR experiments

In order to determine whether or not changes in expression of AChR transcripts in whole retina varied across layers of the retina, LCM was used to isolate cells of the outer INL (oINL), the inner INL (iINL), and the GCL. As a negative control, samples were also collected from the IPL. Samples were sectioned and prepared for LCM within 48 hours of enucleation to prevent tissue degradation. In order to prepare for LCM, slide mounted sections were dehydrated and processed at room temperature in sequential incubations of 75% ethanol for thirty seconds, two changes of RNAse-free distilled water for thirty seconds, 75% ethanol for thirty seconds, 95% ethanol for thirty seconds, 100% ethanol for one minute, and xylene for five minutes. The sections were dried for 5 minutes at room temperature and then laser capture microdissection was performed using a Veritas Microdissection System (Molecular Devices; Sunnyvale, CA). For each layer (GCL, iINL, oINL) three caps containing 8-10 retinal sections were obtained for each animal. Representative images documenting laser capture were captured with the Veritas Microdissection System software. Brightness and contrast were adjusted using Adobe Photoshop; adjustments were identical for all images in a series (Adobe Systems; San Jose, CA). RNA was isolated using a Pico Pure extraction kit (Applied Biosystems; Carlsbad, CA) according to the manufacturer's protocol. As expected, RNA could not be extracted from samples collected within the IPL. RNA extracted from the three caps obtained from the same animal and capturing the same layer (GCL, iINL, or oINL) was

pooled. A total of 11 WT and 11 α7 nAChR KO mice were used. Fold change, statistical significance, and DNA product validation was determined as previously described.

Results

ChAT Wholemount Immunohistochemistry

We first assessed the distribution and number of ChAT immunoreactive cells in the WT and α7 nAChR KO mouse retina. ChAT is the enzyme that synthesizes ACh; thus, theoretically, a reduced number of ChAT immunoreactive cells could indicate a reduction in overall levels of ACh. The distribution of ChAT immunoreactivity in the WT mouse has been previously described and our studies yielded similar results, with immunoreactivity in a subset of amacrine cells in the INL and displaced amacrine cells in the GCL, with two bright bands in the second and fourth sublamina of the IPL (Galli-Resta et al., 2000; Haverkamp & Wassle, 2000). The number of ChAT immunoreactive amacrine cells in the INL was higher than in the GCL (Figure 1). This higher number of ChAT immunoreactive cells in the INL as compared to the GCL was observed for both WT ($t(8) = -2.987$, $p<0.05$) and α7 nAChR KO ($t(8) = -9.519$, $p<0.001$) mice. In the WT retina, the INL contained 1390.6 per mm^2 (SD=162.14) ChAT immunoreactive amacrine cells, while the GCL contained 1016.8 per mm^2 (SD=75.79) ChAT immunoreactive amacrine cells. In the α7 nAChR KO retina, the INL contained 1349.33 per mm^2 (SD=61.49) ChAT immunoreactive amacrine cells, while the GCL contained 1142.67 per mm^2 (SD=73.22) ChAT immunoreactive amacrine cells. There was not a significant difference in the number or distribution pattern of ChAT immunoreactive cells in the α7 nAChR KO mouse as compared to WT, in either the INL or GCL. Thus, the absence of

α7 nAChRs did not appear to grossly affect the cholinergic cell populations, thus any changes in the expression of nAChR subunits or mAChR subtypes in the α7 nAChR KO mouse was most likely not due to altered levels of retinal ACh.

qPCR screening

In order to screen for changes in expression of many different candidate genes at one time, qPCR custom SuperArrays were used. SuperArrays included primers for a wide variety of targets, including the members of the ligand gated ion channel superfamily and receptors that activate the same protein cascades as the mAChRs. qPCR screening results indicated a significant 1.19 (SEM=0.082) fold up-regulation ($t(14) = -2.200$, $p < 0.05$) of the β2 $GABA_A$ receptor, indicating that β2 $GABA_A$ containing receptor expression was significantly higher in KO mice than in WT mice. There was also a significant -1.50 (SEM=0.182) fold down-regulation ($t(14) = 2.290$, $p < 0.05$) of the α5 nAChR subunit, a -1.78 (SEM=0.252) fold down-regulation ($t(12) = 2.185$, $p < 0.05$) of the m1 mAChR subtype, and a -1.98 (SEM=0.225) fold down-regulation ($t(12) = 2.884$, $p < 0.05$) of the inwardly rectifying potassium, subfamily J, member 4 channel (Kcnj4). This indicates that these targets (α5 nAChR, m1 mAChR, and Kcnj4) were significantly down-regulated in KO mice than in WT mice (Figure 2). As primer sets in SuperArrays are proprietary, sequence homology could not be determined. Since we were unable to sequence the products and several AChR subunits showed changes that trended towards significance, we chose to confirm the results and perform a more fine-tuned analysis with custom designed and optimized AChR primers. Due to the small

differences in expression of Kcnj4 and β2 $GABA_A$ receptors, we chose to focus on nAChR transcript expression.

Whole Retina AChR qPCR

To confirm the changes in mRNA expression observed using the SuperArrays and ensure product sequence homology, custom primers for AChRs, designed against mouse sequences, were optimized for qPCR. qPCR products were subjected to electrophoresis on a 2.5% agarose gel and single bands of the expected molecular weight were obtained (Figure 3). Homology of product sequences to mouse nAChR and mAChR sequences ranged from 81-100% (Table 2). RNA extracted from α7 nAChR KO mouse showed no product when qPCR was performed using the α7 nAChR primer set. RNA extracted from α9 nAChR KO mouse also showed no amplification when qPCR was perfomed using the α9 nAChR primer set. Similarly, RNA extracted from α10 nAChR KO mouse showed no amplification when qPCR was performed using the α10 nAChR primer set. qPCR results, using RNA extracted from WT and α7 nAChR KO mouse retinas, indicated a significant 3.11 fold (SEM=0.263) up-regulation ($t(16) = -4.280$, $p < 0.001$) of the α2 nAChR subunit, 3.5 fold (SEM=0.586) up-regulation ($t(15) = -2.118$, $p < 0.05$) of the α9 nAChR subunit, 2.66 fold (SEM=0.553) up-regulation ($t(18) = -1.831$, $p < 0.05$) of the α10 nAChR subunit, 1.49 fold (SEM=0.107) up-regulation ($t(18) = -3.693$, $p < 0.001$) of the β4 nAChR subunit, 3.81 fold (SEM=0.627) up-regulation ($t(18) = -2.087$, $p < 0.05$) of the m1 mAChR subtype, and 6.22 fold (SEM=0.589) up-regulation ($t(15) = -2.941$, $p < 0.01$) of the m4 mAChR subtype. Results also indicated significant -2.95 fold (SEM=0.582) down-regulation ($t(16) = 1.768$, $p < 0.05$) of the α5 nAChR subunit (Figure 4).

LCM AChR qPCR

In order to determine whether AChR expression varied in specific populations of cells in the retina, LCM was used to extract cells in the GCL, the inner INL (iINL), and the outer INL (oINL). The GCL is composed of ganglion and displaced amacrine cell populations. The iINL is composed of amacrine and bipolar cells, while the oINL is composed of horizontal and bipolar cells. Representative images of retinal tissue before and after each laser capture are shown in Figure 5. The IPL was also collected (image not shown) as a negative control and, as expected, there were no RNA transcripts present.

nAChRs qPCR- Retinal Layers

qPCR results indicated significant 3.11 fold (SEM=0.263) up-regulation ($t(16) = -4.280$, $p < 0.001$) of the α2 nAChR subunit in whole retina. However, none of the captured regions of the retina showed up-regulation of the α2 nAChR subunit. Instead there was actually statistically significant -3.07 fold (SEM=0.504) down-regulation ($t(13) = 2.243$ $p < 0.05$) in the iINL. There was a significant 2.95 fold (SEM=0.582) down-regulation ($t(16) = 1.768$, $p < 0.05$) of the α5 nAChR subunit in whole retina, and non-statistically significant down-regulation in the oINL, iINL, and GCL. There was a significant 3.5 fold (SEM=0.586) up-regulation ($t(18) = -1.831$, $p < 0.05$) of the α9 nAChR subunit in whole retina and non-statistically significant up-regulation in the oINL and GCL. However, there was a significant -6.26 fold (SEM=0.575) down-regulation ($t(14) = 3.521$, $p < 0.01$) of the α9 nAChR subunit in the iINL. Finally, there was a 2.66 fold (SEM=0.553) up-regulation ($t(18) = -1.831$, $p < 0.05$) of the α10 nAChR subunit in whole retina with a non-statistically significant up-regulation in the oINL and GCL with

a non-statistically significant down-regulation in the iINL. To summarize, α2 nAChR subunits were up-regulated in whole retina but down-regulated in the GCL and INL. α5 nAChR subunits were down-regulated in whole retina and inner retina. α9 nAChR subunits were up-regulated in whole retina, GCL, and oINL, and significantly down-regulated in iINL. Finally, α10 nAChR subunits were up-regulated in whole retina, oINL, and GCL, and down-regulation in iINL (Figure 6 and Figure 7).

There was a non-statistically significant up-regulation of the β2 nAChR subunit in whole retina. However, there was statistically significant 3.36 fold (SEM=0.379) up-regulation ($t(17) = -3.218$, $p < 0.01$) of the β2 nAChR subunit in the oINL and a non-statistically significant down-regulation in the iINL and GCL. There was a non-statistically significant up-regulation of the β3 nAChR subunit in whole retina. Conversely, there was statistically significant -2.54 fold (SEM=0.246) down-regulation ($t(19) = 3.844$, $p < 0.001$) of the β3 nAChR subunit in the GCL and a non-statistically significant down-regulation in the INL. Finally, there was 1.49 fold (SEM=0.107) up-regulation ($t(18) = -3.693$, $p < 0.001$) of the β4 nAChR subunit in whole retina and 1.15 fold (SEM=0.079) up-regulation ($t(20) = -1.751$, $p < 0.05$) in the oINL. However, there was a statistically significant -1.60 fold (SEM=0.067) down-regulation ($t(18) = -2.087$, $p < 0.001$) of the β4 nAChR subunit in the iINL and 2.90 fold (SEM=0.097) down-regulation ($t(19) = 11.060$, $p < 0.001$) in the GCL.

mAChRs qPCR- Retinal Layers

There was a statistically significant 3.81 fold (SEM=0.627) up-regulation ($t(18) = -2.087$, $p < 0.05$) of the m1 mAChR subtype in whole retina with a non-statistically

significant up-regulation in the oINL and GCL and a non-statistically significant down-regulation in the iINL. There was a non-statistically significant up-regulation of the m2 mAChR in whole retina and a significant 5.58 fold (SEM=0.335) up-regulation ($t(10) = -5.234$, $p < 0.001$) in the GCL. However, there was also a non-statistically significant down-regulation in the oINL and statistically significant -5.08 fold (SEM=0.637) down-regulation ($t(18) = 2.604$, $p < 0.01$) in the iINL. Finally, there was a statistically significant 6.22 fold (SEM=0.589) up-regulation ($t(15) = -2.941$, $p < 0.01$) of the m4 mAChR subtype in whole retina, 2.48 fold (SEM=0.502) up-regulation ($t(9) = -1.885$, $p < 0.05$) in the oINL, and 2.63 fold (SEM=0.289) up-regulation ($t(10) = -3.415$, $p < 0.01$) in the GCL. However, there was also a statistically significant -2.00 fold (SEM=0.311) down-regulation ($t(14) = 2.268$, $p < 0.05$) of the m4 mAChR subtype in the iINL. To summarize, m1 mAChR subtypes were up-regulated in whole retina, up-regulated in the oINL and GCL, and down-regulated in the iINL. m2 mAChR subtypes were up-regulated in whole retina, up-regulated in GCL, and down-regulated in the INL. Finally, m4 mAChR subtypes were up-regulated in whole retina, oINL, and GCL but down-regulated in iINL.

Discussion

There are many possible effects of the elimination of α7 nAChRs during development. To assess the possibility that there were changes in the overall level of ACh release in the retina, we first determined if there were any alterations in distribution or number of ChAT immunoreactive cells, an indirect method of assessing ACh within the retina. Alternatively, there is a decrease in ACh levels in AD as well as a decrease in α7

nAChRs, so the loss of the α7 nAChR earlier in development could be related to the reduction in levels of ACh in the brain (Coyle et al., 1983; Wevers et al., 1999; Oddo & LaFerla, 2006; Ni et al., 2013). The activity of ChAT, the enzyme that synthesizes ACh, has been shown to be reduced in the primary visual cortex of patients with early stage AD; however, this may be an indicator of reduced availability of choline and not reduced ChAT activity (Ikonomovic et al., 2005).

Consistent with previous reports in rabbit, mouse, and other mammals, ChAT immunoreactivity was observed in amacrine cell bodies in the INL, displaced amacrine cell bodies in the GCL and two distinct bands of labeling in the IPL (Galli-Resta et al., 2000; Haverkamp & Wassle, 2000). There was, as expected, a significantly higher number of ChAT positive amacrine cells in the INL compared to the GCL for both WT and KO retinas ($p<0.05$, $p<0.001$ respectively). There were no significant differences in the numbers of cholinergic cells in WT versus α7 nAChR KO, suggesting that the release of ACh in the α7 nAChR KO is equivalent to that in the WT mouse.

In this study we also assessed the abundance of AChR transcripts in the α7 nAChR KO mouse as compared to WT in order to determine whether or not there were quantitative changes that may be associated with the loss of the α7 nAChR. To this end we had three general sets of qPCR experiments. To begin with we completed whole retinal qPCR superarray screening experiments using a custom designed plate of pre-optimized, proprietary primers for a variety of targets that we speculated had the potential to differ in the KO based on the mild retinal phenotype of the KO mouse (Table 1). Subsequently, unique AChR qPCR primers were designed, optimized, and tested in whole retinal qPCR experiments. Finally, laser capture microdissection was employed to

isolate cell populations in the GCL, iINL, and oINL. AChR expression levels in each of these retinal layers were then determined using the AChR primers from the second set of experiments.

qPCR screening results indicated a significant down-regulation of α5 nAChR subunit and m1 mAChR subtype mRNA. The α5 nAChR result was confirmed via qPCR using custom designed AChR primers but the m1 mAChR result was not confirmed. SuperArrays were helpful for screening of a large number of targets, but without access to specific validation and optimization of the proprietary primers, as well as the overall small changes identified in the screening, we chose to focus on specifically designed and validated primers for AChRs.

An immunoprecipitation study by Origlia et al., 2012, indicated no significant difference in protein expression of α2, α5 and β4 nAChRs in the α7 nAChR KO mouse retina. This could be an indication that while these targets show up-regulation at the RNA level, there is not a statistically significant increase in protein levels. However, the Origlia study used whole retina protein extract and did not determine protein expression in different retinal cell populations. As we observed in our LCM experiments, variations in expression within different cell populations may be masked in whole retina extracts.

The qPCR screening results also indicated a significant up-regulation of the β2 $GABA_A$ receptor subunit and a significant down-regulation of the Kcnj4 channel. The Kcnj4 channel is an inwardly-rectifying K+ channel, responsible for depolarizing a hyperpolarized membrane back to the K+ resting potential (Kubo et al., 2005). The β2 $GABA_A$ receptor subunit is in the same super-family as nAChRs (Hadingham et al., 1994). A decrease in Kcnj4 and an increase in the β2 $GABA_A$ receptor subunit may result

in an increase in hyperpolarization. These results are counterintuitive; as we speculated that a decrease in α7 nAChR mediated excitation might be correlated with a decrease in inhibitory $GABA_A$ or an increase in Kcnj4, a channel that reduces the length of time a cell is hyperpolarized. However, α7 nAChR activation can cause changes in Ca^{2+} dependent Cl^- channel activity, and removing this effect could be related to the observed decrease in Kcnj4 and increase in β2 $GABA_A$ (Yamashita & Isa, 2003; Zhang & Berg, 2007). Confirmation of these changes with custom designed primers warrants further experimentation.

A comparison of results of the different qPCR experiments helped to further parse out differences in AChR expression in the α7 nAChR KO mouse retina (Figure 7). Although, whole retina qPCR results indicated a significant up-regulation of α2 nAChR subunit transcripts, there was significant down-regulation in cells of the GCL and a non-statistically significant down-regulation in the INL. This up-regulation in whole retina, but not GCL and INL, suggests that changes in expression of α2 nAChR subunits occur in other areas of the retina possibly within the retinal vasculature observed at the level of the outer plexiform layer (OPL) or in retinal macroglial cells whose somas are in the OPL (Arias et al., 2009; Liu et al., 2009). The β3 nAChR subunit had the same pattern of expression as the α2 nAChR subunit; overall up-regulation but significant down-regulation in the oINL, iINL, and GCL. This implies that both α2 and β3 nAChR subunits are increased in cell populations other than retinal neurons, such as within blood vessels or in macrophages, which have been shown to express nAChR subunits (Arias et al., 2009).

While whole retina qPCR, using both superarray and custom primers, showed a significant down-regulation of the α5 nAChR subunit, the down-regulation in individual layers of the retina were not statistically significant. This suggests that the overall down-regulation of the α5 nAChR subunit was spread across the retina and not specific to a particular area of the retina, but combined together did result in overall down-regulation. The α5 nAChR subunit is usually expressed as a heteromer in conjunction with α3β4 subunits (Sargent, 1993; Gotti et al., 1997). Down-regulation of the α5 nAChR subunit mRNA is consistent with a possible decrease in α3α5β4 receptors. This suggests a shift in the ratio of α3α5β4 to α3β4 nAChRs in the retina of the α7 nAChR KO mouse. The α5-containing nAChRs are less sensitive to nicotine than other nAChRs, so a decrease in the number of these receptors might indicate an overall increase in sensitivity to nicotine (Jackson et al., 2010). The β2 and β4 nAChR subunit transcripts had similar patterns of expression in the α7 nAChR KO; overall up-regulation in whole retina, up-regulation in oINL and down-regulation in the GCL and iINL. This suggests that the β2 and β4 containing nAChR were likely decreased in ganglion and amacrine cells and increased in bipolar cells and horizontal cells.

The α9 nAChR subunit was significantly up-regulated overall, with non-statistically significant up-regulation in the oINL and the GCL. However, there was also a significant down-regulation of the α9 nAChR subunit in the iINL. This could indicate reductions of α9 nAChR subunits within populations of amacrine cells in the iINL. While the α9 nAChR subunit is predominantly homomeric, there have been reports of α9α10 nAChR heteromers (Weisstaub et al., 2002; Plazas et al., 2005). In whole retina, there was an overall increase in both α9 and α10 nAChR subunit expression in the α7 nAChR

KO, raising the possibility that throughout the retina there is an increase in the α9 nAChR and α10 nAChRs as compared to WT. These increases were likely limited to the GCL, as both α9 nAChR subunit and α10 nAChR subunit transcripts were reduced in RNA extracted from INL cells gathered by LCM. α9 and α10 nAChR subunits were good candidates for up-regulation because of their physiological similarities to α7 nAChRs. Our data suggest that they may indeed partially compensate for the loss of α7 nAChRs, although the expression patterns, as determined by localized changes in RNA transcript, differs from that of α7 nAChRs.

There were also localized changes detected in number of mAChR transcripts. While the m2 mAChR subtypes showed no significant change in expression in whole retina, there was a significant up-regulation in the GCL and a significant down-regulation in the iINL. These localized changes in opposite directions resulted in no overall change, but did suggest the possibility of increased inhibition via m2 mAChR subunits in the GCL and a decrease in inhibition in the iINL. This pattern suggests the potential for decreased inhibition of presumptive amacrine cells in the iINL, due to decreased m2 mAChR, which might result in an increase in GABA, glycine, and ACh release from amacrine cells. Thus, predicting a possible increase in β2 $GABA_A$ receptor subunit expression, as was observed in superarray qPCR, in order to maintain an optimal balance of excitation and inhibition. The m4 mAChR subtype was significantly up-regulated in whole retina as well as in the oINL and GCL, and significantly down-regulated in the iINL. This suggests that there may also be an increase in inhibition via m4 mAChRs in the oINL and GCL and a decrease of inhibition in the iINL. While this raises the possibility of an increase in excitatory neurotransmitter release due to decreased

inhibition of amacrine cells in the iINL, this may also be balanced by increased inhibition via m2 and m4 mAChRs in the oINL and GCL.

The findings of the current study indicate that the absence of α7 nAChRs was not simply correlated with changes in mRNA expression of other AChR subunits or subtypes. Instead, there is a complex picture of increased and decreased expression of different AChR subunits or subtypes, with variation within different retinal cell populations. Pharmacological treatments of AD or schizophrenia by means of simple up-regulation of cholinergic activity, as with the use of acetylcholinesterase inhibitors, may not provide enough specific up- or down-regulation of the appropriate AChR subunits or subtypes to treat visual symptoms. However, cholinergic agents with more specific subtype activity, such as α5 nAChR blockers, may be viable targets for drug development.

References

Alexander, S.P., Mathie, A. & Peters, J.A. (2007). Guide to Receptors and Channels, 2nd edition (2007 Revision). British Journal of Pharmacology, 150, 1-168.

Alkondon, M. & Albuquerque, E.X. (2001). Nicotinic acetylcholine receptor α7 and α4β2 subtypes differentially control GABAergic input to CA1 neurons in rat hippocampus. Journal of Neurophysiology, 86, 3043-3055.

Arias, H.R. (2000). Localization of agonist and competitive antagonist binding sites on nicotinic acetylcholine receptors. Neurochemistry International, 36, 595-645.

Arias, H.R., Richards, V.E., Ng, D., Ghafoori, M.E., Le, V. & Mousa, S.A. (2009). Role of non-neuronal nicotinic acetylcholine receptors in angiogenesis. The International Journal of Biochemistry and Cell Biology, 41, 1441-1451.

Baldridge, W.H. (1996). Optical recordings of the effects of cholinergic ligands on neurons in the ganglion cells layer of mammalian retina. Journal of Neuroscience, 16, 5060-5072.

Brown, D.A., Abogadie, F.C., Allen, T.G., Buckley, N.J., Caulfield, M.P., Delmas, P., Haley, J.E., Lamas, J.A. & Selvanko, A.A. (1997). Muscarinic mechanisms in nerve cells. Life Sciences, 60, 1137-1144.

Caulfield, M.P. & Birdsall, N.J. (1998). International Union of Pharmacology. XVII. Classification of muscarinic acetylcholine receptors. Pharmacological Review, 50, 279-290.

Clementi, F., Fornasari, D. & Gotti, C. (2000). Neuronal nicotinic acetylcholine receptors: from structure to therapeutics. Trends in Pharmacological Sciences, 21, 35-37.

Coyle, J.T., Price, D.L. & DeLong, M.R. (1983). Alzheimer's disease: a disorder of cortical cholinergic innervation. Science, 219, 1184-1190.

Dmitrieva, N.A., Strang, C.E. & Keyser, K.T. (2007). Expression of α 7 nicotinic acetylcholine receptors by bipolar, amacrine, and ganglion cells of the rabbit retina. Journal of Histochemical Cytochemistry, 55, 461-476.

Dulon, D., Lenoir, M. (1996). Cholinergic responses in developing outer hair cells of the rat cochlea. European Journal of Neuroscience, 8, 1945-1952.

Elgoyhen, A.B., Vetter, D.E., Katz, E., Rothlin, C.V., Heinemann, S.F. & Boulter, J. (2001). α10: A determinant of nicotinic cholinergic receptor function in mammalian vestibular and cochlear mechanosensory hair cells. Proceedings of the National Academy of Sciences, 98, 3501-3506.

Erostegui, C., Norris, C.H., Bobbin, R.P. (1994). In vitro characterization of a cholinegic receptor on outer hair cells. Hearing Research, 74, 135-147.

Evans, M. (1996). Acetylcholine activates two currents in guinea-pig outer hair cells. Journal of Physiology, 491, 563-578.

Fuchs, P.A. & Murrow, B.W. (1992). A novel cholinergic receptor mediates inhibition of chick cochlear hair cells. Proceedings: Biological Sciences, 248, 35-40.

Galli-Resta, L., Novelli, E., Volpini, M. & Strettoi, E. (2000). The spatial organization of cholinergic mosaics in the adult mouse retina. European Journal of Neuroscience, 12, 3819-3822.

Gerzanich, V., Wang, F., Kuryatov, A. & Lindstrom, J. (1998). α5 subunit alters desensitization, pharmacology, Ca^{++} permeability and Ca^{++} modulation of human neuronal α3 nicotinic receptors. The Journal of Pharmacology and Experimental Therapeutics, 286, 311-320.

Gotti, C., Fornasaru, D. & Clementi, F. (1997). Human neuronal nicotinic receptors. Progress in Neurobiology, 53, 199-237.

Gu, Y.H., Zhang, Z.M., Long, T., Li, L., Hou, B.K., & Guo, Q. (2003) A naturally occurring rat model of X-linked cone dysfunction. Investigative Ophthalmology and Visual Science, 44, 5321-5326.

Hadingham, K.L., Wingrove, P.B., Wafford, K.A., Bain, C., Kemp, J.A., Palmer, K.J., Wilson, A.W., Wilcox, A.S., Sikela, J.M., Ragan, C.I. & Whiting, P.J. (1994). Role of the beta subunit in determining the pharmacology of human gamma-aminobutyric acid type A receptors. Molecular Pharmacology, 44, 1211-1218.

Haverkamp, S. & Wassle, H. (2000). Immunocytochemical analysis of the mouse retina. The Journal of Comparative Neurology, 424, 1-23.

Housley, G.D., Ashmore, J.F. (1991). Direct measurement of the action of acetylcholine on isolated outer hair cells of the guinea pig cochlea. Proceedings of the Royal Society London B, 244, 161-167.

Ikonomovic, M.D., Mufson, E.J., Wuu, J., Bennett, D.A. & DeKosky, S.T. (2005). Reductio of choline acetyltransferase activity in primary visual cortex in mild to moderate Alzheimer's disease. Archives of Neurology, 62, 425-430.

Jackson, K.J., Marks, M.J., Vann, R.E., Chen, X., Gamage, T.E., Warner, J.A. & Damaj, M.I. (2010). Role of alpha5 nicotinic acetylcholine receptors in pharmacological and behavioral effects of nicotine in mice. Journal of Pharmacology and Experimental Therapeutics, 334, 137-146.

Johnson, D., Martinez, J., Elgoyhen, A., Heinemann, S., McIntosh, J. (1995). α-Conotoxin Im1 exhibits subtype-specific nicotinic acetylcholine receptor

blockade: preferential inhibition of homomeric α7 and α9 receptors. Molecular Pharmacology, 48, 194-199.

Karlin, A. (2002). Emerging structure of the nicotinic acetylcholine receptors. National Review of Neuroscience, 3, 102-114.

Katz, E., Verbitsky, M., Rothlin, C.V., Vetter, D.E., Heinemann, S.F. & Elgoyhen, A.B. (2000). High calcium permeability and calcium block of the alpha9 nicotinic acetylcholine receptor. Hearing Research, 141, 117-128.

Keyser, K.T., MacNeil, M.A., Dmitrieva, N., Wang, F., Masland, R.H. & Lindstrom, J.M. (2000). Amacrine, ganglion, and displaced amacrine cells in the rabbit retina express nicotinic acetylcholine receptors. Visual Neuroscience, 17, 743-752.

Khiroug, S.S., Harkness, P.C., Lamb, P.W., Sudweeks, S.N., Khiroug, L., Millar, N.S. & Yakel, J.L. (2002). Rat nicotinic ACh receptor α7 and β2 subunits co-assemble to form functional heteromeric nicotinic receptor channels. Journal of Physiology, 540, 425-434.

Kittila, C.A. & Massey, S.C. (1997). Pharmacology of directionally selective ganglion cells in the rabbit retina. Journal of Neurophysiology, 77, 675-689.

Kubo, Y., Adelman, J.P., Clapham, D.E., Jan, L.Y., Karschin, A., Kurachi, Y., Lazdunski, M., Nichols, C.G., Seino, S. & Vandenberg, C.A. (2005). International Union of Pharmacology. LIV. Nomenclature and molecular relationships of inwardly rectifying potassium channels. Pharmacological Reviews, 57, 509-526.

Leonard, S. & Freedman, R. (2006). Genetics of chromosome 15q13-q14 in schizophrenia. Biological Psychiatry, 60, 115-122.

Lindstrom, J., Anand, R., Gerzanich, V., Peng, X., Wang, F. & Wells, G. (1996). Structure and function of neuronal nicotinic acetylcholine receptors. Progress in Brain Research, 109, 125-137.

Lindstrom, J.M. (2000). The structures of neuronal nicotinic receptors. In Handbook of Experimental Pharmacology, Vol 144, ed. Clementi, F., Fornasari, D. & Gotti, C., pp. 101-162. Berlin Heidelburg: Springer-Verlag.

Liu, J., McGlinn, A.M., Fernandes, A.I., Milam, A.H., Strang, C.E., Andison, M.E., Lindstrom, J.M., Keyser, K.T. & Stone, R.A. (2009). Nicotinic acetylcholine receptor subunits in rhesus monkey retina. Investigative Ophthalmology and Vision Sciences, 50, 1408-1415.

McGehee, D.S. (1999). Molecular diversity of neuronal nicotinic acetylcholine receptors. Annals of the New York Academy of Sciences, 868, 565-577.

Morley, B.J. & Rodriguez-Sierra, J.F. (2004). A phenotype for the α7 nicotinic acetylcholine receptor null mutant. Brain Research, 1023, 41-47.

Nolan, T., Hands, R.E. & Bustin, S.A. (2006). Quantification of mRNA using real-time RT-PCR. Nature Protocols, 1, 1559-1582.

Nordberg, A. (1999). PET studies and cholinergic therapy in Alzheimer's disease. Review Neurology, 155, 53-S63.

Origlia, N., Valenzano, D.R., Moretti, M., Gotti, C. & Domenici, L. (2012). Visual acuity is reduced in alpha 7 nicotinic receptor knockout mice. Investigative Opthalmology and Visual Science, 53, 1211-1218.

Paylor, R., Nguyen, M., Crawley, J.N., Patrick, J., Beaudet, A. & Orr-Urtreger, A. (1998). α7 nicotinic receptor subunits are not necessary for hippocampal-dependent learning or sensorimotor gating: a behavioral characterization of Acra7-deficient mice. Learning and Memory, 5, 302-316.

Plazas, P.V., Katz, E., Gomez-Casati, M.E., Bouzat, C. & Elgoyhen, B. (2005). Stoichiometry of the α9/α10 nicotinic cholinergic receptor. The Journal of Neuroscience, 25, 10905-10912.

Rothlin, C., Verbitsky, M., Katz, E., Elgoyhen, A.B. (1999). The α9 nicotinic acetylcholine receptor shares pharmacological properties with type A γ-aminobutyric acid, glycine and type 3 serotonin receptors. Molecular Pharmacology, 55, 248-254.

Sargent, P. (1993). The diversity of neuronal nicotinic acetylcholine receptors. Annual Review of Neuroscience, 16, 403-443.

Strang, C.E., Renna, J.M., Amthor, F.R. & Keyser, K.T. (2007). Nicotinic acetylcholine receptor expression by directionally selective ganglion cells. Visual Neuroscience, 24, 523-533.

Strang, C.E., Renna, J.R., Amthor, F.R. & Keyser, K.T. (2010). Muscarinic acetylcholine receptor localization and activation effects on ganglion response properties.

Taylor, P. (1990). Cholinergic agonists. The Pharmacological Basis of Therapeutics. Permagon Press, New York, 122-149.

Tichopad, A., Dilger, M., Schwarz, G. & Pfaffl, M.W. (2003). Standardized determination of real-time PCR efficiency from a single reaction set-up. Nucleic Acids Research, 31, 122.

Weisstaub, N., Vetter, D.E., Elgoyhen, A.B. & Katz, E. (2002). The alpha9alpha10 nicotinic receptor is permeable to and is modulated by divalent cations. Hearing Research, 167, 122-135.

Xu, J., Pato, M.T., Torre, C.D., Medeiros, H., Carvalho, C., Basile, V.S., Bauer, A., Dourado, A., Valente, J., Soares, M.J., Macedo ,A.A., Coelho, I., Ferreira, C.P., Azevedo, M.H., Macciardi, F., Kennedy, J.L. & Pato, C.N. (2001). Evidence for

linkage disequilibrium between the α7-nicotinic receptor gene (CHRNA7) locus and schizophrenia in Azorean families. American Journal of Medical Genetics, 105, 669-674.

Yamahita, T. & Isa, T. (2003). Fulfenamic acid sensitive, Ca(2+)-dependent inward current induced by nicotinic acetylcholine receptors in dopamine neurons. Neuroscience Research, 19, 465-480.

Zhang, J. & Berg, D.K. (2007). Reversible inhibition of GABAA receptors by α7-containing nicotinic receptors on the vertebrate postsynaptic neurons. Journal of Physiology, 579, 753-763.

Zhou, Z.J. & Zhao, D. (2000). Coordinated transitions in neurotransmitter systems for the initiation and propagation of spontaneous retinal waves. Journal of Neuroscience, 20, 6570-6577.

Table 1. Superarray qPCR Screening Targets and Fold Change between WT and α7 nAChR KO Mice

Target	Description	Fold Change
Accn1	amiloride-sensitive cation channel 1, neuronal, hair cell	-1.03
Accn2	neuronal asic 1a	-1.17
Accn3	amiloride-sensitive cation channel 3, dorsal root ganglion	1.06
Cacna1a	calcium channel, voltage-dependent, P/Q type, α 1A, brain	1.17
Cacna1b	calcium channel, voltage-dependent, N type, α 1B, brain sensory	1.00
Cacna1g	calcium channel, voltage-dependent, T type cardiac and brain	-1.03
Cacna1h	calcium channel, voltage-dependent, T type, α 1H, neuronal	-1.08
Cacnb3	calcium channel, voltage-dependent, β 3 subunit, olfactory bulb	-1.03
Cacnb4	voltage gated calcium channel lymphocytes, cardiac and absence seizures	-1.07
Cftr	CFTR	1.15
Chat	choline acetyltransferase (Chat)	1.09
Chrm1	cholinergic receptor, muscarinic 1 brain	**-1.78***
Chrm2	cholinergic receptor, muscarinic 2, cardiac	1.18
Chrm3	cholinergic receptor, muscarinic 3, cardiac	1.17
Chrm4	cholinergic receptor, muscarinic 4 brain	1.12
Chrm5	cholinergic receptor, muscarinic 5 brain	-1.16
Chrna1	cholinergic receptor, nicotinic, α polypeptide 1	-1.08
Chrna2	cholinergic receptor, nicotinic, α polypeptide 2	1.06
Chrna3	cholinergic receptor, nicotinic, α polypeptide 3	-1.15
Chrna4	cholinergic receptor, nicotinic, α polypeptide 4, brain	-1.12
Chrna5	cholinergic receptor, nicotinic, α polypeptide 5	**-1.50***
Chrna6	cholinergic receptor, nicotinic, α polypeptide 6	-1.07
Chrna7	cholinergic receptor, nicotinic, α polypeptide 7	**-103.61*****
Chrna9	cholinergic receptor, nicotinic, α polypeptide 9	1.72
Chrna10	cholinergic receptor, nicotinic, α polypeptide 10	1.33
Chrnb1	cholinergic receptor, nicotinic, β polypeptide 1, motor neurons	1.18
Chrnb2	cholinergic receptor, nicotinic, β polypeptide 2	1.00
Chrnb4	cholinergic receptor, nicotinic, β polypeptide 4	-1.06
Htr3a	5HT 3a	-1.13
Chrnb3	cholinergic receptor, nicotinic, β polypeptide 3	1.05
Clca1	chloride channel calcium activated 1 (Clca1), brain	-1.03
Clcn2	chloride channel 2, astrocytes, salivary gland	1.20
Clcn4-2	chloride channel 4-2 (Clcn4-2), taste bud, brain	1.15
Clcn6	chloride channel 6 , brain	-1.07
Gabra1	λ-aminobutyric acid (GABA-A) receptor, subunit α 1	1.02
Gabra2	λ-aminobutyric acid (GABA-A) receptor, subunit α 2	-1.10
Gabra3	λ-aminobutyric acid (GABA-A) receptor, subunit α 3	-1.07
Gabra4	λ-aminobutyric acid (GABA-A) receptor, subunit α 4	1.15
Gabra5	λ-aminobutyric acid (GABA-A) receptor, subunit α 5	1.08
Gabra6	λ-aminobutyric acid (GABA-A) receptor, subunit α 6	NA
Gabrb2	λ-aminobutyric acid (GABA-A) receptor, subunit β 2	**1.19***
Gabrb3	λ-aminobutyric acid (GABA-A) receptor, subunit β 3	1.07
Gabrd	λ-aminobutyric acid (GABA-A) receptor, subunit Δ	1.03
Gabrg1	λ-aminobutyric acid (GABA-A) receptor, subunit λ 1	1.08

* $p<0.05$ ***$p<0.001$

Table 1 cont. Superarray qPCR Screening Targets and Fold Change between WT and α7 nAChR KO Mice

Target	Description	Fold Change
Gabrg2	λ-aminobutyric acid (GABA-A) receptor, subunit λ 2	1.16
Gabrp	λ-aminobutyric acid (GABA-A) receptor, π	-1.36
Gabrq	λ-aminobutyric acid (GABA-A) receptor, subunit θ	-1.04
Gabrr1	λ-aminobutyric acid (GABA-C) receptor, subunit ρ 1	-1.09
Gabrr2	λ-aminobutyric acid (GABA-A) receptor, subunit ρ 2	1.10
Gabrr3	λ-aminobutyric acid (GABA-A) receptor, subunit ρ 3	1.07
Glra1	glycine receptor α 1	1.09
Glra2	glycine receptor, α 2 subunit	1.15
Glra3	glycine receptor, α 3 subunit	-1.20
Glra4	glycine receptor, α 4	1.01
Glrb	glycine receptor, β subunit	-1.06
Kcna2	potassium voltage-gated channel, shaker-related, brain and spinal cord	1.02
Kcna6	potassium voltage-gated channel, shaker-related, brain	-1.04
Kcnc4	potassium voltage gated channel, Shaw-related, neurotransmitter release	1.06
Kcnd1	potassium voltage-gated channel, Shal, brain	-1.01
Kcnh2	potassium voltage-gated channel, subfamily H, brain , ear	-1.03
Kcnj3	potassium inwardly-rectifying channel, subfamily J, spinal interneurons	-1.09
Kcnj4	frontal cortex pyramidal neurons HCN, Kir2, and Kleak	**-1.98***
Kcnj6	potassium inwardly-rectifying channel, subfamily J, brain	1.01
Kcnn2	potassium channel calcium-activated, subfamily N, synaptic plasticity	1.21
Kcnn3	potassium intermediate/small conductance, Ca^{2+} activated, N type, brain	-1.28
Kcnq2	potassium voltage-gated channel, subfamily Q, hippocampus	1.02
Kcnq3	potassium voltage-gated channel, subfamily Q, member 3, brain	1.18
Ryr3	ryanodine receptor 3	1.22
Scn1a	sodium channel, voltage-gated, type I, brain	1.08
Scn1b	sodium channel, voltage-gated, type I, β brain & cardiac	-1.12
Scn5a	sodium channel, voltage-gated, type V, cardiac and brain	1.29
Scn7a	sodium channel, voltage-gated, type VII, sodium concentration sensor, taste	1.07
Slc5a7	solute carrier family 5 (high affinity choline transporter), member 7	-1.01
Gria1	AMPA 1 cereblum	1.03
Gria2	AMPA 2 synaptic	1.14
Gria3	AMPA 3, als	1.14
Gria4	AMPA 4 alcohol use	1.19
Grik1	kainate 1 presynaptic	1.06
Grik2	kainate 2 mossy fiber, synaptic plasticity	1.11
Grik5	kainate 5 mossy fiber	1.15
Grin1	NMDA NR1 brain	-1.05
Grin2a	NMDA NR2a brain	-1.08
Grin2b	NMDA NR2b brain	1.17
Grin2c	NMDA NR2c brain	1.13
Grin2d	NMDA NR2d brain	-1.16
Grin3a	NMDA NR3a	1.04
Grin3b	NMDA3b motor neurons	1.09
Vdac1	voltage-dependent anion channel 1	1.02
Hsp90ab1	heat shock protein 90 α (cytosolic), class B member 1	1.16
Actb	actin, β	Avg Ct=22.3
Gapdh	glyceraldehyde-3-phosphate dehydrogenase	Avg Ct=23.4
Gusb	glucuronidase, β	Avg Ct=32.6
Hprt1	hypoxanthine guanine phosphoribosyl transferase 1	Avg Ct=23.8
MGDC	mouse genomic DNA contamination	No amp
RTC	reverse transcription control	No amp
PPC	positive PCR control	Avg Ct=18

* $p<0.05$ ***$p<0.001$

Table 2. Acetylcholine Receptor Primer Pairs

Subunit	Accession Number	F- Sense R- Antisense	Product (bp)	Temp (C°)	Primer Ratio (nmol)	Product Homology to Mouse Sequence
α2 nAChR	NM_144803	**F-** GTGCCCAACACTTCCGATG **R-**TGTAGTCATTCCATTCCTGCTTT	126	55.8	F400:R600	92%
α3 nAChR	NM_145129	**F-** CCAGTTTGAGGTGTCTATGTC **R-** TCGGCGTTGTTGTAAAGC	198	55.8	F300:R200	99%
α4 nAChR	NM_015730	**F-**CTCAGATGTGGTCCTTGTC **R-** GAGTTCAGATGGGATGCG	178	62.6	F500:R400	95%
α5 nAChR	NM_176844	**F-** CATCGTTTTGTTTGATAATGC **R-** TGCGTCCAAGTGACAGTG	90	55.8	F500:R300	84%
α6 nAChR	NM_021369	**F-** TGTCTCCGATCCCGTCAC **R** TTGTTATACAGAACGATGTCAGG	213	62.6	F600:R500	98%
α7 nAChR	NM_007390	**F-**GGTCATTTGCCCACTCTG **R-** GACAGCCTATCGGGTGAG	130	57.6	F500:R500	99%
α9 nAChR	NM_001081104	**F-** ACAAGGCCACCAACTCCA **R-** ACCAACCCACTCCTCCTCTT	152	54.0	F400:R400	81%
α10 nAChR	NM_001081424	**F-** TCTGACCTCACAACCCACAA **R-** TCCTGTCTCAGCCTCCATGT	168	54.0	F500:R400	94%
β2 nAChR	NM_009602	**F-**CCGGCAAGAAGCCGGGACCT **R-** CTCGCTGACACAAGGGCTGCG	152	62.6	F300:R400	97%
β3 nAChR	NM_173212	**F-** AAGAAGCAGACTCCTACC **R-** AACAACCTGACTGATGAAG	123	62.6	F200:R600	90%
β4 nAChR	NM_148944	**F-** CTACAGGAAGCATTAGAGG **R-** CAGAATACACACAATCACG	146	50.0	F300:R200	84%
m1 mAChR	NM_007698	**F-**GACCCTACAGACCCCTCTCC **R-** CCCTTCCTCCAGTCACAAGA	165	66.2	F600:R500	93%
m2 mAChR	NM_203491	**F-**CGGCTTTCTATCTGCCTGTC **R-** GGCATGTTGTTGTTGTTTGG	169	50.0	F100:R400	96%
m3 mAChR	NM_033269	**F-**GTACAACCTCGCCTTTGTTTCC **R-** GACAAGGATGTTGCCGATGATG	244	62.6	F400:R200	99%
m4 mAChR	NM_007699	**F-**GCCTTCATCCTCACCTGGAC **R-** AGTGGCATTGCAGAGTGCAT	146	62.6	F400:R200	99%
m5 mAChR	NM_205783	**F-** CCATGGACTGTGGGAAGTCA **R-** CAGCGTCCCATGAGGATGTA	215	62.6	F300:R200	99%
RyR3	NM_177652	**F-** AAGGTCATACTCCATCAGG **R-** AATAAGGCGGTTGTGTTC	110	50.0	F400:R200	98%

*Primers adapted from Smith et al., 2013, in preparation.

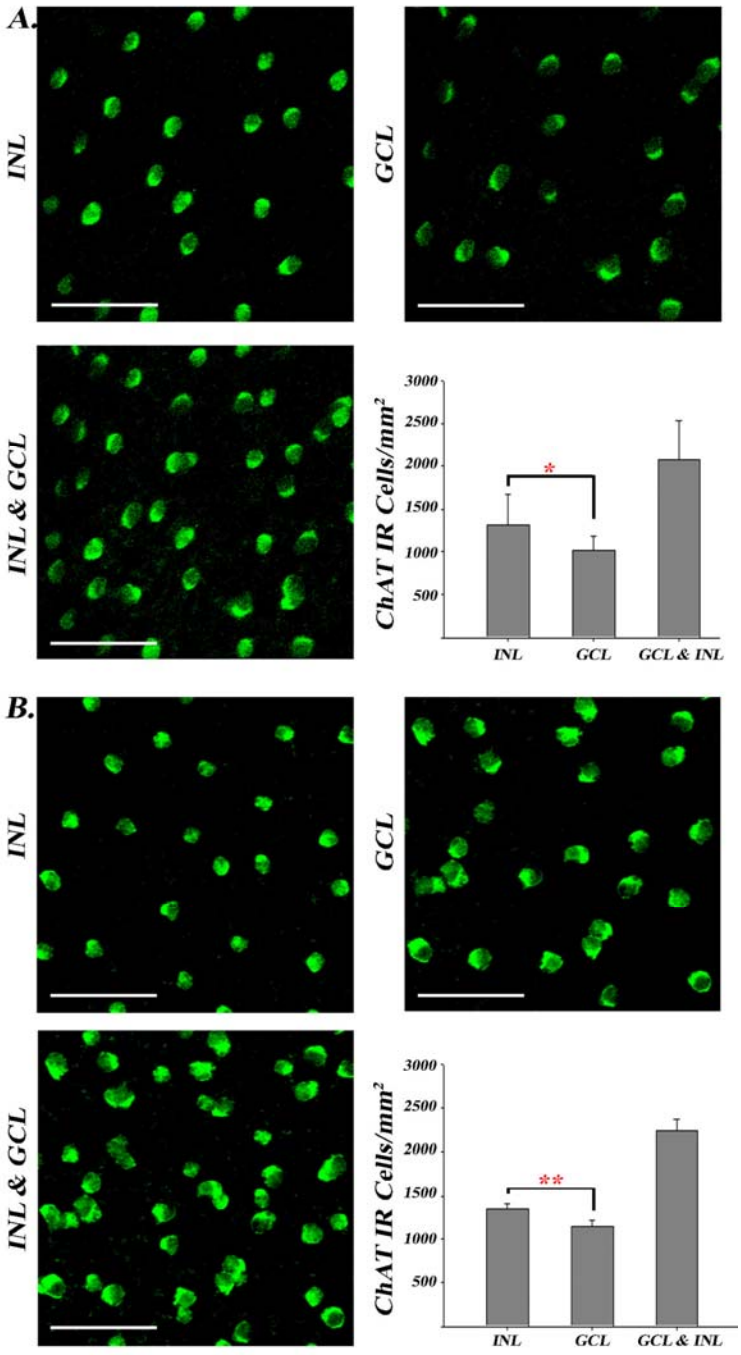

Figure 1. Wholemount ChAT IHC. Showed a significant increase in the number of ChAT immunoreactive amacrine cells in the INL as compared to the GCL in both WT C57BL/6J mice ($p<0.05$) and the α7 nAChR KO mice ($p<0.001$). There was no significant difference between WT and α7 nAChR KO mice. Scale bar, 50μm.

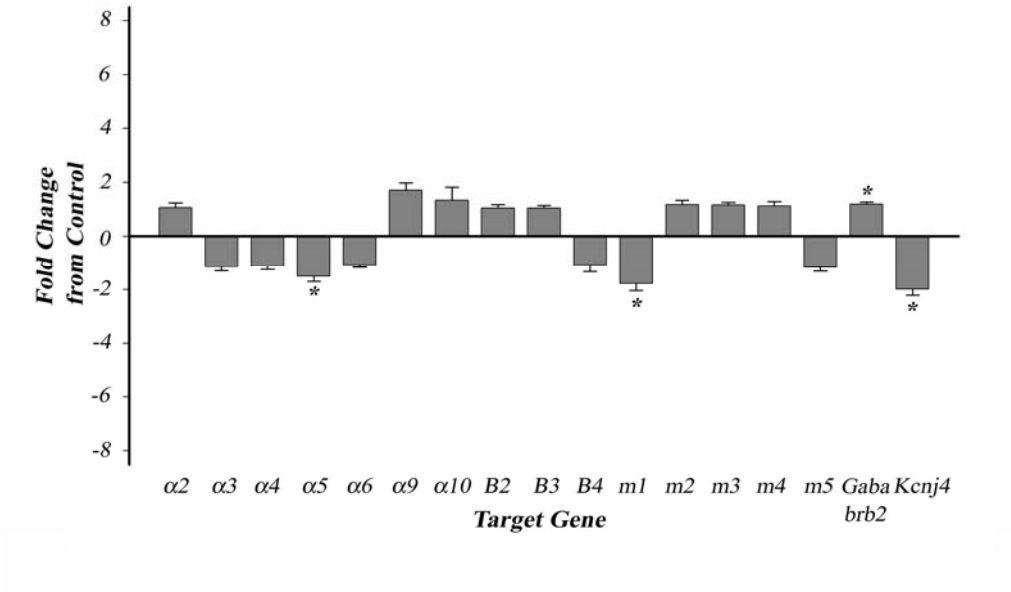

Figure 2. Superarray qPCR screening fold changes in mouse retina. Error bars represent standard error of the mean. *$p < 0.05$

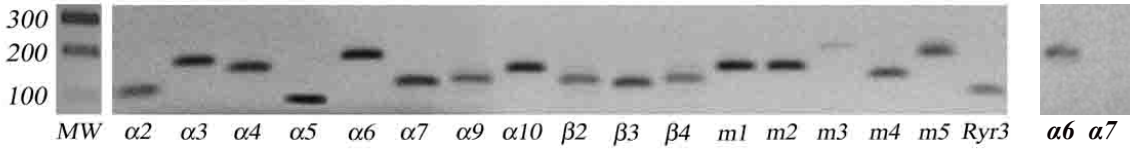

Figure 3. 2.5% agarose gel of acetylcholine receptor qPCR products. (Left) Products obtained from WT mouse retinal RNA extracts, using custom designed primers for α2-α7, α9, α10 and β2-β4 nAChR subunits as well as m1-m5 mAChR subtypes are shown. (Right) Products obtained from α7 nAChR KO retinal RNA extracts, using primers for α6 and α7 nAChR subunits.

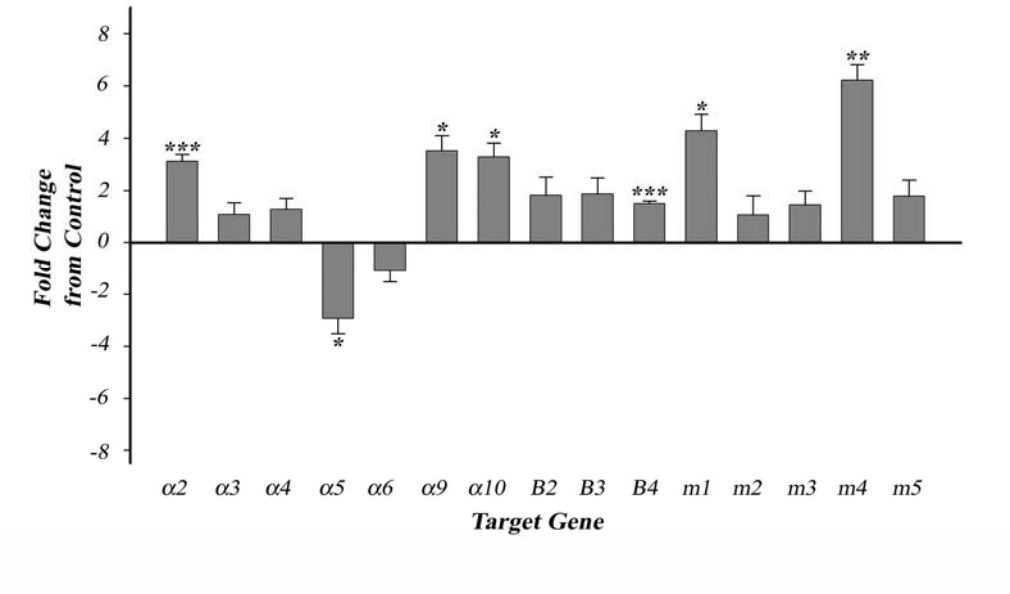

Figure 4. Acetylcholine receptor qPCR fold changes in whole mouse retina. Error bars represent standard error of the mean. *p < 0.05, **p < 0.01, ***p < 0.001

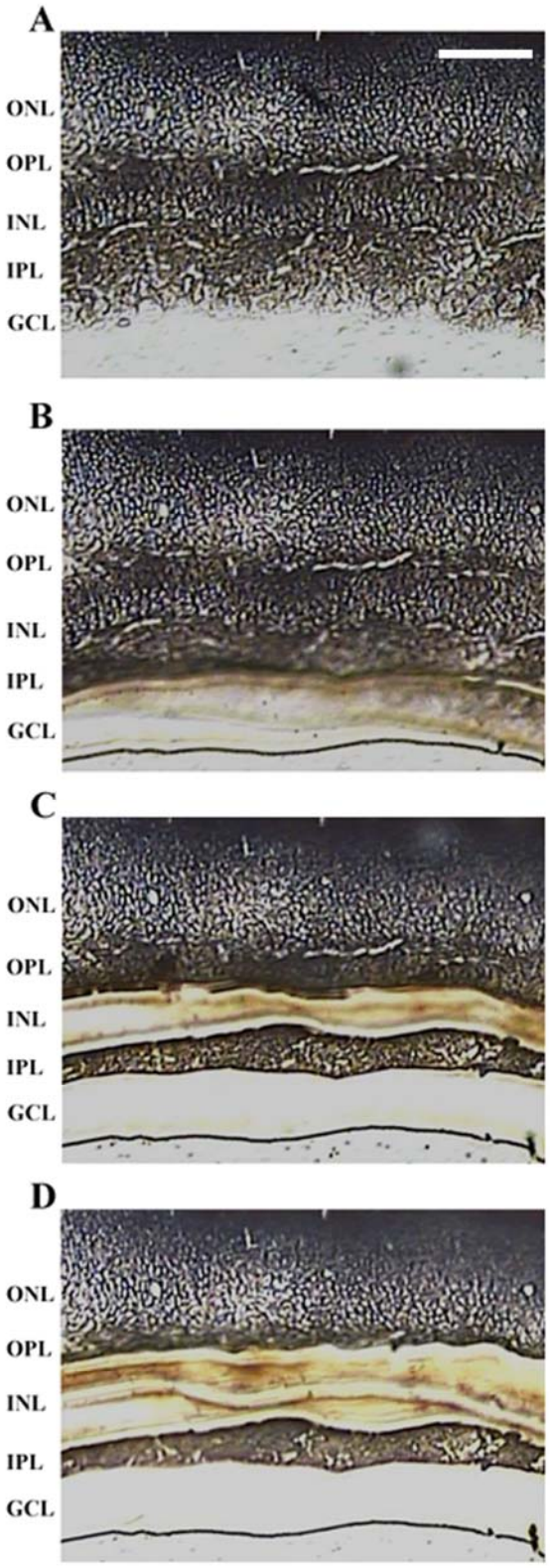

Figure 5. Images of vertical sections depicting laser capture microdissection of the unfixed mouse retina. Vertical section of unfixed, mouse retina (A) before laser capture microdissection, (B) after dissection of GCL, (C) after LCM of GCL and the inner portion of the INL, and (D) after dissection of the GCL, the inner portion of the INL and the outer portion of the INL.

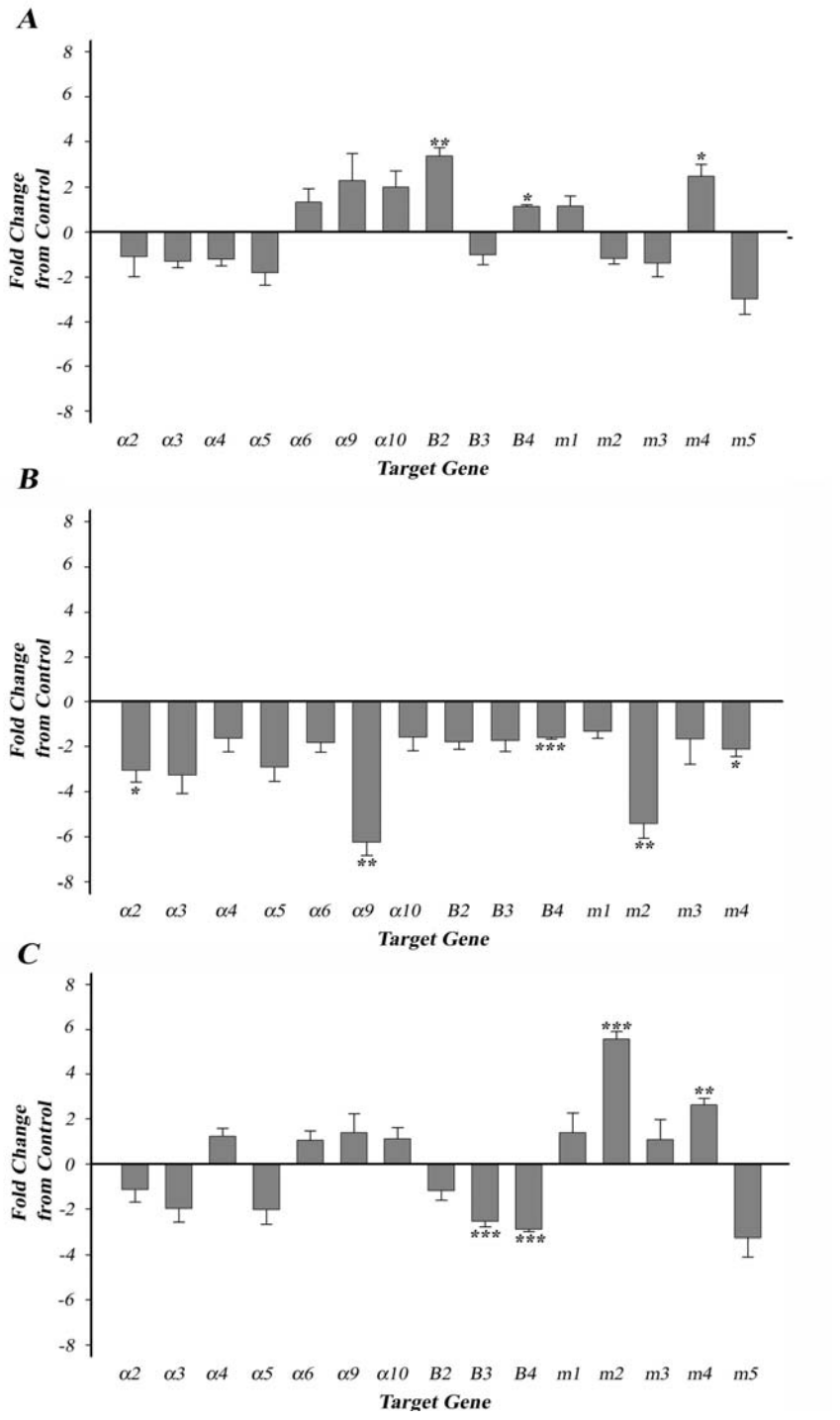

Figure 6. Acetylcholine receptor qPCR fold changes in the mouse outer INL, inner INL, and GCL. Fold changes in the (A) outer INL, (B) inner INL, and (C) GCL. Error bars represent standard error of the mean. *p < 0.05, **p < 0.01, ***p < 0.001

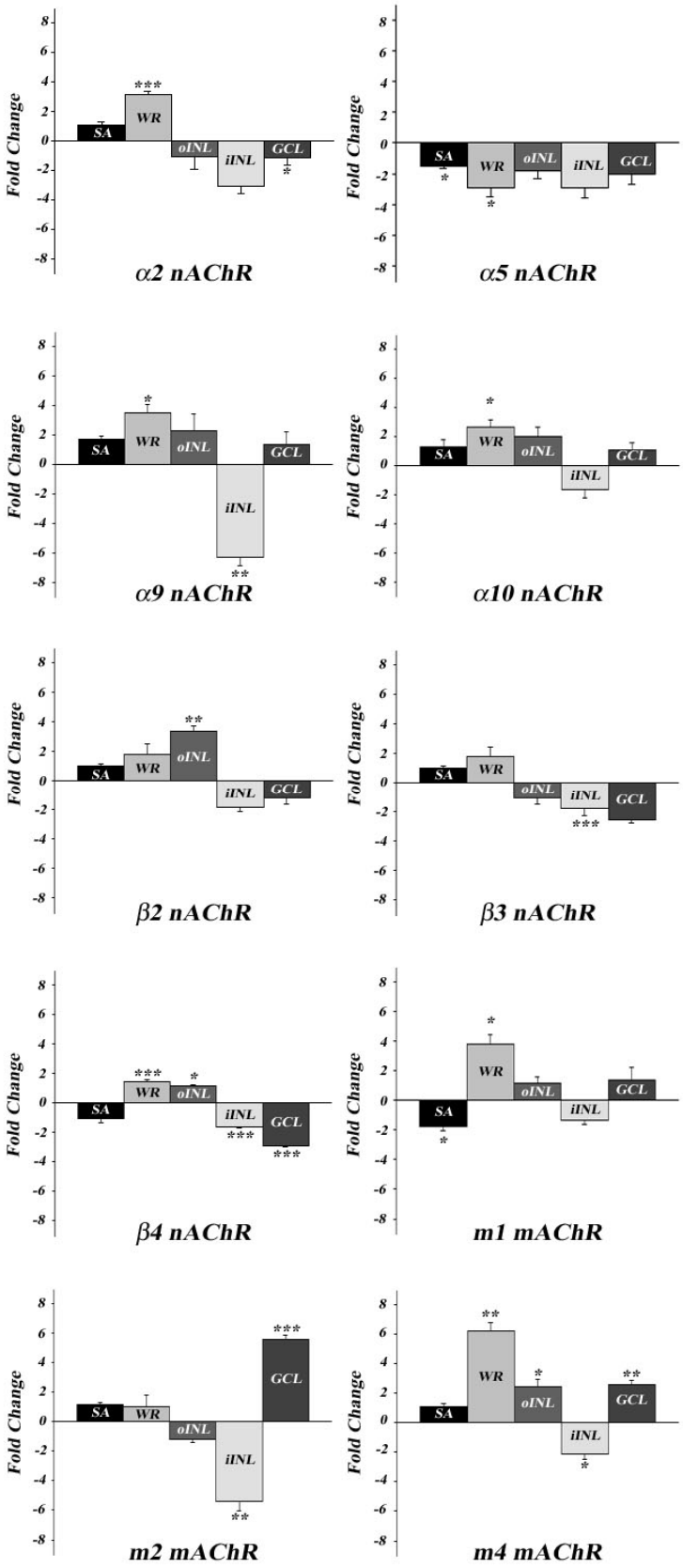

Figure 7. Comparison of significant qPCR targets across experiments. Error bars represent standard error of the mean. SA- superarray, WR- whole retina, oINL- outer portion of INL, iINL- inner portion of INL, GCL- ganglion cell layer *p < 0.05, **p < 0.01, ***p < 0.001

GLOBAL SUMMARY

AChRs are expressed throughout the nervous system, including within the retinal inner neurons (Keyser et al., 2000; Dmitrieva et al., 2007; Liu et al., 2007). Despite the existence of several AChR KO mice, the distribution in the mouse retina has not been previously examined. Of particular interest to us was the α7 nAChR KO mouse model. We are interested in the α7 nAChR KO mouse model because not only are α7 nAChRs expressed throughout the retina, but these receptors are affected in disease states such as AD and schizophrenia, which have visual deficits (Coyle et al., 1983; Nordberg et al., 1999; Xu et al., 2001; Leonard & Freedman, 2006; Dmitrieva et al., 2007). While it is not clear if the link between α7 nAChRs and disease is causal, one could predict that an α7 nAChR KO mouse would display significant phenotypic effects. However, the phenotype of the α7 nAChR KO mouse is quite mild, which could be attributed to the absence of the α7 nAChR throughout development as opposed to changes after reaching adulthood. The nervous system is more plastic early in development than it is upon adulthood, so it is possible that the nervous system simply compensated for the loss in the KO mouse by up-regulating other receptors. This led to the hypothesis that the mild phenotype was due to compensatory up-regulation of other AChRs with similar characteristics to α7 nAChR, particularly those with high calcium permeability. This compensation would not occur naturally in the less plastic adult nervous system, but mimicking any compensatory changes observed in the α7 nAChR KO mouse could provide treatment options in AD and schizophrenia. Prior to investigation of compensatory effects in the α7 nAChR KO

mouse, AChR expression patterns in the mouse retina needed to be established. In order to investigate the mild phenotype of the α7 nAChR KO mouse, the following aims were proposed; 1) to determine the expression patterns of cholinergic amacrine cells and AChRs in the retina of the WT C56BL/6J mouse and 2) to determine if there is compensatory up- or down-regulation of AChRs in the retina of the α7 nAChR KO mouse. We hypothesized that the expression patterns of cholinergic amacrine cells and AChRs in the mouse retina would be similar to the patterns seen in other species and that there would be up-regulation of other nAChR subunits or mAChR subtypes to balance the absence of the α7 nAChR subunit in the α7 nAChR KO mouse.

Specific Aim I

Data for Specific Aim I partially confirmed the hypothesis that the expression patterns of AChRs in the mouse retina would be similar to other mammals. We investigated the expression of AChR RNA in WT mice with RT-PCR, resulting in detection of α2, α3, α4, α5, α6, α7, α9, α10, β2, β3, and β4 nAChRs as well as m1-m5 mAChRs. Then we investigated the protein expression of AChR in WT mice with immunohistochemistry. For the most part expression patterns of AChRs in the mouse retina were similar to other mammals, with a few exceptions. Amacrine cells, bipolar cells, ganglion cells, and much of the IPL were immunoreactive to antibodies against α3 and α5 nAChR subunits. However, in the rabbit retina, bipolar cells were not immunoreactive to antibodies against α3 and α5 nAChR subunits. Additionally, antibodies specific for α4 nAChRs showed immunoreactivity similar to that seen with mAb 210. These results suggest that in the mouse retina, bipolar cells express α3, α4, and

α5 nAChR subunits. Thus, in other mammals, α7 nAChRs were expressed by bipolar cells, but in the mouse non-α7 nAChRs were expressed by bipolar cells (Dmitrieva et al., 2007). Activation of α7 nAChRs results in a transient response with fast desensitization; however activation of non-α7 nAChRs, for the most part, results in a more sustained response with slower desensitization (Papke et al., 2000). Thus, the nicotinic-dependent response of bipolar cells may be more sustained and have an influence on the ganglion cell light response in the mouse retina.

Another exciting finding in the mouse retina is the presence of α9 and α10 nAChR subunits, which have never been reported within the retina before. α9 nAChR immunoreactivity was displayed by presumptive bipolar, amacrine and ganglion cells as well as within a dense, broad band in the center of the IPL, within sublamina 2, sublamina 3 and sublamina 4. The single band in westerns using WT retina protein and the elimination of immunoreactivity in western blot experiments using protein from α9 nAChR KO mouse retina confirmed the specificity of the α9 nAChR subunit antibody. α9 nAChR physiology is most similar to α7 nAChR physiology, but with no affinity for nicotine as the other nAChRs do, suggesting a mixed nicotinic-muscarinic physiology (Housley & Ashmore, 1991; Fuchs & Murrow, 1992; Elgoyhen et al., 1994; Erostegui et al., 1994; Johnson et al., 1995; Dulon & Lenoir, 1996; Evans, 1996; Rothlin et al., 1999; Katz et al., 2000). The presence of α9 nAChR subunits within the retina is not just exciting because of its uniqueness; the unique physiology and pharmacology of α9 nAChRs most likely affects the retinal physiology within the mouse retina.

The expression patterns of mAChRs also showed a few differences in mouse as compared to the patterns described in other mammals, and this is the first description of

mAChR expression patterns in the mouse retina. Processing with antibodies specific to m1 mAChRs showed immunoreactivity by ganglion cells and processes in two bands in the IPL. However, in the rabbit, m1 mAChR immunoreactivity was seen in horizontal and amacrine cells as well (Strang et al., 2010). Thus, in the mouse there is a decrease in the excitatory m1 mAChR in the INL as compared to rabbit. There were also differences in expression patterns of the inhibitory m2 and m4 mAChRs. In the rabbit retina, m2 mAChR were expressed by ganglion cells, bipolar cells, and amacrine cells along with intense immunoreactivity in processes in the central sublaminae of the IPL and less intense immunoreactivity in processes in the outer sublaminae of the IPL (Strang et al., 2010). Patterns of m2 mAChR immunoreactivity in mouse were similar, except that immunoreactivity in the IPL was observed in two intense narrow bands within the second and fourth sublamina. This suggests that the types of bipolar cells expressing m2 mAChRs in the rabbit and mouse retina differ. Finally, there was m4 mAChR immunoreactivity displayed by ganglion cells, bipolar cells, amacrine cells and throughout the IPL in mice. In the rabbit, while the expression patterns were similar to mouse, there were no mAb 210 immunoreactive bipolar cells. Thus, in the mouse there was a potential increase in inhibitory mAChRs in the INL as well as a decrease in the excitatory m1 mAChR. While the majority of AChRs showed patterns of immunoreactivity similar to those observed in other mammals, there were some differences, particularly by the bipolar cells. Even small changes in expression patterns of AChRs could affect the physiology of the retina. Thus, these differences in expression of AChRs in the mouse retina suggest that the physiology of the mouse retina differs from

that of other mammals. These differences may be attributed to the different visual needs of the mouse compared to rabbit and non-human primate.

Once we had determined the general distribution of AChRs in the WT mouse, we then addressed Specific Aim II, using qPCR to determine expression of AChRs in WT compared to the α7 nAChR KO mouse.

Specific Aim II

Data for Specific Aim II partially confirmed our hypothesis that there was up-regulation of other AChRs in the α7 nAChR KO mouse. However, while some AChRs were up-regulated in the α7 nAChR KO mouse, other AChRs were down-regulated and expression differences seen in whole retina differed across retinal cell populations. Thus, the differences observed between the WT and the α7 nAChR KO mice retinas were more complex than simple up-regulation of a few AChRs throughout the retina.

ChAT Distribution

One possible mechanism for compensation for the absence of α7 nAChRs in the KO mouse, could be an increase in ACh. Another reason we were interested in ACh levels is that there is evidence of reduced ACh in AD and schizophrenia, which have been linked to reductions in α7 nAChRs. In order to establish any potential differences in ACh levels, we determined the number of ChAT immunoreactive cells within the α7 nAChR KO mouse retina. ChAT immunoreactivity was consistent with that previously reported in the mouse retina as well as other mammals; immunoreactivity within amacrine cells and displaced amacrine cells as well as within two distinct bands in the

IPL (Galli-Resta et al., 2000; Haverkamp & Wassle, 2000). Also consistent with previous reports, there were significantly higher numbers of ChAT immunoreactive cells in the INL than the GCL. However, this was also true for the α7 nAChR KO mouse and there were no statistically significant differences between the WT and α7 nAChR KO mice in regards to the number of ChAT immunoreactive cells. This suggests that there are no differences in level of ChAT and thus ACh in the α7 nAChR KO mouse. So, retinal ACh levels are likely to be equivalent in WT and α7 nAChR KO mouse.

RNA Expression of nAChRs

We hypothesized that AChRs with similar chracteristics to α7 nAChRs, such as high Ca^{2+} permeability, would be up-regulated in the α7 nAChR KO mouse. However, instead of simple up-regulation of AChRs with similar characteristics to α7 nAChRs, there was a more complex change in RNA expression including both up- and down-regulation of AChRs with similar and differing characteristics to α7 nAChRs. Additionally, these changes varied between different retinal cell populations.

Specifically, α2 nAChR subunits were up-regulated in whole retina but down-regulated in the GCL and trending towards down-regulation in the iINL and oINL. α5 nAChR subunits were down-regulated in whole retina and trended towards down-regulation in the oINL, iINL, and GCL. α9 nAChR subunits were up-regulated in whole retina and GCL, trended towards up-regulation in oINL, and significantly down-regulated in iINL. α10 nAChR subunits were up-regulated in whole retina, trended towards up-regulation in oINL and GCL, and trended towards down-regulation in iINL. β2 nAChR subunits trended towards up-regulation in whole retina, were up-regulated in the oINL,

and trended towards down-regulation in the iINL and GCL. B3 nAChR subunits trended towards up-regulation in whole retina, were down-regulated in the iINL, and trended towards down-regulation in the oINL and GCL. β4 nAChR subunits were up-regulated in whole retina and the oINL and down-regulated in the iINL and GCL. m1 mAChR subtypes were up-regulated in whole retina, trended towards up-regulation in the oINL and GCL, and trended towards down-regulation in the iINL. m2 mAChR subtypes trended towards up-regulation in whole retina, were up-regulated in GCL, trended towards down-regulation in the oINL, and were down-regulated in the iINL. Finally, m4 mAChR subtypes were up-regulated in whole retina, oINL, and GCL but down-regulated in iINL.As expected, the α7 nAChR was essentially undetectable in whole retina, GCL, iINL, and oINL, as would be expected for the α7 nAChR in the KO mouse.

The α2 nAChR was up-regulated in whole retina, but was significantly down-regulated in the iINL and trended towards significant down-regulation in the GCL and oINL. The up-regulation of the α2 nAChR seen in whole retina was due to possible changes in expression with the retinal vasculature within the IPL or in macroglial cells within the IPL and was most likely not due to up-regulation in ganglion cells, amacrine cells, horizontal cells, or bipolar cells as our qPCR indicated down-regulation of α2 nAChRs within those cell populations.

The pattern of expression of β3 nAChRs was similar to that of the α2 nAChRs; up-regulation was observed in whole retina, but down-regulation observed within the GCL, iINL and oINL. This suggests that the β3 nAChR may also be decreased within retinal cell populations, but increased within vascular endothelial cells or macroglial cells. Changes in the expression of the α5 nAChR were less complex; the α5 nAChR was

down-regulated in whole retina, GCL, iINL, and oINL. This indicated an overall reduction in α5 nAChR transcripts within ganglion cells, bipolar cells, amacrine cells, and horizontal cells. The α5 nAChRs are less sensitive to nicotine and ACh (Jackson et al., 2010), thus, a reduction of α5 nAChR transcripts suggests decreased α5 nAChRs, which may result in an increased sensitivity to nicotine and ACh in the α7 nAChR KO mice.

Both the α9 nAChR and the α10 nAChR subunits showed overall up-regulation, trends towards up-regulation in the GCL and oINL, and down-regulation in the iINL. This suggests that these nAChR subunits were increased in the ganglion cells, bipolar cells, and horizontal cells while being decreased in the amacrine cells. The α9 nAChRs and the α9α10 nAChRs were the best single candidates for up-regulation in the absence of α7 nAChRs, since the have similar pharmacology and calcium permeability. However, reports also suggest that α9 nAChRs and the α9α10 nAChRs are blocked by nicotine as well as many traditional nAChR agonists (Verbitsky et al., 2000). Thus, expression of other subunits may also need to be changed to perfectly mimic α7 nAChR function in an α7 nAChR KO mouse.

β2 containing nAChRs trended towards up-regulation in the whole retina and were significantly up-regulated in the oINL, but they also trended towards down-regulation in the GCL and iINL. The β4 nAChR had similar patterns of expression as the β2 nAChR; significant up-regulation in whole retina and oINL, but significant down-regulation in GCL and iINL. The β2 and β4 nAChRs were likely increased in bipolar and horizontal cells, but decreased in ganglion and amacrine cells.

RNA Expression of mAChRs

The m1 mAChR subytpe was significantly up-regulated in whole retina, trended towards up-regulation in the GCL and oINL, and trended towards down-regulation in the iINL. In most cell populations within the retina, m1 mAChRs were up-regulated. The effect of m1 mAChR activation is generally excitatory, indicating a possible increase in excitation in the α7 nAChR KO mouse. The m2 mAChR transcripts only trended towards up-regulation in the whole retina, was significantly up-regulated in the GCL, was significantly down-regulated in the iINL, and trended towards down-regulation in the oINL. The m2 mAChR is generally inhibitory, indicating an increase in inhibition in the GCL, but a decrease in inhibition in the INL. Finally, the m2 mAChR was significantly up-regulated in whole retina, GCL, and oINL, but significantly down-regulated in iINL. The m2 mAChR is also generally inhibitory, indicating an increase in inhibition in the GCL and oINL, but a decrease in inhibition in the iINL.

Changes in expression of AChRs in the α7 nAChR KO mouse were complex and varied across retinal cell populations. These results indicate that treatments aimed at simply up-regulating or down-regulating a single nAChR subunit or mAChR subtype is not going to be effective in compensating for the loss of the α7 nAChR. Changes in expression targeted at improving disease states such as AD and schizophrenia must also be as complex as was observed in the α7 nAChR KO mouse. Pharmacological interventions cannot simply affect one target throughout the nervous system; they must instead target several nAChR subunits and mAChR subtypes and, ideally, have different effects in different neuronal cell populations. Furthermore, pharmacological treatments currently in use include acetylcholinesterase inhibitors, which increase cholinergic

activity, would not provide the specific up- and down-regulation changes found in the α7 nAChR KO mouse. However, cholinergic agents with more specific AChR activity, such as α5 nAChR blockers, may be more viable targets for drug development.

GENERAL REFERENCES

Adler, L.E., Hoffer, L.J., Griffith, J., Waldo, M.C. & Freedman, R. (1992). Normalization by nicotine of deficient auditory sensory gating in the relatives of schizophrenics. Biological Psychiatry, 32, 607-616.

Aizenman, E., Frosch, M.P. & Lipton, S.A. (1988). Responses mediated by excitatory amino acid receptors in solitary retinal ganglion cells from rat. The Journal of Physiology, 396, 75-91.

Albuquerque, E.X., Pereira, E.F., Mike, A., Eisenberg, H.M., Maelicke, A. & Alkondon, M. (2000). Neuronal nicotinic receptors in synaptic functions in humans and rats: physiological and clinical relevance. Behavioural Brain Research, 113, 131-141.

Alexander, S.P., Mathie, A. & Peters, J.A. (2007). Guide to Receptors and Channels, 2nd edition (2007 Revision). British Journal of Pharmacology, 150, 1-168.

Alkondon, M., Pereira, E.F. & Albuquerque, E.X. (1998). α-bungarotoxin- and methyllycaconitine-sensitive nicotinic receptors mediate fast synaptic transmission in interneurons of rat hippocampal slices. Brain Research, 810, 257-263.

Alkondon, M. & Albuquerque, E.X. (2001). Nicotinic acetylcholine receptor α7 and α4β2 subtypes differentially control GABAergic input to CA1 neurons in rat hippocampus. Journal of Neurophysiology, 86, 3043-3055.

Arias, H.R. (2000). Localization of agonist and competitive antagonist binding sites on nicotinic acetylcholine receptors. Neurochemistry International, 36, 595-645.

Ambrosini, A., Bresciani, L., Fracchia, S., Brunello, N. & Racagni, G. (1995). Metabotropic glutamate receptors negatively coupled to adenyatle cyclase inhibit N-methyl-D-aspartate receptor activity and prevent neurotoxicity in mesencephalic neurons in vitro. Molecular Pharmacology, 47, 1057-1064.

Amthor, F.R., Oyster, C.W. & Takahashi, E.S. (1984). Morphology of on-off direction-selective ganglion cells in the rabbit retina. Brain Research, 298, 187-190.

Amthor, F.R., Takahashi, E.S. & Oyster, C.W. (1989a). Morphologies of rabbit retinal ganglion cells with complex receptive fields. Journal of Comparative Neurology, 280, 97-121.

Amthor, F.R., Takahashi, E.S. & Oyster, C.W. (1989b). Morphologies of rabbit retinal ganglion cells with concentric receptive fields. Journal of Comparative Neurology, 280, 72-96.

Amthor, F.R. & Grzywacz, N.M. (1993). Directional selectivity in vertebrate retinal ganglion cells. Reviews of Oculomotor Research, 5, 79-100.

Badea, T.C. & Nathans, J. (2004). Quantitative analysis of neuronal morphologies in the mouse retina visualized by using a genetically directed reporter. The Journal of Comparative Neuroscience, 480, 331-351.

Baldridge, W.H. (1996). Optical recordings of the effects of cholinergic ligands on neurons in the ganglion cells layer of mammalian retina. Journal of Neuroscience, 16, 5060-5072.

Barlow, H.B., Hill, R.M. & Levick, W.R. (1964). Retinal ganglion cells responding selectively to direction and speed of image motion in the rabbit. The Journal of Physiology, 173, 377-407.

Berridge, M.J., Lipp, P. & Bootman, M.D. (2000). The versatility and universality of calcium signaling. Nature Reviews Molecular Cell Biology, 1, 11-21.

Bertrand, D., Ballivet, M. & Rungger, D. (1990). Activation and blocking of neuronal nicotinic acetylcholine receptor reconstituted in Xenopus oocytes. Proceedings of the National Academy of Science, 87, 1993-1997.

Blanks, J.C., Torigoe, Y., Hinton, D.R. & Blanks, R.H. (1996a). Retinal pathology in Alzheimer's disease. 1.. Ganglion cell loss in foveal/parafoveal retina. Neurobiology of Aging, 17, 377-384.

Blanks, J.C., Schmidt, S.Y., Torigoe, Y., Porrello, K.V., Hinton, D.R. & Blanks, R.H. (1996b). Retinal pathology in Alzheimer's disease. 2. Regional neuron loss and glial changes in GCL. Neurobiology of Aging, 17, 385-395.

Bloomfield, S.A. (1994). Orientation-sensitive amacrine and ganglion cells in the rabbit retina. Journal of Neurophysiology, 71, 1672-1691.

Britto, L.R., Hamassaki-Britto, D.E., Ferro, E.S., Keyser, K.T., Karten, H.J. & Lindstrom, J.M. (1992). Neurons of the chick brain and retina expressing both α-bungarotoxin-sensitive and α-bungarotoxin-insensitive nicotinic acetylcholine receptors: an immunohistochemical analysis. Brain Research, 590, 193-200.

Brown, D.A., Abogadie, F.C., Allen, T.G., Buckley, N.J., Caulfield, M.P., Delmas, P., Haley, J.E., Lamas, J.A. & Selvanko, A.A. (1997). Muscarinic mechanisms in nerve cells. Life Sciences, 60, 1137-1144.

Brown, D., Ramlochansingh, C., Manaye, K.F. & Tizabi, Y. (2013). Nicotine promotes survival of cells expressing amyloid precursor protein and presenilin: Implication

for Alzheimer's disease. Neuroscience Letters, 2013 Jan 8. pii: S0304-3940(13)00006-2. doi: 10.1016/j.neulet.2012.12.046. [Epub ahead of print]

Caulfield, M.P. & Birdsall, N.J. (1998). International Union of Pharmacology. XVII. Classification of muscarinic acetylcholine receptors. Pharmacological Review, 50, 279-290.

Chang, K.T. & Berg, D.K. (1999). Nicotinic acetylcholine receptors containing α7 subunits are required for reliable synaptic transmission in situ. Journal of Neuroscience, 19, 3701-3710.

Chen, D. & Patrick, J.W. (1997). The α-bungarotoxin-binding nicotinic acetylcholine receptor from rat brain contains only the α7 subunit. Journal of Biological Chemistry, 272, 24024-24029.

Cheon, E.W., Kuwata, O. & Saito, T. (2001). Muscarinic acetylcholine receptors in the normal developing and regenerating newt retinas. Developmental Brain Research, 127, 9-21.

Chu, Z. & Hablitz, J.J. (2000). Quisqualate induces an inward current via mGluR activation in neocortical pyramidal neurons. Brain Research, 879, 88-92.

Clementi, F., Fornasari, D. & Gotti, C. (2000). Neuronal nicotinic acetylcholine receptors: from structure to therapeutics. Trends in Pharmacological Sciences, 21, 35-37.

Cohen, E.D. & Miller, R.F. (1994). The role of NMDA and non-NMDA excitatory amino acid receptors in the functional organization of primate retinal ganglion cells. Visual Neuroscience, 11, 317-332.

Couturier, S., Bertrand, D., Matter, J.M., Hernandez, M.C., Bertrand, S., Millar, N., Valera, S., Barkas, T. & Ballivet, M. (1990). A neuronal nicotinic acetylcholine receptor subunit (α7) is developmentally regulated and forms a homo-oligomeric channel blocked by α-BTX. Neuron, 5, 847-856.

Coyle, J.T., Price, D.L. & DeLong, M.R. (1983). Alzheimer's disease: a disorder of cortical cholinergic innervation. Science, 219, 1184-1190.

Creese, I., Burt, D.R. & Snyder, S.H. (1976). Dopamine receptor binding predicts clinical and pharmacological potencies of antischizophrenic drugs. Science, 192, 481-483.

Cronin-Golomb, A. (1995). Vision in Alzheimer's disease. Gerontologist, 35, 370-376.

Cronin-Golomb, A., Corkin, S. & Growdon, J.H. (1995). Visual dysfunction predicts cognitive deficits in Alzheimer's disease. Optometry & Vision Science, 72, 168-176.

Dajas-Bailador, F.A. & Wonnacott, S. (2004). Nicotinic acetylcholine receptors and the regulation of neuronal signaling. Trends in Pharmacological Sciences, 25, 317-324.

Dani, J.A. (2001). Overview of nicotinic receptors and their roles in the central nervous system. Biological Psychiatry, 49, 166-174.

Debski, E.A. & Cline, H.T. (2002). Activity-dependent mapping in the retinotectal projection. Current Opinions in Neurobiology, 12, 93-99.

Dingledine, R., Borges, K., Bowie, D. & Traynelis, S.F. (1999). The glutamate receptor ion channels. Pharmacological Reviews, 51, 7-61.

Dmitrieva, N.A., Pow, D.V., Lindstrom, J.M. & Keyser, K.T. (2003). Identification of cholinoceptive glycinergic neurons in the mammalian retina. Journal of Comparative Neurology, 456, 167-175.

Dmitrieva, N.A., Strang, C.E. & Keyser, K.T. (2007). Expression of α 7 nicotinic acetylcholine receptors by bipolar, amacrine, and ganglion cells of the rabbit retina. Journal of Histochemical Cytochemistry, 55, 461-476.

Dulon, D., Lenoir, M. (1996). Cholinergic responses in developing outer hair cells of the rat cochlea. European Journal of Neuroscience, 8, 1945-1952.

Dutescu, R.M., Li, Q.X., Crowston, J., Masters, C.L., Baird, P.N. & Culvenor, J.G. (2009). Amyloid precursor protein processing and retinal pathology in mouse models of Alzheimer's disease. Graefes Archive for Clinical & Experimental Ophthalmology, 247, 121-1221.

Dziewczapolski, G., Glogowski, C.M., Masliah, E. & Heinemann, S.F. (2009). Deletion of the α7 nicotinic acetylcholine receptor gene improves cognitive deficits and synaptic pathology in a mouse model of Alzheimer's disease. Neuroscience, 29, 8805-8815.

Egea, J., Rosa, A.O., Sobrado, M., Gandia, L., Lopez, M.G. & Garcia, A.G. (2007). Neuroprotection afforded by nicotine against oxygen and glucose deprivation in hippocampal slices is lost in α7 nicotinic receptor knockout mice. Neuroscience, 145, 866-872.

Elgoyhen, A.B., Johnson, D.S., Boulter, J., Veter, D.E. & Heinemann, S. (1994) A9; an acetylcholine receptor with novel pharmacological properties expressed in rat cochlear hair cells. Cell, 79, 705-715.

Endoh, T. (2004). Characterization of modulatory effects of postsynaptic metabotropic glutamate receptors on calcium currents in rat nucleus tractus solitarius. Brain Research, 1024, 212-224.

Erostegui, C., Norris, C.H., Bobbin, R.P. (1994). In vitro characterization of a cholinegic receptor on outer hair cells. Hearing Research, 74, 135-147.

Euler, T., Schneider, H. & Wassle, H. (1996). Glutamate responses of bipolar cells in a slice preparation of the rat retina. The Journal of Neuroscience, 16, 2934-2944.

Evans, M. (1996). Acetylcholine activates two currents in guinea-pig outer hair cells. Journal of Physiology, 491, 563-578.

Famiglietti, E.V. & Kolb, H. (1976). Structural basis of "On-" and "Off-" centre responses in retinal ganglion cells. Science, 194, 196-195.

Famiglietti, E.V. (1983). Starburst amacrine cells and cholinergic neurons: mirror-symmetric on and off amacrine cells of rabbit retina. Brain Research, 261, 138-144.

Feller, M.B. (2002). The role of nAChR-mediated spontaneous retinal activity in visual system development. Journal of Neurobiology, 53, 556-567.

Fernandes, C., Hoyle, E., Dempster, E., Schalkwyk, L.C. & Collier, D.A. (2006). Performance deficit of α7 nicotinic receptor knockout mice in a delayed matching-to-place task suggests a mild impairment of working/episodic-like memory. Genes Brain Behavior, 5, 433-440.

Frazier, C.J., Buhler, A.V., Weiner, J.L. & Dunwiddie, T.V. (1998). Synaptic potentials mediated via α-bungarotoxin-sensitive nicotinic acetylcholine receptors in rat hippocampal interneurons. Neuroscience, 18, 8228-8235.

Freedman, R., Adler, L.E., Gerhardt, G.A., Waldo, M., Baker, N., Rose, G.M., Drebing, C., Nagamoto, H., Bickford-Wimer, P., Franks, R. (1987). Neurobiological studies of sensory gating in schizophrenia. Schizophrenia Bulletin, 13, 669-678.

Freedman, R., Adler, L.E., Bickford, P., Byerley, W., Coon, H., Cullum, C.M., Griffith, J.M., Harris, J.G., Leonard, S., Miller, C. & . (1994). Schizophrenia and nicotinic receptors. Harvard Review Psychiatry, 2, 179-192.

Freedman, R., Coon, H., Myles-Worsley, M., Orr-Urtreger, A., Olincy, A., Davis, A., Polymeropoulos, M., Holik, J., Hopkins, J., Hoff, M., Rosenthal, J., Waldo, M.C., Reimherr, F., Wender, P., Yaw, J., Young, D.A., Breese, C.R., Adams, C., Patterson, D., Adler, L.E., Kruglyak, L., Leonard, S. & Byerley, W. (1997). Linkage of a neurophysiological deficit in schizophrenia to a chromosome 15 locus. Proceedings in the National Academy of Sciences U.S.A, 94, 587-592.

Freedman, R., Adams, C.E. & Leonard, S. (2000). The α7-nicotinic acetylcholine receptor and the pathology of hippocampal interneurons in schizophrenia. Journal of Chemical Neuroanatomy, 20, 299-306.

Fuchs, P.A. & Murrow, B.W. (1992). A novel cholinergic receptor mediates inhibition of chick cochlear hair cells. Proceedings: Biological Sciences, 248, 35-40.

Fucile S. (2004). Ca^{2+} permeability of nicotinic acetylcholine receptors. Cell Calcium, 35, 1-8.

Fukuda, Y. & Stone, J. (1974). Retinal distribution and central projections of Y-, X-, ad W-cells of the cat's retina. The Journal of Neurophysiology, 37, 749-772.

Galli-Resta, L., Novelli, E., Volpini, M. & Strettoi, E. (2000). The spatial organization of cholinergic mosaics in the adult mouse retina. European Journal of Neuroscience, 12, 3819-3822.

Gerzanich, V., Wang, F., Kuryatov, A. & Lindstrom, J. (1998). α5 subunit alters desensitization, pharmacology, Ca^{++} permeability and Ca^{++} modulation of human neuronal α3 nicotinic receptors. The Journal of Pharmacology and Experimental Therapeutics, 286, 311-320.

Ghosh, K.K, Bujan, S., Haverkamp, S., Feigenspan, A., & Wassle, H. (2004). Types of bipolar cells in the mouse retina. Journal of Comparative Neurology, 476, 202-203.

Grabus, S.D., Martin, B.R., Batman, A.M., Tyndale, R.F., Sellers, E. & Damaj, M.I. (2005). Nicotine physical dependence and tolerance in the mouse following chronic oral administration. Psychopharmacology, 178, 183-192.

Greeve, I., Kretzschmar, D., Tschape, J.A., Beyn, A., Brellinger, C., Schweizer, M., Nitsch, R.M. & Reifegerste, R. (2004). Age-dependent neurodegeneration and Alzheimer-amyloid plaque formation in transgenic drosophila. Journal of Neuroscience, 24, 2899-2906.

Griffith, J.M, O'Neill, J.E., Petty, F., Garver, D., Young, D. & Freedman, R. (1998). Nicotinic receptor desensitization and sensory gating deficits in schizophrenia. Biological Psychiatry, 44, 98-106.

Grzywacz, N.M, Amthor, F.R. & Merwine, D.K. (1998). Necessity of acetylcholine for retinal directionally selective responses to drifting gratings in rabbit. Journal of Physiology, 512, 575-581.

Hardy, J. & Selkoe, D.J. (2002). The amyloid hypothesis of Alzheimer's disease: progress and problems on the road to therapeutics. Science, 297, 353-356.

Haverkamp, S. & Wassle, H. (2000). Immunocytochemical analysis of the mouse retina. The Journal of Comparative Neurology, 424, 1-23.

Hinton, D.R., Sadun, A.A., Blanks, J.C. & Miller, C.A. (1986). Optic-nerve degeneration in Alzheimer's disease. New England Journal of Medicine, 315, 485-487.

Housley, G.D., Ashmore, J.F. (1991). Direct measurement of the action of acetylcholine on isolated outer hair cells of the guinea pig cochlea. Proceedings of the Royal Society London B, 244, 161-167.

Hughes, J.R., Hatsukami, D.K., Mitchell, J.E. & Dahlgren, L.A. (1996). Prevalence of smoking among psychiatric outpatients. Experimental Clinical Psychopharmacology, 143, 993-997.

Hutton, J.T., Morris, J.L., Elias, J.W. & Poston, J.N. (1993). Contrast sensitivity dysfunction in Alzheimer's disease. Neurology, 43, 2328-2330.

Ikeda, H. & Sheardown, M.J. (1982) Acetylcholine may be an excitatory transmitter mediating visual excitation of "transient" cells with the periphery effect in the cat retina: iontophoretic studies in vivo. Neuroscience, 7, 1299-1308.

Johnson, D., Martinez, J., Elgoyhen, A., Heinemann, S., McIntosh, J. (1995). α-Conotoxin Im1 exhibits subtype-specific nicotinic acetylcholine receptor blockade: preferential inhibition of homomeric α7 and α9 receptors. Molecular Pharmacology, 48, 194-199.

Jones, I.W. & Wonnacott, S. (2005). Why doesn't nicotinic ACh receptor immunoreactivity knock out? Trends in Neuroscience, 28, 343-345.

Jonnala, R.R. & Buccafusco, J.J. (2001). Relationship between the increased cell surface α7 nicotinic receptor expression and neuroprotection induced by several nicotinic receptor agonists. Journal of Neuroscience Research, 66, 565-572.

Jonnala, R.R., Graham, J.H., Terry, A.V.J., Beach, J.W., Young, J.A. & Buccafusco, J.J. (2003). Relative levels of cytoprotection produced by analogs of choline and the role of α7-nicotinic acetylcholine receptors. Synapse, 47, 262-269.

Kandal, E.R., Schwartz, J.H. & Jessell, T.M. (2000). Principles of Neuroscience, 4th edition. McGraw-Hill, New York.

Karlin, A. (2002). Emerging structure of the nicotinic acetylcholine receptors. National Review of Neuroscience, 3, 102-114.

Kaskie, B. & Storandt, M. (1995). Visuospatial deficit in dementia of the Alzheimer type. Archives Neurology, 52, 422-425.

Katz, B. & Rimmer, S. (1989). Ophthalmologic manifestation of Alzheimer's disease. Survey of Ophthalmology, 34, 34-43.

Katz, E., Verbitsky, M., Rothlin, C.V., Vetter, D.E., Heinemann, S.F. & Elgoyhen, A.B. (2000). High calcium permeability and calcium block of the alpha9 nicotinic acetylcholine receptor. Hearing Research, 141, 117-128.

Keyser, K.T., Hughes, T.E., Whiting, P.J., Lindstrom, J.M. & Karten, H.J. (1988). Cholinoceptive neurons in the retina of the chick: an immunohistochemical study of the nicotinic acetylcholine receptors. Visual Neuroscience, 269, 109-117.

Keyser, K.T., MacNeil, M.A., Dmitrieva, N., Wang, F., Masland, R.H. & Lindstrom, J.M. (2000). Amacrine, ganglion, and displaced amacrine cells in the rabbit retina express nicotinic acetylcholine receptors. Visual Neuroscience, 17, 743-752.

Khiroug, S.S., Harkness, P.C., Lamb, P.W., Sudweeks, S.N., Khiroug, L., Millar, N.S. & Yakel, J.L. (2002). Rat nicotinic ACh receptor α7 and β2 subunits co-assemble to form functional heteromeric nicotinic receptor channels. Journal of Physiology, 540, 425-434.

Kleckner, N.W. & Dingledine, R. (1988). Requirement for glycine in activation of NMDA receptors expressed in *Xenopus* oocytes. Science, 241, 835-837.

Kihara, T., Shimohama, S., Sawada, H., Honda, K., Nakamizo, T., Shibasaki, H., Kume, T. & Akaike, A. (2001). α7 nicotinic receptor transduces signals to phosphatidylinositol 3-kinase to block A β-amyloid-induced neurotoxicity. Journal of Biological Chemistry, 276, 13541-13546.

Kittila, C.A. & Massey, S.C. (1997). Pharmacology of directionally selective ganglion cells in the rabbit retina. Journal of Neurophysiology, 77, 675-689.

Kolb, H. & Famiglietti, E.V. (1974). Rod and cone pathways in the inner plexiform of the cat. Science, 186, 47-49.

Kolb, H. (1979). The inner plexiform layer in the retina of the cat: electron microscopic observations. Journal of Neurocytology, 8, 295-329.

Kolb, H., Nelson, R. & Mariani, A. (1981). Amacrine cells, bipolar cells and ganglion cells of the cat retina: a Golgi study. Vision Research, 21, 1081-1114.

Kolb, H. & Marshak, D. (2003). The midget pathways of the primate retina. Documenta Ophthalmologica, 106, 67-81.

Kong, J.H., Fish, D.R., Rockhill, R.L. & Masland, R.H. (2005). Diversity of ganglion cells in the mouse retina: unsupervised morphological classification and its limits. The Journal of Comparative Neuroscience, 489, 293-310.

Koronyo-Hamaoui, M., Koronyo, Y., Ljubimov, A.V., Miller, C.A., Ko, M.K., Black, K.L., Schwartz, M. & Farkas, D.L. (2011). Identification of amyloid plaques in retinas from Alzheimer's patients and noninvasive in vivo optical imaging of retinal plaques in a mouse model. Neuroimage, 54, S204-S217.

Koronyo, Y., Salumbides, B.C., Black, K.L. & Koronyo-Hamaoui, M. (2012). Alzheimer's disease in the retina: imaging retinal Aβ plaques for early diagnosis and therapy assessment. Neurodegenerative Diseases, 10, 285-293.

Lea, P.M., Custer, S.J., Vicini, S. & Fade, A.I. (2002). Neuronal and glial mGluR5 modulation prevents stretch-induced enhancement of NMDA receptor current. Pharmacology Biochemistry and Behavior, 73, 287-298.

Leicester, J. & Stone, J. (1967). Ganglion, amacrine and horizontal cells of the cat's retina. Vision Research, 7, 695-705.

Leonard, S. & Freedman, R. (2006). Genetics of chromosome 15q13-q14 in schizophrenia. Biological Psychiatry, 60, 115-122.

Leventhal, A.G., Rodieck, R.W. & Dreher, B. (1981). Retinal ganglion cell classes in the old world monkey: morphology and central projections. Science, 213, 1139-1142.

Leventhal, A.G., Rodieck, R.W. & Dreher, B. (1985). Central projections of the cat retinal ganglion cells. The Journal of Comparative Neurology, 237- 216-226.

Levick, W.R. (1967). Receptive fields and trigger features of ganglion cells in the visual streak of the rabbit retina. Journal of Physiology, 188, 285-307.

Levin, E.D. (1992). Nicotinic systems and cognitive function. Psychopharmacology, 108, 417-431.

Lindstrom, J., Anand, R., Gerzanich, V., Peng, X., Wang, F. & Wells, G. (1996). Structure and function of neuronal nicotinic acetylcholine receptors. Progress in Brain Research, 109, 125-137.

Lindstrom, J. (1997). Nicotinic acetylcholine receptors in health and disease. Molecular Neurobiology, 15, 193-222.

Lindstrom, J.M. (2000). The structures of neuronal nicotinic receptors. In Handbook of Experimental Pharmacology, Vol 144, ed. Clementi, F., Fornasari, D. & Gotti, C., pp. 101-162. Berlin Heidelburg: Springer-Verlag.

Liu, B., Rasool, S., Yang, Z., Glabe, C.G., Schreiber, S.S., Ge, J. & Tan, Z. (2009). Amyloid-peptide vaccinations reduce beta-amyloid plaques but exacerbate vascular deposition and inflammation in the retina of Alzheimer's transgenic mice. American Journal of Pathology, 175, 2099-2110.

Liu, J., McGlinn, A.M., Fernandes, A.I., Milam, A.H., Strang, C.E., Andison, M.E., Lindstrom, J.M., Keyser, K.T. & Stone, R.A. (2009). Nicotinic acetylcholine receptor subunits in rhesus monkey retina. Investigative Ophthalmology and Vision Sciences, 50, 1408-1415.

Loffler, K.U., Edward, D.P. & Tso, M.O. (1995). Immunoreactivity against tau, amyloid precursor protein, and beta-amyloid in the human retina. Investigative Ophthalmology and Vision Sciences, 36, 24-31.

Luntz-Leybman, V., Bickford, P.C. & Freedman, R. (1992). Cholinergic gating of response to auditory stimuli in rat hippocampus. Brain Research, 587, 130-136.

Marchi, M., Risso, F., Viola, C., Cavazzani, P. & Raiteri, M. (2002). Direct evidence that release-stimulating α7 nicotinic cholinergic receptors are localized on human and rat brain glutamatergic axon terminals. Journal of Neurochemistry, 80, 1071-1078.

Masland, R.H & Ames, A. (1976). Responses to acetylcholine of ganglion cells in an isolated mammalian retina. Journal of Neurophysiology, 39, 1220-1235.

Masland, R.H., Mills, J.W. & Cassidy, C. (1984). The functions of acetylcholine in the rabbit retina. Proceedings of the Royal Society B: Biological Sciences, 223, 121-139.

Massey, S.C. & Miller, R.F. (1988). Glutamate receptors of ganglion cells in the rabbit retina: evidence for glutamate as a bipolar cell transmitter. The Journal of Physiology, 405, 635-655.

Massey, S.C. & Miller, R.F. (1990). N-methyl-D-aspartate receptors of ganglion cells in rabbit retina. Journal of Neurophysiology, 63, 16-30.

Mathew, S.V., Law, A.J., Lipska, B.K., vila-Garcia, M.I., Zamora, E.D., Mitkus, S.N., Vakkalanka, R., Straub, R.E., Weinberger, D.R., Kleinman, J.E. & Hyde, T.M. (2007). α7 nicotinic acetylcholine receptor mRNA expression and binding in postmortem human brain are associated with genetic variation in neuregulin 1. Human Molecular Genetics, 16, 2921-2932.

McGehee, D.S. (1999). Molecular diversity of neuronal nicotinic acetylcholine receptors. Annals of the New York Academy of Sciences, 868, 565-577.

McGhie, A. & Chapman, J.S. (1961). Disorders of attention and perception in earlier schizophrenia. British Journal of Medical Psychology, 34, 103-116.

Meuser, K.T. & McGurk, S.R. (2004). Schizophrenia. Lancet, 363, 2063-2072.

Merwine, D.K., Amthor, F.R. & Grzywacz, N.M. (1995). Interaction between center and surround in rabbit retinal ganglion cells. Journal of Neurophysiology, 73, 1547-1567.

Morley, B.J., Warr, W.B & Rodriquez-Sierra, J.F. (2004). Transient expression of acetylcholinesterase in the posterior ventral cochlear nucleus of rat brain. Journal of the Association for Research in Otolaryngology, 5, 391-403.

Morley, B.J. & Rodriguez-Sierra, J.F. (2004). A phenotype for the α7 nicotinic acetylcholine receptor null mutant. Brain Research, 1023, 41-47.

Nelson, R., Famiglietti, E.V. & Kolb, H. (1978). Intracellular staining reveals different levels of stratification for On- and Off-centre ganglion cells in cat retina. The Journal of Neurophysiology, 41, 472-483.

Nelson, R. & Kolb, H. (1985). A17: a broad-field amacrine cell in the rod system of the cat retina. Journal of Neurophysiology, 54, 592-614.

Nelson, M.E. & Lindstrom, J. (1999). Single channel properties of human α3 AChRs: impact of β2, β4 and α5 subunits. Journal of Physiology, 516, 657-678.

Ni, R., Marutle, A. & Nordberg, A. (2013). Modulation of α7 nicotinic acetylcholine receptor and fibrillar amyloid-β interactions in Alzheimer's disease brain. Journal of Alzheimer's Disease, 2013 Jan 1;33(3):841-51. doi: 10.3233/JAD-2012-121447, [epub ahead of print].

Ning, A., Cui, J., To, E., Ashe, K.H. & Matsubara, J. (2008). Amyloid-beta deposits lead to retinal degeneration in a mouse model of Alzheimer disease. Investigative Ophthalmology & Visual Science, 49, 5136-5143.

Nordberg, A. & Svensson, A.L. (1998). Cholinesterase inhibitors in the treatment of Alzheimer's disease: a comparison of tolerability and pharmacology. Drug Safety, 19, 465-480.

Nordberg, A. (1999). PET studies and cholinergic therapy in Alzheimer's disease. Review Neurology, 155, 53-S63.

Oddo, S. & LaFerla, F.M. (2006). The role of nicotinic acetylcholine receptors in Alzheimer's disease. Journal of Physiology, 99, 172-179.

Origlia, N., Valenzano, D.R., Moretti, M., Gotti, C. & Domenici, L. (2012). Visual acuity is reduced in alpha 7 nicotinic receptor knockout mice. Investigative Opthalmology and Visual Science, 53, 1211-1218.

Orr-Urtreger, A., Goldner, F.M., Saeki, M., Lorenzo, I., Goldberg, L., De, B.M., Dani, J.A., Patrick, J.W. & Beaudet, A.L. (1997). Mice deficient in the α7 neuronal nicotinic acetylcholine receptor lack α-bungarotoxin binding sites and hippocampal fast nicotinic currents. Neuroscience, 17, 9165-9171.

Palmer, A.M. (2002). Pharmacotherapy for Alzheimer's disease: progress and prospects. Trends in Pharmacological Science, 23, 426-433.

Papke, R.L., Bencherif. M. & Lippiello, P. (1996). An evaluation of neuronal nicotinic acetylcholine receptor activation by quaternary nitrogen compounds indicates that choline is selective for the α7 subtype. Neuroscience Letters, 213, 201-204.

Papke, R.L., Meyer, E. & Uteshev, V.V. (2000). α7 Receptor-selective agonists and modes of α7 receptor activation. European Journal of Pharmacology, 393, 179-195.

Parisi, V., Restuccia, R., Fattapposta, F., Mina, C., Bucci, M.G. & Pierelli, F. (2001). Morphological and functional retinal impariment in Alzheimer's disease patients. Clinical Neurophysiology, 112, 1860-1867.

Parisi, V. (2003). Correlation between morphological and functional retinal impairment in patients affected by ocular hypertensions, glaucoma, demyelinating optic neuritis and Alzheimer's disease. Seminars in Ophthalmology, 18, 50-57.

Paylor, R., Nguyen, M., Crawley, J.N., Patrick, J., Beaudet, A. & Orr-Urtreger, A. (1998). α7 nicotinic receptor subunits are not necessary for hippocampal-dependent learning or sensorimotor gating: a behavioral characterization of Acra7-deficient mice. Learning and Memory, 5, 302-316.

Perez, S.E., Lumayag, S., Kovacs, B., Mufson, E.J. & Xu, S. (2009). Beta-amyloid deposition and functional impairment in the retina of the APPswe/ps1DeltaE9 transgenic mouse model of Alzheimer's disease. Investigative Ophthalmology & Visual Science, 50, 793-800.

Perry, V.H., Oehler, R. & Cowey, A. (1984). Retinal ganglion cells that project to the dorsal lateral geniculate nucleus in the macaque monkey. Neuroscience, 12, 1101-1123.

Perry, V.H. & Cowey, A. (1984). Retinal ganglion cells that project to the superior colliculus and pretectum in the macaque monkey. Neuroscience, 12, 1125-1137.

Perry, E., Martin-Ruiz, C., Lee, M., Griffiths, M., Johnson, M., Piggott, M., Haroutunian, V., Buxbaum, J.D., Nasland, J., Davis, K., Gotti, C., Clementi, F., Tzartos, S., Cohen, O., Soreq, H., Jaros, E., Perry, R., Ballard, C., McKeith, I. & Court, J. (2000). Nicotinic receptor subtypes in human brain ageing, Alzheimer and Lewy body diseases. European Journal of Pharmacology, 393, 215-222.

Pin, J.P. & Duvoison, R. (1995). Review: Neurotransmitter receptors. I. The metabotropic glutamate receptors: structure and functions. Neuropharmacology, 34, 1-26.

Plazas, P.V., Katz, E., Gomez-Casati, M.E., Bouzat, C. & Elgoyhen, A.B. (2005). Stoichiometry of the alpha9alpha10 nicotinic cholinergic receptor. Journal of Neuroscience, 25, 10905-10912.

Reed, B.T., Amthor, F.R. & Keyser, K.T. (2002). Rabbit retinal ganglion cell responses mediated by alpha-bungarotoxin-sensitive nicotinic acetylcholine receptors. Visual Neuroscience, 19, 427-438.

Reed, B.T., Amthor, F.R. & Keyser, K.T. (2004). MLA-sensitive cholinergic receptors involved in the detection of complex moving stimuli in retina. Visual Neuroscience, 21, 861-872.

Renna, J.M., Strang, C.E., Amthor, F.R. & Keyser, K.T. (2007). Strychnine, but not PMBA, inhibits neuronal nicotinic acetylcholine receptors expressed by rabbit retinal ganglion cells. Visual Neuroscience, 24, 503-511.

Rothlin, C., Verbitsky, M., Katz, E., Elgoyhen, A.B. (1999). The α9 nicotinic acetylcholine receptor shares pharmacological properties with type A γ-aminobutyric acid, glycine and type 3 serotonin receptors. Molecular Pharmacology, 55, 248-254.

Sadun, A.A. & Bassi, C.J. (1990). The visual system in Alzheimer's disease. Research Publications - Association for Research in Nervous and Mental Disease, 67, 331-347.

Sasaki, T. & Kaneko, A. (1996). L-Glutamate-induced responses in OFF-type bipolar cells of the cat retina. Vision Research, 36, 787-795.

Schmidt, M., Humphrey, M.F. & Wassle, H. (1987). Action and localization of acetylcholine in the cat retina. Journal of Neurophysiology, 58, 997-1015.

Seeman, P., Chau-Wong, M., Tedesco, J. & Wong, K. (1975). Brain receptors for antipsychotic drugs and dopamine: direct binding assays. Proceedings in the National Academy of Sciences U.S.A., 72, 4376-4380.

Skeberdis,V.A., Lan, J., Opitz, T., Zheng, X., Bennett, M.V., Zukin, R.S. (2001). mGluR1-mediated potentiation of NMDA receptors involves a rise in intracellular calcium and activation of protein kinase C. Neuropharmacology, 40, 856-865.

Slaughter, M.M. & Miller, R.F. (1981). 2-Amino-4-phosphobutyric acid: a new pharmacological tool for retina research. Science, 211, 182-184.

Slaughter, M.M. & Miller, R.F. (1983). The role of excitatory amino acid transmitters in the mudpuppy retina: an analysis with kainic acid and N-methyl aspartate. The Journal of Neuroscience, 3, 1701-1711.

Stanke, J.J., Lehman, B. & Fischer, A.J. (2008). Muscarinic signaling influences the patterning and phenotype of cholinergic amacrine cells in the developing chick retina. BMC Developmental Biology, 8, 13.

Stevens, E.R., Esquerra, M., Kim, P.M., Newman, E.A., Snyder, S.H., Zahs, K.R. & Miller, R.F. (2003). D-serine and serine racemase are present in the vertebrate retina and contribute to the physiological activation of NMDA receptors. Proceedings of the National Academy of Sciences, 100, 6789-6794.

Strang, C.E., Andison, M.E., Amthor, F.R. & Keyser, K.T. (2005). Rabbit retinal ganglion cells express functional α7 nAChRs. American Journal of Physiology-Cell Physiology, 289, 644-C655.

Strang, C.E., Renna, J.M., Amthor, F.R. & Keyser, K.T. (2007). Nicotinic acetylcholine receptor expression by directionally selective ganglion cells. Visual Neuroscience, 24, 523-533.

Strang, C.E., Renna, J.R., Amthor, F.R. & Keyser, K.T. (2010). Muscarinic acetylcholine receptor localization and activation effects on ganglion response properties.

Swanson, C.J., Bures, M., Johnson, M.P., Linden, A.M., Monn, J.A. & Schoepp, D.D. (2005). Metabotropic glutamate receptors as novel targets for anxiety and stress disorders. Nature Reviews Drug Discovery, 4, 131-144.

Syed, M.M., Lee, S., Zheng, J. & Zhou, Z.J. (2004). Stage-dependent dynamics and modulation of spontaneous waves in the developing rabbit retina. Journal of Physiology, 560, 533-549.

Taylor, W.R. & Smith, R.G. (2012). The role of starburst amacrine cells in visual signal processing. Visual Neuroscience, 29, 73-81.

Trojanowski, J.Q., Schmidt, M.L., Shin, R.W., Bramblett, G.T., Rao, D. & Lee, V.M. (1993). Altered tau and neurofilament proteins in neuro-degenerative diseases: diagnostic implications for Alzheimer's disease and Lewy body dementias. Brain Pathology, 3, 45-54.

Uhlmann, R.F., Larson, E.B., Koepsell, T.D., Rees, T.S. & Duckert, L.G. (1991). Visual impairment and cognitive dysfunction in Alzheimer's disease. Journal of General Internal Medicine, 6, 126-132.

van Os, J. & Kapur, S. (2009). Schizophrenia. Lancet, 374, 635-645.

Verbitsky, M., Rothlin, C.V., Katz, E. & Elgoyhen, A.B. (2000). Mixed nicotinic-muscarinic properties of the α9 nicotinic cholinergic receptor. Neuropharmacology, 39, 2515-2524.

Viertio, S., Laitinen, A., Perala, J., Saarni, S.I., Koskinen, S., Lonnqvist, J. & Suvisaari, J. (2007). Visual impairment in persons with psychotic disorder. Social Psychiatry and Psychiatric Epidemiology, 42, 902-908.

Volgyi, B., Chheda, S. & Bloomfield, S.A. (2009). Tracer coupling patterns of the ganglion cell subtypes in the mouse retina. The Journal of Comparative Neurology, 51, 664-687.

Waldo, M.C., Carey, G., Myles-Worsley, M., Cawthra, E., Adler, L.E., Nagamoto, H.T., Wender, P., Byerley, W., Plaetke, R. & Freedman, R. (1991). Codistribution of a sensory gating deficit and schizophrenia in multi-affected families. Psychiatry Research, 39, 257-268.

Wang, H.Y., Lee, D.H., D'Andrea, M.R., Peterson, P.A., Shank, R.P. & Reitz, A.B. (2000). β-Amyloid(1-42) binds to α7 nicotinic acetylcholine receptor with high

affinity. Implications for Alzheimer's disease pathology. Journal of Biological Chemistry, 275, 5626-5632.

Wassle, H. & Boycott, B.B. (1991). Functional architecture of the mammalian retina. Physiological Reviews, 71, 447-480.

Weisstaub, N., Vetter, D.E., Elgoyhen, A.B. & Katz, E. (2002). The alpha9alpha10 nicotinic receptor is permeable to and is modulated by divalent cations. Hearing Research, 167, 122-135.

Wess, J., Liu, J., Blin, N., Yun, J., Lerche, C. & Kostenis, E. (1997). Structural basis of receptor/G protein coupling selectivity studied with muscarinic receptors as model systems. Life Sciences, 60, 1007-1014.

Wevers, A., Monteggia, L., Nowacki, S., Bloch, W., Schutz, U., Lindstrom, J., Pereira, E.F., Eisenberg, H., Giacobini, E., de Vos, R.A., Steur, E.N., Maelicke, A., Albuquerque, E.X. & Schroder, H. (1999). Expression of nicotinic acetylcholine receptor subunits in the cerebral cortex in Alzheimer's disease: histotopographical correlation with amyloid plaques and hyperphosphorylated-tau protein. European Journal of Neuroscience, 11, 2551-2565.

Wolin, M.J. (1994). Alzheimer's disease and the eye. Journal of the South Carolina Medical Association, 90, 534-538.

Xu, J., Pato, M.T., Torre, C.D., Medeiros, H., Carvalho, C., Basile, V.S., Bauer, A., Dourado, A., Valente, J., Soares, M.J., Macedo ,A.A., Coelho, I., Ferreira, C.P., Azevedo, M.H., Macciardi, F., Kennedy, J.L. & Pato, C.N. (2001). Evidence for linkage disequilibrium between the α7-nicotinic receptor gene (CHRNA7) locus and schizophrenia in Azorean families. American Journal of Medical Genetics, 105, 669-674.

Yamada, E.S., Dmitrieva, N., Keyser, K.T., Lindstrom, J.M., Hersh, L.B. & Marshak, D.W. (2003). Synaptic connections of starburst amacrine cells and localization of acetylcholine receptors in primate retinas. Journal of Comparative Neurology, 16, 76-90.

Young, J.W., Crawford, N., Kelly, J.S., Kerr, L.E., Marston, H.M., Spratt, C., Finlayson, K. & Sharkey, J. (2007). Impaired attention is central to the cognitive deficits observed in α7 deficient mice. European Neuropsychopharmacology, 17, 145-155.

Yu, W.F, Guan, Z.Z., & Nordberg, A. (2007) Postnatal upregulation of α4 and α3 nicotinic receptor subunits in the brain of α7 nicotinic receptor-deficient mice. Neuroscience, 146, 1618-1628.

Zhang, J. & Berg, D.K. (2007). Reversible inhibition of GABAA receptors by α7-containing nicotinic receptors on the vertebrate postsynaptic neurons. Journal of Physiology, 579, 753-763.

Zhou, Z.J. & Zhao, D. (2000). Coordinated transitions in neurotransmitter systems for the initiation and propagation of spontaneous retinal waves. Journal of Neuroscience, 20, 6570-6577.

Zucker, C. & Yazulla, S. (1982). Localization of synaptic and nonsynaptic nicotinic-acetylcholine receptors in the goldfish retina. Journal of Comparative Neurology, 204, 188-195.